MSE High-z Team: Science Report

Simon Driver (Chair), Helen Courtois, Luke Davies, Sarah Gallagher, Aaron Robotham, Carlo Schmid

23rd January 2015

Executive Summary

We have identified 7 compelling science cases for MSE (nominal design):

(1) A study of the evolution of structure, galaxies, and AGN over the past 12Gyrs
(2) A high-S/N study of galaxies and AGN in 1Gyr intervals over a 10Gyr timeline
(3) Mapping of the IGM at z=2-2.5 along with a study of associated galaxy population
(4) The use of AGN reverberation mapping to study the central engines of AGN
(5) A peculiar velocity study out to 1Gpc to fully understand the CMB dipole
(6) Mapping of the dark matter distribution using velocity sheer
(7) Coordinated opportunities with LSST, Euclid, WFIRST and SKA

While the goals of these surveys are (mostly) achievable with the nominal design, the science topics drive MSE towards large aperture (12+m), higher-fibre number & density (5000-10000), a broader field-of-view (2+deg), with modest IFU capability (100 ~19fibre modules), and most importantly the capacity to sample the broadest possible wavelength range (300nm – 2.5micron) within a single instrument.

We also note that MSE will fulfill three distinct roles in the 2025+ era: dedicated science programmes (as discussed here), coordinated survey programmes (as briefly touched upon), and ELT feeder programmes (not discussed here). All three roles are critical, transformational, and will lead to major advancements in the area of structure formation, galaxy evolution, AGN physics, our understanding of the IGM, and the underlying Dark Matter distribution. We particularly note the synergy between LSST, Euclid, WFIRST and the SKA, and highlight the need for strong communication channels between these facilities to coordinate survey footprints and survey designs.

2 Science Overview

Within the MSE high-z science team we consider the science potential of MSE at distances greater than a few hundred Mpc and hence epochs prior to the present ($z > 0.1$, Ages > 1Gyr), i.e., the extra-galactic spatially unresolved regime spanning a broad range of masses (typically with stellar masses $> 10^9 M_\odot$), environments (pairs, groups, clusters, tendrils, filaments and voids), and epochs (0 to ~12.5Gyrs, i.e., $z < 5.5$).

A crucial factor to state clearly from the outset is the recognition that MSE will not be a cosmology machine/experiment but rather will have a transformational impact in extra-galactic astrophysics; in particular unscrambling the non-linear regime (small scale clustering, mergers, groups, tendrils and filaments), the baryon regime (i.e., metallicity/chemical evolution), and the evolution and interplay of galaxies, AGN, and the IGM, incorporating environmental factors (i.e., the key energy production pathways).

In the 2025 era the specific constraint of cosmological parameters will be conducted on dedicated facilities/experiments which are optimised to provide measurements to better than 1% via wide-area deep optical and near-IR imaging facilities (e.g., Euclid, WFIRST, LSST), via combinations of weak lensing (high-resolution imaging), BAO analysis (using photometric-redshifts), and RSD analysis (DESI, 4MOST). In these areas numbers rather than redshift accuracy or spectrum continuum signal-to-noise is paramount, and while MSE will undoubtedly have a vital role in quantifying bias, cosmic variance, and other calibratory factors, its forte will be the detailed study of astrophysics rather than cosmology. A key implication is to acknowledge that MSE, in the $z > 0.1$ arena should be unashamedly optimised for studying the evolution of galaxies, AGN, and the environmental factors likely to influence this evolution. In exploring the science potential it is also clear that the $z > 0.1$ case will not drive the evolution towards high-spectral resolution, $R \approx 3000$ is sufficient for almost all astrophysical objectives because of the inherent motion within the structures being studied), similarly IFUs will not be critical for high-z operations where the resolution of the majority of targets will be comparable to the native seeing of the site. However the high-z case will drive the wavelength range to as long-ward and over as broad a range of wavelengths as is financially feasible (with the implicit acknowledgment that the high-z limit will be set by this factor rather than any particular science cut-off). With these factors in mind the high-z team has settled upon the following six areas of critical important with some further consideration of the landscape and unique synergy opportunities which will arise in the 2020 era (e.g., with Euclid, WFIRST, SKA and other potential imaging, time domain or responsive facilities).

The relevant astrophysical measurements MSE is capable of providing are low and intermediate resolution spectroscopy spanning the optical-near-IR range — high resolution spectroscopy is potentially redundant due to the internal dynamics of the systems being studied unless one can resolve the Lyman-α forest which requires exceptionally high resolution ($R > 150,000$). Processes which generate energy at these wavelengths are predominantly star-formation and accretion, potentially triggered via environmental factors such as dynamical interactions, mergers and/or interactions with the inter-galactic (IGM) or intra-cluster medium (ICM). Complimentary external information will naturally arise from panchromatic imaging facilities from the x-ray to the radio, providing potentially high-spatial resolution imaging and potentially spatially resolved spectroscopy for well-defined sub-samples. Initially we focus on what MSE might achieve alone and later consider briefly some of the synergistic opportunities.

Environment may or may not be a red herring outside the very rich cluster environment, in terms of its influence on AGN and galaxy formation. However, the small scale clustering of galaxies in the form of merger rates, halo-occupation distributions, and the evolution of the 3D web from a uniform 3D structure into firstly flattened planes/sheets, and ultimately tendrils/filaments have all emerged relatively late in the Universe ($z < 3$) and therefore their appearance, abundances, morphologies and corresponding evolution all provide rich fodder for comparisons to similar structures in numerical simulations. At the heart of all of MSEs investigations needs to be a detailed fully sampled study of the evolution of small scale structure (i.e., 20kpc – 100Mpc scales).

[MSE-highz-SRO1] *Multi-Scale Clustering with MSE: In this SRO we consider*

clustering experiments on 20kpc to 100Mpc scales (i.e., pair to void/filament scales), and with contiguous volumes to allow for maximal scientific utility. At the smallest (sub Mpc) scales the ultra-high completeness that MSE opens up will produce the best possible HOD dataset. It will also produce merger rates out to z ~ 4, allowing a full model of mass growth via mergers and star formation (via Hα) measurements. Small scale clustering studies are very much driven by the requirement for excellent completeness at the smallest scales down to very faint galaxies requiring close fibre-placement and/or repeat observations/passes.

This extensive low-S/N redshift sample naturally provides not only the environmental information but of course the individual spectral measurements for those systems (galaxies and/or AGN) defining the structures. Hence one can obtain information on, for example, the evolution of the AGN space-density or the galaxy luminosity densities and mass-distributions. However the extraction of more sophisticated measurements such as the mass-metallicity relation versus redshift, and environment requires significantly higher-S/N spectra (S/N~20-30). The second SRO is therefore designed to complement the first by selecting appropriate volume-limited samples at regular time steps building up S/N through repeated integrations.

[MSE-highz-SRO2] *The chemical evolution of galaxies and AGN: This SRO is very much a follow-up of (MSE-highz-SRO1) where we take advantage of the mirror capacity to obtain high-S/N spectra (20-30) for intermediate mass ($10^9 M_\odot$) galaxies to significant redshifts (z~2) to measure both the gas and stellar phase metallicities. The science objective is to be able to construct a full empirical blueprint for the evolution of metals as a function stellar mass, redshift and environment. Crucial for the success of this survey will be the successful construction of a broader low-S/N redshift survey in which the environment is fully defined and from which suitable subsamples can be selected.*

Not all structure will be revealed by the distribution of galaxies/AGN, and in particular the gaseous content of the IGM, representing the bulk of the baryons. However this can be probed through the absorption and attenuation of light from a background galaxy population as it transits through the IGM. Hence our third SRO focuses on exploring the 3D structure of the gaseous IGM. This SRO also extends the study of metallicity to z~2.5.

[MSE-highz-SRO3] *Connecting high redshift galaxies to their local environment - 3D mapping of the structure and composition of the IGM, and the galaxies which are embedded within it: This SRO will simultaneously use high-z (z>2.5) Quasi-Stellar Objects (QSOs) and bright galaxy sight-lines to probe the Lyman-α forest and metal content of the IGM at z~2-2.5, and target photometrically selected faint galaxies within ~1Mpc of each sight-line to directly identify sources associated with the IGM structure. Moderate resolution (R~5000), deep spectra would be obtained for all sources to target wavelengths from Lyman-α to OIII, and intervening stellar absorption lines, at z~2-2.5. This will push the capabilities of MSE, requiring good sensitivity and moderate spectral resolution from 3600Å to 1.8μm – with the primary instrumentation requirement of excellent sensitivity at 3600-4250Å. Such a study would allow a reconstruction of the dark matter distribution and associated galaxies at high-z, detailed modeling of galactic*

scale outflows via emission lines, investigations of the complex interplay between metals in galaxies and the IGM, and the first comprehensive, moderate resolution analysis of large samples of galaxies at this epoch.

Co-evolving with the galaxy population is the AGN population where the underlying physical processes driving AGN remain uncertain. Repeat observations at the appropriate cadence (hours, days, weeks, months, years) can allow one to probe the energy progression through the accretion disc mapping into the very heart of the AGN process. Our fourth SRO is therefore focused on deciphering the AGN cores via reverberation mapping.

[MSE-highz-SRO4] *Mapping the Broad Line Region and Measuring Black Hole Masses in High Redshift Quasars: With its wide field of view and sensitivity, MSE will be an ideal facility to conduct a ground-breaking reverberation-mapping campaign on luminous quasars at the peak of the quasar epoch from z = 1 − 3. With appropriate time-sampling cadence and wavelength coverage from the rest-frame UV through optical, the accretion disk continuum and a suite of lines that probe the broad-line region on all scales will be accessible. The responses of these lines to continuum changes will reveal the structure of the broad-line region, and enable accurate dynamical black hole mass measurements for 100s of high-z quasars.*

An additional probe of the nearby dark matter distribution comes from the local peculiar velocity field as best revealed through the comparison of a broad redshift distribution against direct distance estimates via Tully-Fischer or Fundamental Plane type analysis. Our fifth SRO is designed to provide the definitive measurement of the gravitational conglomerates and provide a complete explanation for the CMB dipole.

[MSE-highz-SRO5] *Peculiar velocity survey up to 1 Gpc/h in the northern hemisphere: A velocity survey covering effective 10000 deg^2, adopting the Fundamental Plane method to measure the distance of early-type galaxies up to redshift z < 0.1 and with galaxy number density and sampling similar to Cosmicflow-2, would represent the northern sky counterpart of the TAIPAN survey. It will allows (i) the reconstruction of the velocity-based cosmic web, resolving cosmic structures down to 0.1Mpc/h; (ii) the direct measurement of RSD, not limited by cosmic variance unlike galaxy redshift surveys and without any assumption about bias; (iii) the direct probe of the back-reaction conjecture (accelerated expansion from small-scale inhomogeneities), by measuring the morphology of the velocity potential.*

MSE also provides new opportunities to explore the intervening DM distribution in a manner which is complementary to weak lensing, for example instead of exploring spatial distortions one can explore velocity distortions, and even more powerful is the combination of the two. Hence our sixth SRO is somewhat high-risk and speculative, in that the technique is yet to be fully demonstrated, but provides great potential for opening up a new field of investigation.

[MSE-highz-SRO6] *Direct measure of weak-lensing from galaxy velocity maps: Gravitational lensing deforms the velocity field of disk galaxies and their luminosity*

profile in a different way, yielding a non- vanishing angle between their projected major axis and the gradient of the velocity field. Using fiber bundles to map the velocity field of galaxies at redshift $z \leq 0.5$ and measuring their profile, one can directly estimate the gravitational shear induced by foreground clusters, with a smaller number of galaxies than required by traditional (statistical) methods.

Finally its is arguable that some of the very best science will come from the unique opportunity provided by cross-facility campaigns, hence our final SRO briefly highlights some of these opportunities.

[MSE-highz-SRO7] *Big facility synergies and likely operational/modes coordination: The next decade will see an emergence of new frontier facilities. Opportunities will exist to coordinate observations between these facilities, to cross-calibrate data, and to pursue science objectives which use a combination of data. Key facilities include: EUCLID, WFIRST, LSST, SKA, eROSITA etc. Here we look to identify some of these synergies and particularly those likely to influence design or operational modes, e.g., transients, TOOs (GRBs, SN), coordinated observations and supporting observations (e.g., photo-z calibration).*

Science explicitly not covered includes the swathe of cosmology experiments: BAO, RSD, weak-lensing. These are critically important and MSE *can and will* provide vital supporting data in the form of calibration of photo-zs, tracer particle bias and sample (cosmic) variance issues. These are briefly discussed as part of MSE-highz-SRO7. We also have not explored high spatial resolution spectroscopy, i.e., IFU on sub-arcsecond scales which would require the incorporation of both active and adaptive options (Multi-conjugate Adaptive Optics) which will be aggressively pursued on the 8m and upcoming ELT facilities. MSE will of course be fundamentally vital in providing suitably selected samples for such follow-up. MSE has a unique role to play, not only in its own right, and through combined cross-facility surveys but also acting as a bridging facility between the 8m ground-based and space-based imaging facilities, and the 30+m class ELTs. These three roles: dedicated science, cross-facility science and bridging science are all key roles for MSE in the 2025+ landscape.

3 Science synergies with other facilities

Fig. 1a,b,c & d provides a comprehensive summary of the upcoming facilities (taken from https://asgr.shinyapps.io/ganttshiny/) and with arguably optimistic timelines. All of these ongoing and upcoming imaging facilities have the potential for significant scientific complementarity. In MSE-highz-SRO7 we highlight some of those synergies pertaining to Cosmology experiments, transient surveys, and radio surveys with a key focus on LSST, Euclid/WFIRST and SKA in particular.

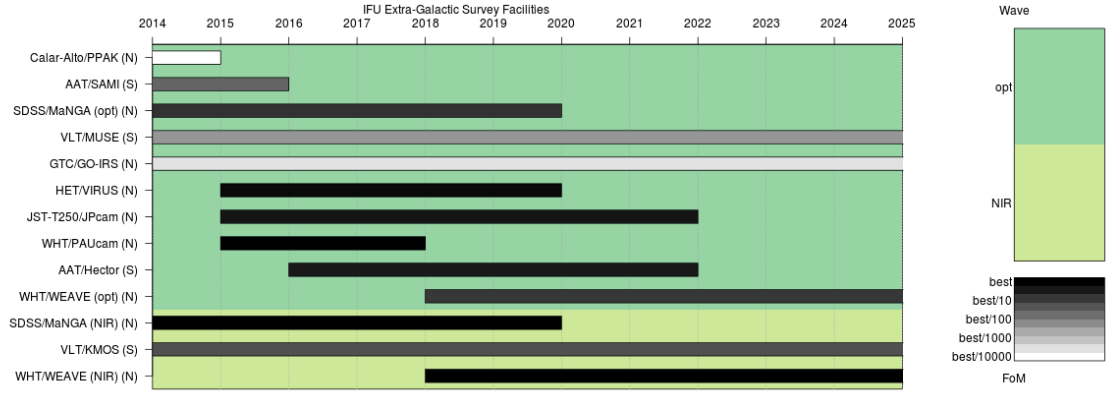

Figure 1: (a) Gantt-Chart comparing various extra-galactic IFU survey facilities that will operate between now and 2025. Figure of merit (FoM) is calculated using $\text{Area.FoV.N}_{\text{fib}}/(\text{FWHM}^2)$. FoM shading is scaled within a wavelength subset.

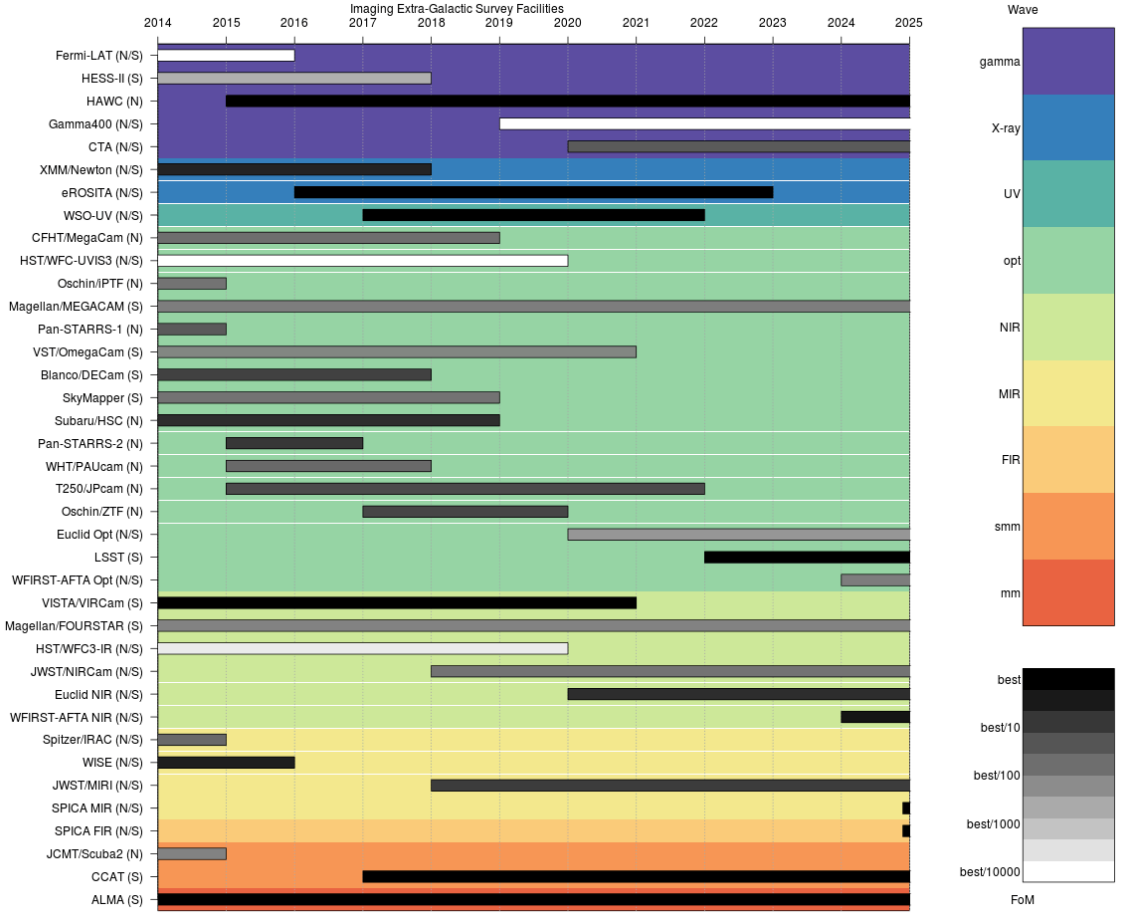

Figure 1: (b) Gantt-Chart comparing various extra-galactic imaging survey facilities that will operate between now and 2025. Figure of merit (FoM) is calculated using $\text{Area.FoV}/(\text{FWHM}^2)$. FoM shading is scaled within a wavelength subset.

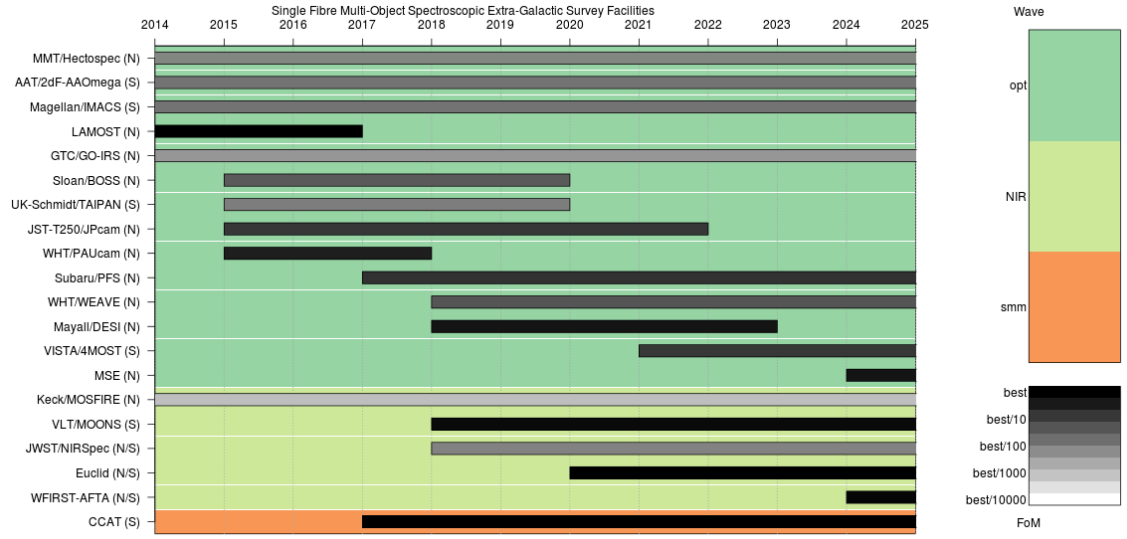

Figure 1: (c) Gantt-Chart comparing various extra-galactic spectroscopic survey facilities that will operate between now and 2025. Figure of merit (FoM) is calculated using $\mathrm{Area.FoV.N_{fib}/(FWHM^2)}$. FoM shading is scaled within a wavelength subset.

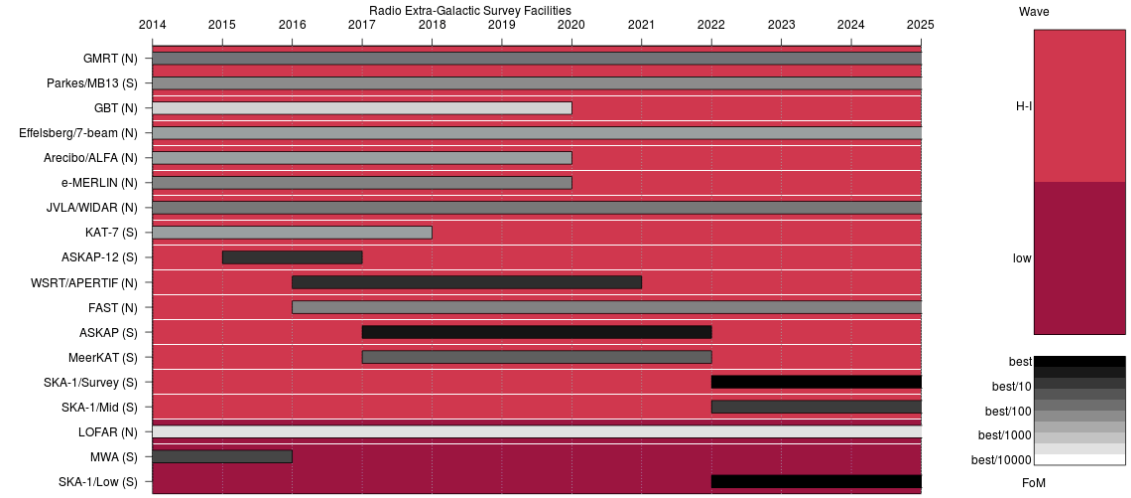

Figure 1: (d) Gantt-Chart comparing various extra-galactic radio survey facilities that will operate between now and 2025. Figure of merit (FoM) is calculated using $\mathrm{(Area/T)^2.FoV/(FWHM^2)}$. FoM shad- ing is scaled within a wavelength subset. 'H-I' corresponds to facilities able to observe H-I in the local Universe, i.e. they can observe at frequencies as high as 1.4 GHz.

Finally on Figure 2 we highlight the survey footprints of a two key surveys LSST and Euclid with other notable wide-area spectroscopic campaigns shown. Also highlighted is a possible survey footprint for MSE-highz-SRO1 our largest area survey. Figure 2 in particular highlights the need to stay firmly connected with the key complementary facilities to maximize science return.

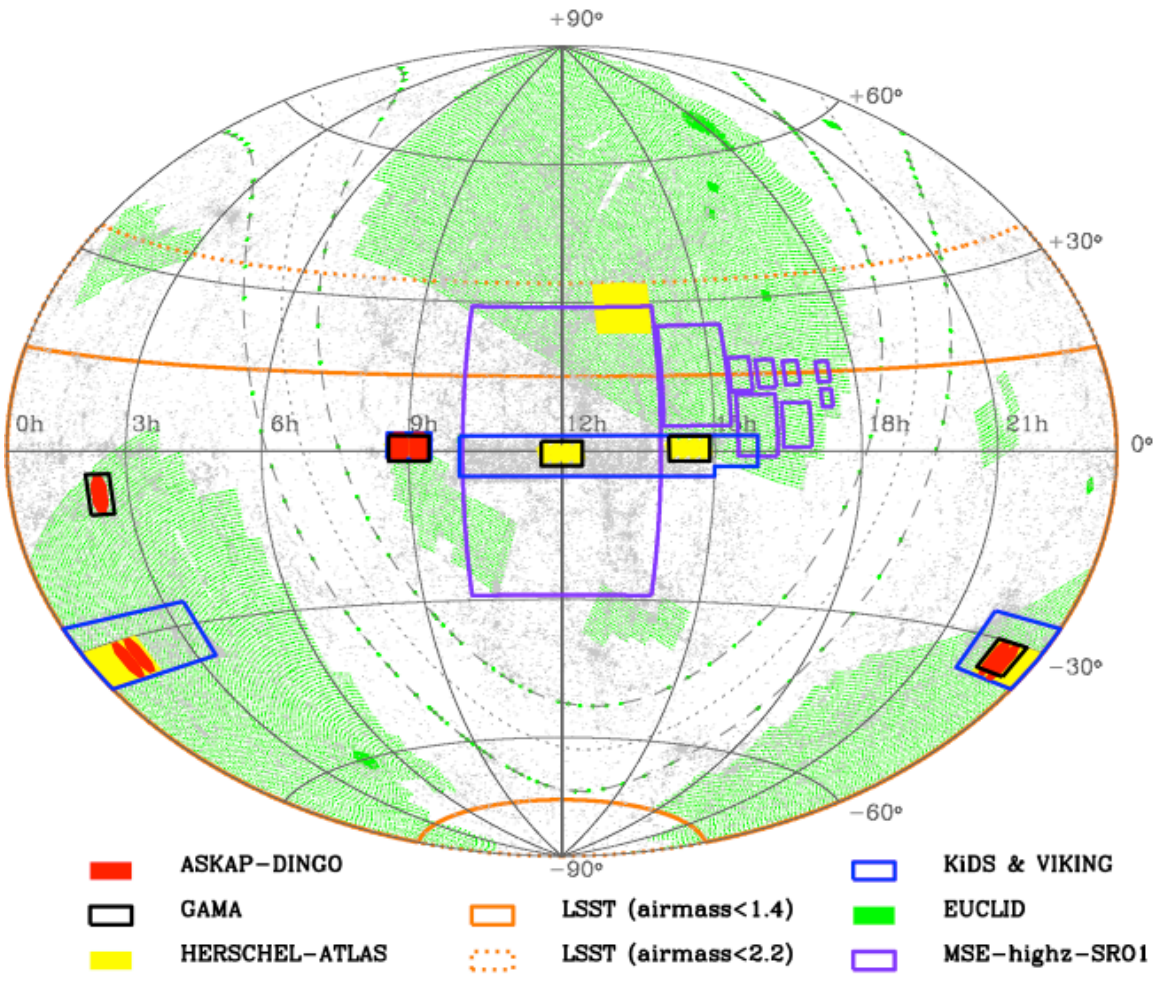

Fig. 2 The currently proposed survey footprint of Euclid and LSST along with main MSE survey we are proposing MSE-highz-SRO1. Also shown are the survey footprints from GAMA, VST KiDS/VIKING, Herschel-Atlas, and the ASKAP Deep Fields (DINGO). Watching these footprints will be critical to maximize the synergies. Note that the Euclid footprint is subject tp change and the WFIRST and SKA footprints are yet to be declared. However it is highly likely the SKA deep fields will lie away from below the equator in the KiDS/VIKING region.

4 Competition

As stated in Section 2 MSE will be out-performed as a standalone cosmology experiment, this is mainly because tracer density, low-mass tracers, high-S/N tracers, and spectroscopic tracers are not critical. DESI very much leads the state-of-the art in spectroscopic surveys spanning several thousand square degrees to faint flux levels, essentially sampling a significant portion of the observable Universe to $z \sim 1.5$. Beyond this redshift EUCLID and WFIRST become the dominant facilities using near-IR photometric redshifts and sample sizes into the many tens of millions. Again MSE, while able to contribute, does not represent a competitive (i.e., Level 4esq) cosmology experiment in its own right. Outside of Cosmology the most competitive facilities for studying galaxy evolution will be Subaru's PFS and ESO's VLT MOONS facilities (with

ESOs 4MOST and the AAT AAOmega facility somewhat further behind, predominantly limited by the 4m aperture of VISTA and the AAT). However this does mean easy low-hanging fruit are within reach of these facilities and will in all likelihood be plucked prior to MSE operations (see timelines indicated in Fig. 1, upper right). There is no doubt the larger MSEs aperture the more unique the facility becomes and moving from 10m to the 12-15m class would be clearly beneficial in setting MSE apart. It is also worth noting the wavelength coverage offered by both Subaru and MOONS, with coverage from 300nm to 2.5micron becoming achievable within a single facility, such as exemplified by ESOs 3-beam X-shooter. A further key advantage for MSE is its intended mode of operation as a dedicated survey facility. Both PFS and MOONS will have to compete with other instruments/survey teams for telescope time, effectively limiting the ambition of the surveys which they can conduct. Finally the Square-Kilometer Array will provide gas and gas dynamical measurements, as well as redshifts (for HI rich systems) suggesting that MSE needs to focus on science beyond redshifts, and resolving the wealth of information uniquely contained within the optical near-IR spectral range, i.e., high-S/N spectroscopy.

5 Key capabilities for MSE to deliver transformative science

(1) Aperture. A 12-15m class would be optimal to conduct unique science beyond Subaru and VLT, best compliment LSST and Euclid and best bridge the 8m to 30+m gap as a feeder facility.

(2) Wavelength coverage, ideally 300nm-2.5micron (as now demonstrated by ESO's X-shooter facility), to allow the maximum number of spectral features to be followed over the broadest possible redshift range. There is no obvious cutoff, however 1.3μm, 1.8μm an 2.5μm essentially opens science to $z<1.5$, <2, and <2.5 respectively (probing all of the main optical emission lines features at each epoch). With the peak of star-formation and AGN activity at $z\sim2$-2.5 the 2.5micron option is most desirable.

(3) Fibre-density. For our most ambitious survey (MSE-highz-SRO1) the survey speed scales directly with fibre-density, with the higher the better up to ~3000-5000 per sq degree. Higher-density also better overcomes fibre-collision bias, a serious concern for clustering and cluster studies.

(4) Field-of-view. There is no direct constraint on field-of-view. 1 degree represents a likely desirable minimum field-of-view to achieve a total fibre number of order 5000.

(5) Synergy. MSE should consider carefully any Dec limits. Given both LSST and SKA are southern hemisphere based facilities, the ability to reach to declinations of -40 is desirable, as this would ensure MSE can cover the likely location of the SKA deep-fields.

Finally a key aspect we hope we have emphasised is the need to have close communications with the key imaging facilities, and in particular: LSST, Euclid, WFIRST, the SKA.

		SRO-1	SRO-2	SRO-3	SRO-4	SRO-5	SRO-6
Mirror Size	**10m (nominal)**	All science viable	Viable	All science viable	All science viable	Science viable	All science viable
	12+m	x1.2+ speed increase	x1.2 speed increase	x1.2+ speed increase	x1.2 + speed increase	increase in science quality	x1.2+ speed increase
FoV	**1.5 deg (nominal)**	All science viable	Viable	All science viable	All science viable	All science viable	All science viable
	2+ deg	No enhancement (for similar fibre density)	No change	No enhancement (for similar fibre density)	Fewer pointings needed	No change	No enhancement (for similar fibre density)
Fibres	**3200 (nominal)**	All science viable	Viable	All science viable	All science viable	All science viable	All science viable
	5000	x1.6 speed increase	x1.6 faster	Increase in either simultaneous FOV coverage or target volume for 2<z<2.5 galaxies	No enhancement	No change	Increase in either simultaneous FOV coverage or target volume for 2<z<2.5 galaxies
Fibre size	**1" (nominal)**	All science viable	Viable	All science viable	Decreased flux calibration/throughput	All science viable	All science viable
	2" -> 3"	Better throughput for extra-galactic sources	No change	Better throughput for extra-galactic sources/inceased fibre collisions	Better flux calibration/throughput	Limits severely the project	Better throughput for extra-galactic sources/inceased fibre collisions
Fibre type	**Single fibres (nominal)**	All science viable	Viable	All science viable	All science viable	Science viable	All science viable
	IFUs available	More efficient for close-clustering	Beneficial for z<0.3 galaxies with opportunities to recover Z gradients etc.	More efficient observations of closely separated galaxies around high-z sightlines	Gravitational lens science	Best option : bundle with 19 fibers	More efficient observations of closely separated galaxies around high-z sightlines
Spec start	**380 nm (nominal)**	All science viable	Viable	IGM tomography/Lyman-a line modelling can only be probed at z>2.125	All science viable	Science viable	IGM tomography/Lyman-a line modelling can only be probed at z>2.125
	300 nm	Ly-a observed at lower z	Opportunity to observe metallicity lines at lower redshift and pick up Lyalpha earlier.	All science viable (360nm requirement)	Increased redshift range for key science (to z>1)	Limited science	All science viable (360nm requirement)
Spec end	**1300 nm (nominal)**	Surveys S1-S7 viable	Viable	All science except gas-phase metalicities	Reduced redshift range for key science (to z<1.7)	OK	All science except gas-phase metalicities
	1800 nm	Surveys S1-S8 viable	propsect to probe to higher redshifts.	All science viable	Reduced redshift range for key science (to z<2.7)	Optimal	All science viable
	2500 nm	Surveys S1-S9 viable	No change	All science viable plus Ha and NII measurements for 2<z<2.5 galaxy sample	Optimal redshift range for key science (to z<4)	OK	All science viable plus Ha and NII measurements for 2<z<2.5 galaxy sample
Spec res	**R2000 (nominal)**	All science viable	Viable	Cannot probe IGM metal contet or individual absorbing/galaxy matching	All science viable	limited science	Cannot probe IGM metal contet or individual absorbing/galaxy matching
	R5000 (nominal)	All science viable (no enhancement)	Improved line measurements	All science viable	All science viable	Best option	All science viable
Synergies	LSST/HSC (e.g. optical deep photo-z selection)	Vital for S1-S9	Vital	Vital for all science	Vital for spectrophotometry and time sampling	vital	Vital for all science
	Euclid/WFIRST (e.g. NIR deep photo-z selection)	Vital for S8-S9	Optimal	Improved stellar mass measurements for M-Z relation	Extra science	vital	Improved stellar mass measurements for M-Z relation
	SKA	Significant science enhancement S1-S5	Extra science	No enhancement	Extra science	can help in selection of targets	No enhancement

Evolution of galaxies, halos, and structure over 12 Gyrs

Tag: **MSE-highz-SRO1/ MSE-lowz-SRO1**

Lead: **Aaron Robotham,** Michael Balogh, Luke Davies, Simon Driver, Carlo Schmid, Yue Shen

1. Abstract

Here we propose an ambitious design of nine photo-z selected survey cubes that will allow MSE to measure the build up of large scale structure, stellar mass, halo occupation and star formation out to z = 5.5. By targeting (300 Mpc/h)^3 boxes, each volume will measure "Universal" values for an array of potential experiments.

At low redshift we will directly observe halo abundances below 10^{12} $M_{\odot}$, which means we can measure the occupation of halos and their abundance over a four decade range in halo mass, accounting for the majority of stellar mass in the low-redshift Universe. At higher redshifts our survey volumes will trace the transition from merger-dominated spheroid formation to the growth of disks, covering the peak in star-formation and merger activity.

This combination of depth, area and photo-z selection is not possible without a combination of LSST and MSE. As such, MSE will be able to produce the definitive survey of structure, halos and galaxy evolution over 12 billion years. With the nominal design of MSE these proposed surveys will take ~7 years to observe.

2. Science Justification

Current surveys that span the low ($z < 0.3$, e.g. GAMA/SDSS), moderate ($z \sim 1$, e.g. zCOSMOS, Lilly et al 2007) and high redshift ($z > 3$, e.g. VVDS, Le Fevre 2013) Universe come from hugely different telescopes. At low redshift the extra-galactic field is dominated by the Sloan Telescope and the Anglo-Australian Telescope (2.5/4m, FoV ~ 3/2 deg) and at higher redshifts a mixture of large facilities dominate (8+m, FoV << 1 deg). Low and high redshift surveys also tend to target photometric data from different facilities. Historically, co-moving volumes for high redshift surveys are tiny (comfortably dominating the error term for any 'Universal measurement') and tend to be high incomplete. In particular, surveys that use Ly-α to obtain redshifts have very poor velocity accuracy (due to the complex nebula component) and only probe a minority of available galaxies within a survey volume (~20%, VVDS, Le Fevre 2013). By designing a suite of surveys with equal co-moving volumes from low redshift ($z \sim 0$) to high redshift ($z \sim 5.5$) MSE will definitively answer a host of science questions over 12 Gyrs in look-back time.

The critical dark matter halo mass range in terms of stellar mass content is the decade around $10^{12}M_{\odot}$ (see **left panel** of Figure 1). This halo mass range contains our own Milky-Way halo and that of our nearest large spiral galaxy M31. To investigate galaxies in their most common environment requires an ambitious experiment. To robustly detect groups with a low false-positive rate we require at least 5 galaxies to be observable within a group/halo, and to measure dynamical halo mass within a factor ~3 accuracy requires 10 or more galaxies to be observed within a group/halo (Robotham et al 2011). Also, to obtain reasonable number statistics for rare massive clusters/halos a large volume of the Universe must be surveyed. If these science cases are combined to coexist within the same volume (both sky coordinates and redshift window aligned) then we require a large sky area and a robust photo-z selection in order to improve the efficiency of the volume overlap. Without a photo-z selection (i.e. only an apparent magnitude selection) we would naturally find more massive clusters at higher redshifts only, and we would have a comparatively small volume that contains the full

range of $10^{12}M_{\odot}$ - $10^{15}M_{\odot}$ halos (see Figure 16 in Robotham et al 2011). Also, without a photo-z selection it becomes extremely inefficient to sample faint galaxies at low redshift, with fainter apparent magnitudes naturally pushing the peak in the n(z) distribution to higher redshifts.

With this aim in mind, and with the knowledge that such a study opens up a large suite of complementary science such as ultra-large dynamic range close-pair and halo occupation distribution (HOD) studies (see Robotham et al 2014), we have designed an ambitious survey that only MSE is reasonably able to conduct on a sensible timescale (~7 years). The basic goal is to observe 3,200 sq deg of the Northern extra-galactic sky (overlapping fully with the proposed LSST survey region and substantially with the current SDSS footprint) between redshift 0 and 0.21 and down to a limiting magnitude of i_{AB}=25.3 selected from LSST standard depth multi-year survey. To efficiently probe down to low mass halos it is advantageous to observe as large an area as possible, and 3,200 sq deg over the suggested redshift extent minimally contains a 300x300x300 Mpc/h co-moving cube. This means our volume is large enough that we reach Universal homogeneity in all three dimensions (Srimgeour et al 2013, Driver & Robotham 2010). By observing to i = 25.3 within z = 0.21 we expect to be deep enough that essentially all $10^{12}M_{\odot}$ mass halos are both detected and have a reasonable mass estimate, with 10 or more galaxies identified (see RHS of Figure 1).

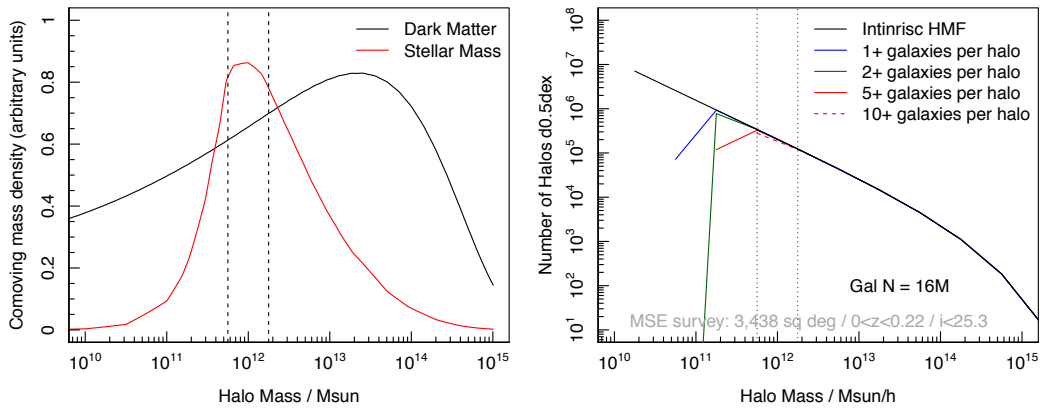

Figure 1: **Left panel** presents the distribution of dark matter and stellar mass as a function of halo mass. It is clear that we expect it to be highly dominated by $10^{12}M_{\odot}$ halos. **Right panel** presents the expected galaxy occupation frequency as a function of halo mass. Our proposed survey will sample the $10^{12}M_{\odot}$ halo mass regime with better than 5 galaxies per halo, allowing for per-halo dynamical mass measurements.

By repeating the basic survey design (in particular the target volume) for this low redshift HOD and halo abundance focused science case, we can open up a new suite of science. Figure 2 shows a basic possible observing strategy, where a co-moving 300 Mpc/h cube is targeted in nine separate redshift windows using a mixture of LSST photo-z selection (S1 to S7) and Euclid photo-z selection (S8 and S9). Each survey region proposed would be targeted down to a different i/Y-band limit but with ~100% completeness within each volume (certainly better than 95%, i.e. ~SDSS). Such a suite of surveys allows detailed halo occupation modelling out to z = 5, spanning the rapid increase and slow decline in universal star-formation (top panel Figure 2), the era of merger dominated mass build-up (z > 2), the transition into galaxy disk formation and in-situ star-formation dominating build-up (z < 2) and the epoch of rapid large-scale structure formation (z > 2). For obtaining robust 'Universal values' for merger rates and star formation history the co-moving volume analysed and the stellar mass depth observed is key. By selecting common 300 Mpc/h cubes we will have sub per-cent sample variance independent of look-back time. By aiming to be complete to stellar masses at least 1 dex below M* for S1 to S4 we can definitely explore the interplay between mass build up through merger and star formation (see Robotham et al 2014 for a z=0.2

version of this experiment). Beyond this range we are limited by the high quality photo-z i < 25.3 sample provided by LSST. Despite this, we can still probe the dominant component of stellar mass (M*) and its halo occupation distribution out to z = 2 with S5 and S6. This takes our galaxy evolution analysis out to 10 Gyrs in consistent co-moving volumes that have high statistical quality.

New survey possibilities are opened up if MSE has a spectral range covering 380-1800 nm or even better 380-2400 nm (rather than the nominal 380-1300 nm). Importantly OII becomes visible out to z = 5.4 (at 2400 nm), i.e. it becomes a common emission feature that S1 to S9 can all observe, offering a consistent star-formation tracer over 12 Gyrs from a single facility. If we have access to Ly-α and OII then direct measurements of the feedback of gas into the inter-stellar medium is possible. With the shorter spectrograph range this experiment could only be conducted in S7. With the extended range this direct fuelling can be measured for S7, S8 and S9. We will also be able to observe Ha, and construct a full BPT diagram out to z = 2/2.5 (i.e. S1 to S6/S7) with an extended spectrograph range (1800/2400 nm).

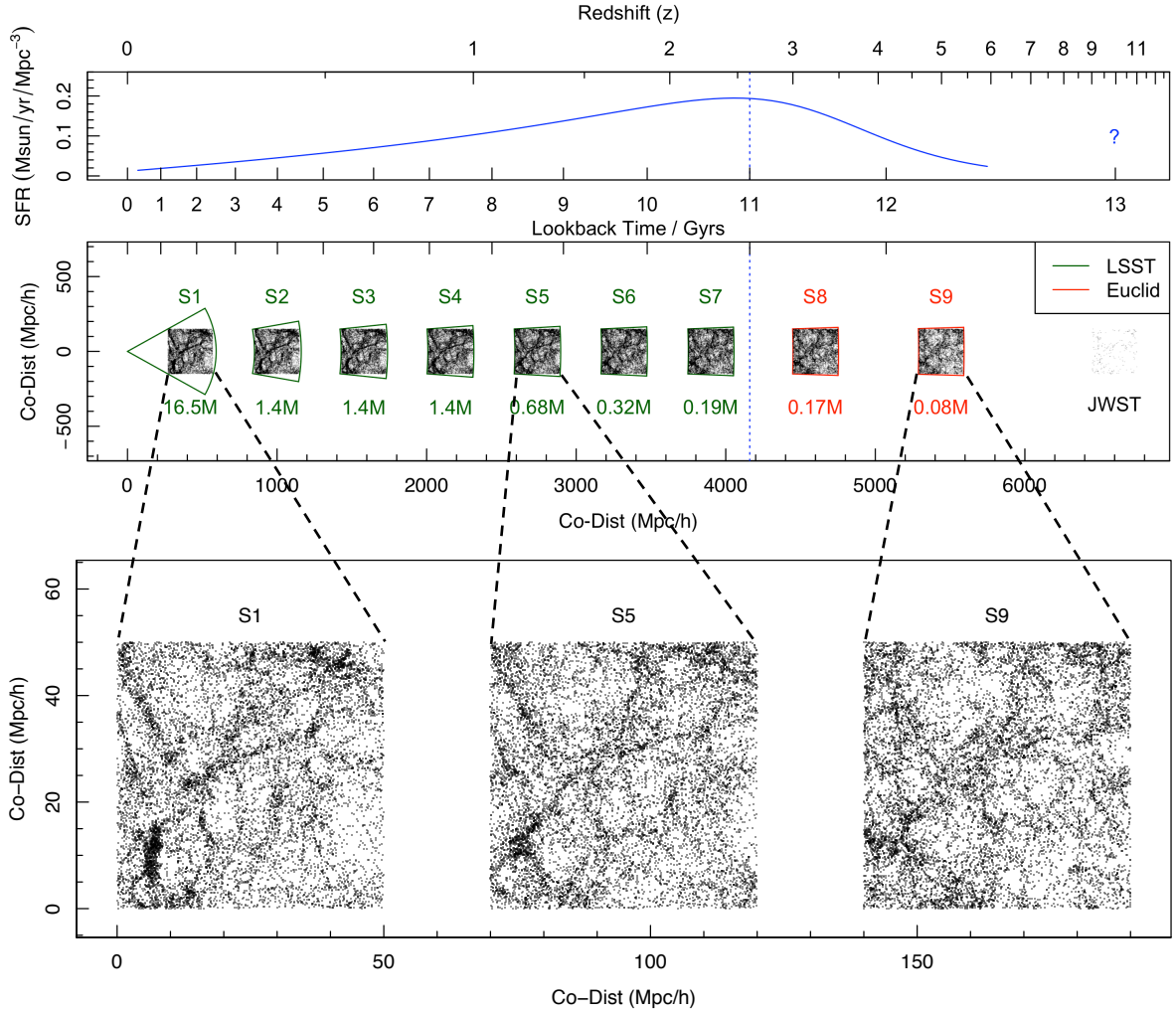

Figure 2: The proposed range of equi-comoving MSE survey cubes (S1 to S9). The top panel shows the cosmic SFH from Hopkins & Beacom 2006. The middle panel shows the proposed surveys. The bottom panel shows enlarged versions of the growth in large-scale structure in TAO simulated (50 mpc/h)^3 survey cubes for S1, S5 and S9 redshifts. The irregular spacing for S8 and S9 is required to avoid the strong sky absorption features, see Figure 3 for details.

It is clear that such a survey suite opens up a vast amount of science that is not accessible to any other facility. A non-exhaustive summary is given below, where we will:

- Measure halo occupation (through group finding) below $10^{12}M_{\odot}$. This combined with an HOD analysis will definitively uncover the interplay between stellar mass and halos, and will put any detailed study of individual halos (e.g. future MilkWay and M31 "archeology" studies) into a proper cosmological context.
- Directly observe the evolution of the massive end of the halo mass function out to redshift 1 (half the age of the Universe). This is step beyond cluster count cosmology, and will be conducted with a homogenous selection with LSST (the selection function is one of the major limitations of current cluster cosmology work).
- Study the evolution of the large-scale structure and cosmic web out to $z = 5$ with a consistent galaxy tracer with homogenous bias.
- Study the merger rate and star-formation history for all galaxies down to M*/10 (covering the converged majority of stellar mass) out to $z = 1$.
- Study the close clustering and merger rate of massive galaxies ($10^{11}M_{\odot}$) out to $z = 5$.
- With photometry from LSST we will be able the majority of the stellar component of the cosmic spectral energy distribution (CSED) out to $z = 2$.
- Together with other next generation telescopes (most significantly LSST, Euclid, WFIRST, SKA, 30+m telescopes) we these surveys will have a vital role in:
    - Measuring morphological evolution to $z = 1$
    - Studying the interplay between gas, dust, stars and environment
    - Providing IFU targets for 30+m telescopes for well understood samples at multiple epochs
    - Offering the sample superset for high S/N observations of individual galaxies in order to ascertain the evolution of metals through cosmic time.
- Especially at higher redshifts, exciting work looking at the clustering of AGN is viable. This would naturally be a subset of the proposed surveys, but extended AGN focused science cases could be constructed and incorporated into the nominal design.

The main competition to MSE in doing such a combined survey is Subaru-PFS (Takada et al 2013) and VLT-MOONS (Cirasulo et al 2012). PFS will have a spectral range 380-1300 nm but in many other respects will have similar capability to MSE. It will nominally be conducting $z < 1$, $i < 21.5$ and $1 < z < 2$, $i < 23.9$ photo-z pre-selection surveys (based on shallower HSC data). In both regimes the surveys discussed here are at least a magnitude deeper (a factor ~3 in stellar mass) and over much larger areas (fixed 16 sq deg for PFS, 400 to 30 sq deg over the same range for MSE. The huge advantage of MSE compared to all of the proposed PFS surveys is that we will be extending to the scale of homogeneity in all three dimensions. For many of the science cases laid out here (and foreshadowed on a smaller scale by PFS) the definitive measurement will be made by MSE, with no further appreciable improvements to be made by moving to larger survey volumes (since many extra-galactic measurements are dominated by sample variance not Poisson statistics of the sample itself).

Regarding potential competition, VLT/MOONS will have a spectral range 680-1800 nm and is focusing on surveys at $z > 1$. Where MSE has a potentially huge advantage is the LSST and Euclid/WFIRST photometric source catalogues. These telescopes will only become available post 2020, and offer a paradigm shift in optical quality. In particular, using LSST allows us to conduct surveys S1 (3,200 sq deg) to S7 (22 sq deg) with identical photometry and photo-z technique. Such homogeneity will improve the robustness of almost every type of analysis made. Given the fast survey speed of MSE, once LSST and Euclid data become available no other facility will be able to keep up with the observing speed of MSE, i.e. it will dominate the next generation of spectroscopic surveys from $0 < z < 6$.

Robotham, 2011, MNRAS, 424
Robotham, 2014, MNRAS, 444
Srimgeour, 2012, MNRAS, 425
Le Fevre, 2013, A&A, 559
Driver, 2010, MNRAS, 407
Hopkins, 2006 ApJ, 651
Lilly, 2007, ApJS, 172
Cirasulo, 2012, arXiv, 1208.5780
Takada, 2013, arXiv, 1206.0737

3. Key astrophysical observables

For all clustering related experiments the core observation will be a redshift. This can be obtained through cross-correlation template fitting using auto-z (Baldry et al 2014) or similar. Value added products would be to get better signal-to-noise for star-formation features (Hα and OII) and for absorption features (Mg and Na). Broadly speaking our required spectral range is $372.7(1+z_{lo})$ to $372.7(1+z_{hi})$ [for tracing OII, our main driver]. Similarly we have $517.5(1+z_{hi})$ [for tracing Mg-b] $589.4(1+z_{hi})$ [for tracing Na] $(656.4*(1+z_{hi})$ [for tracing Hα].

The nominal range of 380-1300nm for MSE is adequate for a large amount of HOD related science (see Figure 3), allowing Hα measurements out to z=1 (S4) and Mg-b absorption out to z=1.5 (S5). For robust redshifts for non-emission galaxies the presence of C-K and g-band (i.e. the 400 nm break feature) is probably a sensible minimum requirement, meaning we can do reasonably unbiased HOD target selection and analysis all the way to an upper limit of z = 2 with the nominal design. This is within the regime of interest, and allows for a possible analysis of the interplay between merging and star-formation at z = 2 (S6). If the spectrograph is extended out to 1800 nm (i.e. H-band limit) then OII (and H-K and g-band) is visible out to S8 (z = 3.5), allowing high fidelity velocity measurements (and therefore HOD analysis, at least for massive halos) for S1 to S8. High quality OII redshifts are only possible in S9 if the spectrograph range is increased to 2400 nm (i.e. K-band limit). It should be noted that the regular spacing of S1 to S7 could not be continued for S8 and S9 because the important OII line becomes highly attenuated by the sky, even at an excellent site such as MSE on Mauna-Kea. The S8 and S9 volumes were therefore adjusted to optimally sit within the H and K bands respectively. By some cosmic conspiracy a 300Mpc/h LoS baseline almost exactly fits within these two bands.

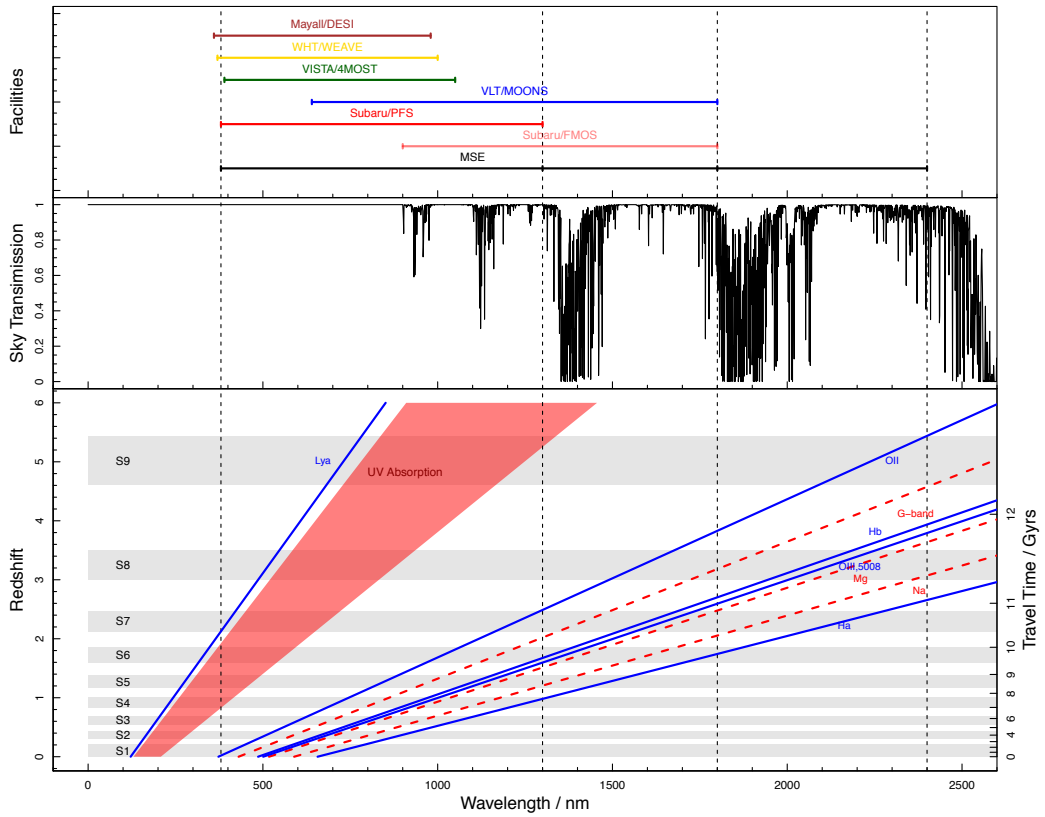

Figure 3: Accessibility of different spectral features for the different proposed volumes. The nominal 380-1300 nm MSE limit is shown as vertical dashed lines, with proposed extensions at 1800 and 2400 nm (H and K band) also displayed. S1-S7 via the OII line are still viable with a 380-1300 nm facility, but S8 and S9 are not viable).

For redshift measurements the key requirement is velocity accuracy. Pragmatically, a velocity accuracy that is within the typical velocity width of individual galaxies is appropriate. With moderate (R~ few thousand) resolution we can expect to obtain a velocity accuracy of a few 10s km/s, where no more than 30 km/s is ideal. $10^{11/12}M_{\odot}$ halos have typical velocity dispersions of 100/200 km/s, and with 10 galaxies in a group we would expect relative velocity dispersion errors of 10% / 5% respectively, which is perfectly adequate for the more stringent group finding and halo occupation analysis requirements. It is not worth attmpeting to get much higher velocity accuracy because the internal dispersion of even a $10^{9}M_{\odot}$ galaxy is ~100 km/s, so velocity accuracy rapidly becomes limited by the complex internal kinematics of galaxies, not the spectral resolution. OII will provide a good estimate of the systemic galaxy velocity for all nine surveys, and Ha will also be an excellent velocity measure where available (to S4/S6/S7 if the spectrograph limit is 1300/1800/2400 respectively). Ly-α is a complex feature that contains high velocity nebula components and severe self-attenuation, so group finding (and associated halo science) based on Ly-α alone is likely to be highly compromised.

To extract the useful information for the data (i.e. redshifts) we would expect to require a basic reduction and then we would run auto-z (Baldry et al 2014) or similar. This is a proven technique for extracting redshifts via absorption or emission lines, and does not rely on good flux calibration or continuum templates. This is a proven process from the GAMA survey, and should work equally well on MSE data given we will be operating in a similar S/N regime.

A successful redshift measurement requires good continuum S/N in the rest-frame optical regime (i.e. S/N of a few). From experience with GAMA, this is typically adequate to extract robust redshifts with a feature cross-correlation fitting code (auto-z, Baldry et al 2014). We expect to be able to obtain emission line equivalent widths and associated star formation rates with data of this quality. We would expect to be able to measure reasonable Ha derived star formation rates (which have higher S/N and are usually more robust than OII derived rates) from S1 to S4/S6/S7 if we have a 380 to 1300/1800/2400 nm spectrograph range. These are also the survey limits in which we can plausibly construct a full BPT diagram to separate AGN/LINERS/star-forming galaxies. Such a division increases the scientific quality of the survey because AGNs and LINERS can otherwise be a strongly contaminating population for any star-formation measurement.

4. Target selection

Table 1 specified the major characteristics of the required surveys. S1-S7 will use a LSST defined survey selection. LSST is being designed to produce robust photometric redshifts for $i < 25.3$ out to $z = 2.5$ and over the entire visible sky, so this comfortably covers the proposed area of S1 (3000+ sq deg) and the redshift limit of S7. For S8 and S9 a Euclid or W-FIRST photo-z selection would be required, using the proposed deep surveys. These are nominally of the required depth, although it is uncertain where on the sky they will be placed. Clearly it is vital they are visible to MSE, since this is the only plausible source of photo-z optimized targeting for S8 and S9. For S2-S7 it is possible that a similar selection could be made using photo-z from the Subaru HSC surveys, but S1 is substantially larger than the proposed HSC fields. Having uniform photometry throughout is optimal, so LSST-based input catalogues for all of S1-S7 is preferable.

Survey	z low	z high	Area / deg^2	Vol / Gpc^3	Photo	Selection	SM lim / $M_\odot$	Gal N (M)	Fibre H (M)	Passes
S1	0	0.214	3233.8	0.0674	LSST	i<25.3	$5x10^7$	16.5	5.7	2.8
S2	0.305	0.435	398.6	0.0399	LSST	i<22.5	$5x10^9$	1.4	0.1	2
S3	0.547	0.695	143.17	0.0345	LSST	i<24.0	$5x10^9$	1.4	0.8	5.4
S4	0.83	1.004	72.792	0.0322	LSST	i<25.3	$5x10^9$	1.4	6.1	10.7
S5	1.171	1.383	43.921	0.031	LSST	i<25.3	$3x10^{10}$	0.68	4	8.6
S6	1.591	1.858	29.347	0.0303	LSST	i<25.3	$1x10^{11}$	0.35	2.5	6.1
S7	2.126	2.472	20.982	0.0298	LSST	i<25.3	$2x10^{11}$	0.2	1.7	5
S8	3.001	3.496	14.906	0.0293	Euclid	Y<25.7	$2x10^{11}$	0.17	2.8	6
S9	4.607	5.43	10.877	0.029	Euclid	Y<26	$2x10^{11}$	0.09	2.7	3.6

Table 1: Main characteristics of the 9 proposed equi-comoving MSE survey volumes.

For S1 to S7 the limiting magnitude is never fainter than i = 25.3 (see Table 1 above, and left panel of Figure 4) for S8 and S9 the input comes from Euclid and/or W-FIRST. In these cases the limiting magnitudes are Y = 25.7 and Y = 26 respectively. It is plausible that LSST and Euclid/WFIRST could be encouraged to survey a region appropriate for S7, S8 and S9 even deeper, allowing an improved stellar mass limit of $10^{11}M_\odot$ throughout all nine survey volumes (approximate limits with current depths are shown in the right panel of Figure 4).

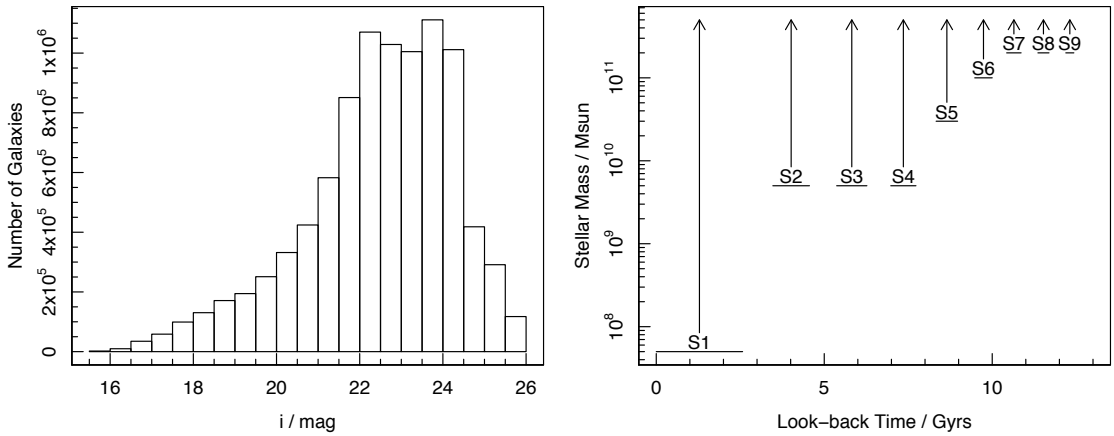

Figure 4: Left panel: Distribution of apparent i-band magnitudes for surveys (S1 to S9). Right panel: approximate stellar mass limits for all surveys as a function of look-back time.

The expected sources density is presented in Table 1. All surveys are effectively 2+ pass (assuming an MSE design of 3200 fibres over 1.8 sq deg). In practice S1 will have significant inhomogeneous structure meaning that where galaxies are targeted the true MSE tiling density is probably a factor of a couple greater. The main mechanism to speed the surveys up is therefore to increase the proposed number of fibres. Even if the number of fibres were doubled (and FoV kept static) the proposed suite of surveys would still make excellent and efficient use of the facility.

Being able to target close-pairs efficiently is a key requirement. With GAMA we found that even with ~1000 targets per square degree we required on average ~10 passes, with some regions obtaining 14 passes, to ensure we were not biased against close-pairs (part of the most important science case for the proposed surveys here). Being able to pack fibres closer than 10" would be hugely beneficial for the proposed surveys, since the number of passes will not actual approach the ~10 of GAMA (i.e. we know that a 2.8 pass average will not be sufficient for S1 if the fibre collision limits are similar to the AAT). The physical size of the MSE focal plane might alleviate some of the difficulty in close fibre positioning, but the design used (e.g. echidna) might introduce further constraints (there might be a hard limit on how many fibres can be close-packed due to patrol area limitations). Related to this, it may

be the case that using a small number of dedicated IFUs to target highly clustered regions could be the most efficient approach to obtaining redshifts. A detailed cost-benefit analysis would need to be made to answer this question using realistic sky simulations.

In total we are proposing to observe 22M galaxies over the nine survey cubes. There is, of course, scope to scale the surveys down, but there are clear scientific compromises to this. The survey volumes have been selected to guarantee the smallest contiguous volume that has obtained homogeneity in all dimensions (Srimgeour et al 2013, Driver & Robotham 2010). This means all measures of large-scale structure (fractal nature, halo abundance) and galaxy evolution (particularly cosmic star formation rate and merger accretion rate) can be directly interpreted as a Universal average. Similar studies over substantially smaller volumes by competing facilities (e.g. Subaru-PFS and VLT-MOONS) will be primarily limited by sample variance, which has been historically a huge source of uncertainty at high redshift. The photo-z pre-selection minimises wasted observations that are not within the windows of high interest, and hence LSST (and at higher redshift Euclid or W-FIRST selection) is vital. The photometric limits are such that beyond S2 we do not attempt to be complete below stellar mass $=5\text{x}10^9$ $M_\odot$ (see right panel of Figur 4). This takes us 1 dex below M* in the range of surveys where the limit is applied, which appears to be enough to ascertain the full Universal fraction of mass accretion through mergers (see Robotham et al 2014) since the integrated mass should be convergent in this regime. This sliding limit is applied for S2 to S4. For S5 and above it is not feasible to get down to such a depth given a hard photo-z pre-selection limit from LSST of i = 25.3, unless there is future deep-field coordination between MSE and LSST. In summary, the current design is the minimum in depth and volume required for the range of potential science outlined.

There is scope to drop entire survey cubes with the loss of potential science. For exploring entirely new parameter domains S1 and S9 are objectively the most compelling for their proposed depth and volume respectively. S8 and S7 are the next most compelling due to the paucity of contiguous volume surveys in these regimes. S5 to S9 collectively span the increase, peak and decline in star-formation, mergers, large-scale structure formation and quasar activity. They also cover the transition between turbulent clumpy star-formation to smoother disk growth mechanisms. For this reason doing all five of S5-S9 is highly compelling. S1 to S4 are the surveys that will have a consistent HOD analysis given their equivalent stellar mass limits (deeper in the case of S1). A case could be made for only doing a subset of S2/S3/S4, perhaps merging S2 and S3 into an intermediate volume. S4 in particular is expensive in terms of fibre-hours required (6.1m, the most of all surveys), but it does offer an 8 Gyr look-back timescale for the HOD science case (over half the age of the Universe), so from a galaxy evolution and halo evolution standpoint it is a more interesting survey regime than S2 or S3. Pragmatically, a merger between S2 and S3 would be the first option to consider, should the survey scale outlined be considered too ambitious for MSE.

We can make an approximate estimate to the total time to conduct all nine surveys using a few assumptions. If we assume MSE will have double the integration efficiency compared to VVDS (conducted using VIMOS an 8.1m VLT since 2003) then we approximately expect to obtain a redshift in T = 0.5 x 4.5^(i – 23), i.e. ~0.5/2/10 hours for i = 23/24/25 respectively. Using this rough estimate we can calculate the number of fibre hours required for each of the nine survey volumes (these numbers are given in Table 1). The distribution of i-band magnitudes is shown in the left panel of Figure 4, where it is clear that only a minority of sources are fainter than i=24, i.e. extreme integration times should be quite rare. In total our 22M objects will require 26M fibre hours (assuming efficient survey tiling, and that we do not integrate longer than required on sources). Assuming we observe for 100 dark/grey nights per year, for 10 hours a night and using a nominal 3,200 multiplex we have 3.2M fibre hours per year for the surveys (this assumes no survey inefficiency, simulations are required to

determine the true fibre placement efficiency). This means all nine surveys will take approximately seven years to complete. The main telescope-side speed-up that is possible is to increase the multiplex of MSE. If MSE has the same multiplex as DESI (5000 fibres) then the combined surveys will take 4.4 years to complete. A survey-side option is to reduce the number of surveys (as outlined above). A strong case can be made for **not** reducing the volumes or depths of the proposed survey volumes, so the first option to consider is whether a subset of the proposed S1 to S9 surveys could be merged. Another survey-side is to spread the RA baseline such that the surveys are observable across all available ~200 dark/dark-grey nights. This could speed up the survey campaign by a factor ~2 (i.e. all nine surveys will take 3.5 years) but at a serious cost to any other dark sky (particularly extra-galactic) science case.

A note on the higher redshift (S8 and S9) volumes: pure drop-out selected z ~ 5+ samples are highly contaminated from M-T dwarf stars and lower-z galaxies (z ~ 1 for z ~ 5 selections), where either saw-tooth-like dwarf stellar spectra or the 400nm break are identified consistently with the target Ly-α break. Ambiguity arises in these selections as they traditionally only observe in three bands (one short-ward and two long-ward of Ly-α at the target redshift, e.g. r/i/z for z~5), and simply aim to select sources with a strong continuum break and relatively flat-continuum - as expected for high-z sources where we are probing the UV-continuum region. With only a single colour in this continuum region it is difficult to differentiate true high-z sources from their low-z counterparts (see Stanway 2008 for a detailed discussion on contamination in high-redshift photometric selections).

However, with additional bands (specifically NIR from Euclid or WFIRST) selections can be improved to rule out such contaminating sources. For example, multiple NIR bands allow for a much more detailed analysis of the spectral slope long-ward of the break, allowing the removal of sources with non-flat spectral shapes. In addition, with high quality data out to K-band, we should be able to identify the 400nm break in high-z sources out to z=5.5 (between H and K). This will significantly improve the fidelity of our photo-z measurements and aid in the removal of contaminating sources.

5. Cadence and temporal characteristics

Repeat observations are not required for the proposed surveys.

6. Calibration Requirements

The wavelength calibration needs to be accurate to better than the desired velocity accuracy throughout (~30 km/s, for reasons outlined above). This is to ensure we do not have any systematic biases in our redshift distributions. The expectation would be to have pixel level or better calibration accuracy.

The main sky features will need to be either well subtracted or potentially (for stronger line) masked entirely. Experience from GAMA suggests that 1% sky subtraction accuracy is probably adequate for obtaining good redshifts.

For the core redshift science the spectrophotometric calibration does **not** need to be especially good. Getting Ha SFR from EW also does not require particularly good flux calibration (only relevant for the low-z HOD science case).

7. Data processing

Instrumental signatures (the major ones) will need to be removed prior to redshift measurements. Auto-z is fairly robust to poor flux calibration and even imperfect sky subtraction issues, but the wavelength calibration would need to be very good throughout. Potentially the exact wavelength calibration could be left as a variable within auto-z, but this is probably non-ideal, and likely to create degenerate solutions.

The zeroeth-order quantity we need from the data is the redshift. We expect to do this using a tool similar to auto-z (Baldry et al 2014). Higher order products, depending on the data quality (since these products will not drive the survey design), are potentially EW for various features. The expectation would be to do this via direct line summation or Gaussian fitting technique (e.g. Hopkins et al 2013). The primary requirement for all nine surveys is redshifts, with additional science made possible if spectral analysis is possible (potentially only for the brighter targets observed).

For the core HOD related science we require robust multi-band photometry (optical and NIR restframe ideally), and stellar mass estimates, for all targeted objects. Since we will be requiring photo-z to enable optimal pre-selection we should expect to have this information in place prior to redshifts being obtained. For various science applications it is possible to imagine further data being obtained (e.g. restframe UV, MIR, FIR and radio), but this is not a specific requirement for the core science cases. The most obvious source for such data over ~3,200 sq deg is LSST and Euclid/WFIRST. Other teams are responsible for producing the photometric data products for these surveys, but there may be an advantage (or even requirement) for MSE to be collaboratively involved with these teams at an early stage.

At a minimum we would expect to return sky subtracted, wavelength calibrated, but **not** flux calibrated, 1D spectra for each targeted object. We would also produce redshift measurements with quality estimates for each object.

8. Any other issues

How the surveys are distributed across the sky and how they are scheduled is a very serious issue that requires careful consideration. As shown in Figure 5, S1 is likely to be appropriately centred close to RA=180 and Dec=0. There is no strong science led reason to require S2 to S6 to overlap on the sky, so serious survey-speed gains might be possible if they are spread out over a large RA baseline. The big difference between traditional extra-galactic surveys (e.g. SDSS, GAMA, z-COSMOS) and the proposed MSE surveys is that they will be photo-z selected, so there is no particular observing gain through stacking them (wedding cake style) in overlapping parts of the sky. They are separated along the co-moving line-of-site such that even large-scale structure is barely associated between adjacently numbered survey volumes. At a minimum the fields should be spread over ~7-8 hours in RA (105-120 deg) to ensure the proposed surveys can be observed efficiently by MSE throughout a night (i.e. if all surveys shared the same central RA then the observing efficiency drops by a factor of a few, meaning the combined survey would take 20+ years).

A number of science cases could be made for placing S7 – S9 within the extent of a foreground field since they will contain extremely bright AGNs. A number of science cases can potentially make use of bright background AGN, e.g. as probes of the inter-galactic medium (IGM) at lower redshifts via the study of absorption features in the spectra of the distant AGN. S7 and S8 in particular are close to specifying the same survey requirements as the SRO concerning the 3D mapping of the IGM.

A lot of thought needs to go into the careful design of the survey regions, with consideration given the historic datasets in certain regions. This is particularly true for the UV and FIR, since this data will not be substantially improved for low redshift studies for a generation (the wide field GALEX and Herschel telescopes are now decommissioned). Thought must also be given to upcoming facilities. In the radio the SKA (based in South Africa and Australia) will be a game-changer for extra-galactic HI and continuum studies out to z = 1+ (current facilities observe to only z ~ 0.1). Clearly the SKA will be optimal for Southern hemisphere fields, and MSE will be located in the Northern hemisphere. To combat this any proposed fields should be close to the equator, making them reasonably observable by facilities in either hemisphere. It is also vital that MSE has some influence and involvement in the location of the future Euclid and WFIRST deep fields. If these are placed at declination below -40 deg then they become unviable for the MSE S8 and S9 volumes because the airmass at Mauna Kea is always poor. In general it is advisable that the MSE survey volumes avoid the ecliptic and Milk-Way plane (possible for S2-S9, see Figure 5) since this at least ensures shallow Euclid coverage with improved resolution compared to LSST.

In summary, a huge amount of coordinated effort is required if maximum science is to be extracted from the proposed MSE surveys.

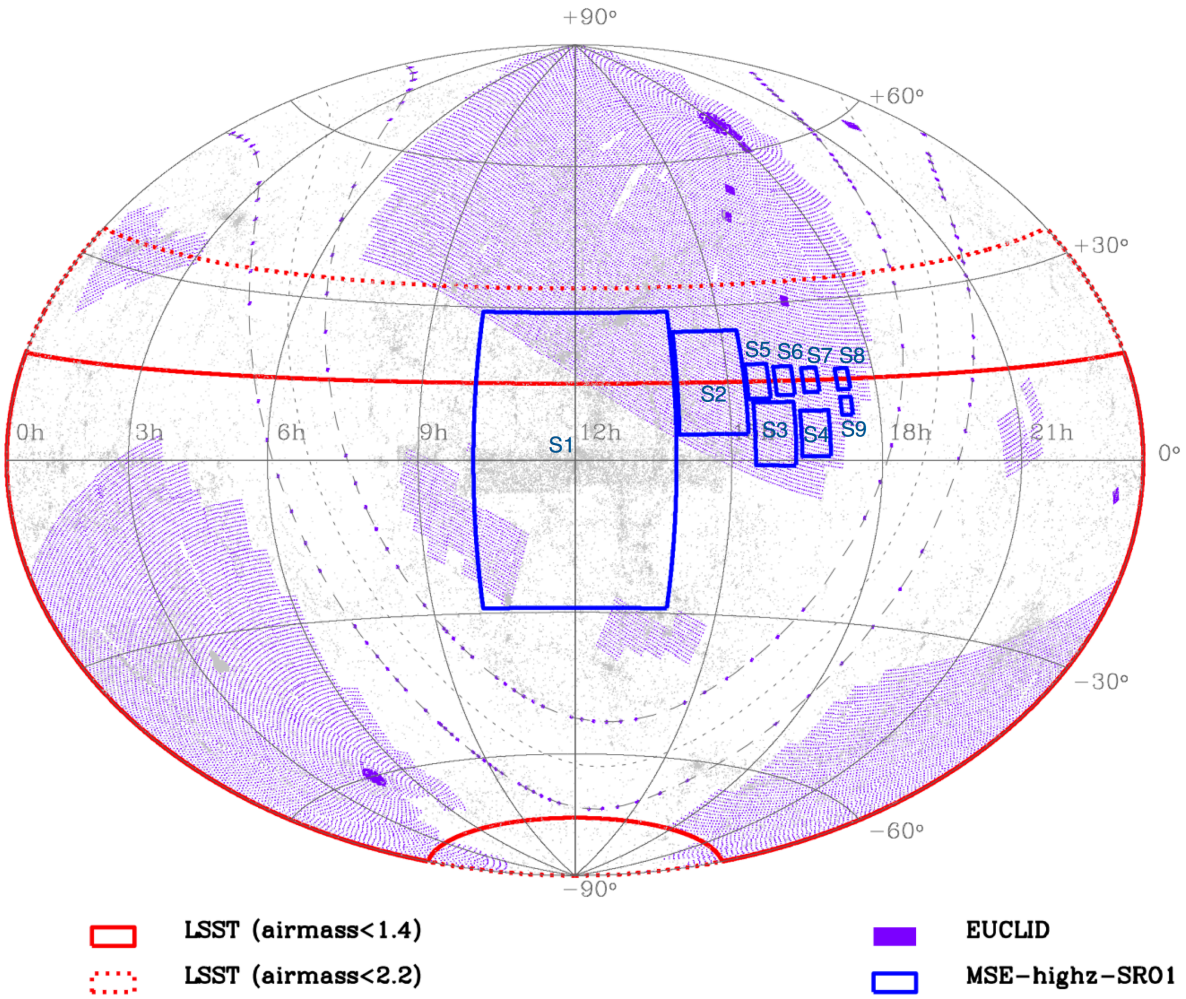

Figure 5: Straw-man locations for proposed S1 – S9 regions, that are visible from both Mauna Kea (+20 deg lat, MSE) and Cerro Pachón (-30 deg lat, LSST). The Milk-Way and Ecliptic can be seen as great circles of avoidance for the proposed Euclid shallow survey (purple). The distribution shown here is such that the proposed MSE survey volumes are only observable in one semester, but with a broad RA baseline allowing them to use full nights efficiently. A number of permutations for the survey design and sky distribution are possible, so effort must be invested into the optimal design of the MSE survey suite.

The size of fibres on sky is a potential issue. The nominal 1” fibre size is clearly optimised for expected point-spread-function at a good seeing site such as Mauna Kea. For extra-galactic work a fibre size of 2” (e.g. AAT) to 3” (e.g. SDSS and the VLT/KMOS IFU unit size) is considered optimal. Galaxy sizes become almost constant for $z > 1$ at ~2-3”, so all of S1-S9 would likely achieve better throughput with larger fibres (especially S1). Having a range of available fibre sizes would also be advantageous. Detailed study of the optimal fibre size distribution is required to fully assess this issue, since uniformly larger fibre size would have a certain negative impact on stellar focussed science.

There are still a significant number of unknowns that could seriously impact any future multi-epoch HOD focussed survey. The core requirement for the highest priority elements of the science case is for high completeness at all angular scales regardless of clustering on sky. How efficiently MSE can do this will clearly be a function of the intrinsic source clustering and the fibre placement technology. Any time estimates could be out by a factor of ~2 if the Universe and technology conspire to make high completeness on small spatial scales difficult. This is a complex issue to overcome, and will require detailed simulations to understand fully.

A mechanism for rapidly assessing whether any given target has a reliable redshift and can therefore be removed from the target list would be hugely beneficial to the survey. Such dynamic feedback would prevent time wasted increasing S/N beyond what is required for the core case. This would require a pipeline that can dynamically reduce, stack and redshift the individual short integrations (e.g. 20 mins) for each galaxy. Scheduling software that can cope with such dynamism (currently not an option at ESO survey facilities) would give MSE an appreciable advantage in the domain of extra-galactic surveys.

The chemical evolution of galaxies and AGN over the past 10billion years (z<2)

Tag: **MSE-highz-SRO2**

Lead: **Simon Driver,** Luke Davies, Bianca Poggianti

1. Abstract

We propose a high-S/N (S/N>30) spectroscopic study of carefully selected volume-limited samples from the present epoch to the peak of star-formation 10 billion years earlier. Each volume-limited sample should contain 10k galaxies uniformly spanning the broadest possible stellar-mass range, and in regular 1Gyr intervals (i.e., 10 volume-limited samples of 10k galaxies resulting in a total survey of 100k galaxies). The volume-limited samples could be selected either from photo-z catalogues identified by LSST, EUCLID or WFIRST, or from a redshift pre-survey of the selected regions (i.e, such as that proposed by MSE-highz-SRO1). Key requirements for this survey are high throughout (i.e., maximum aperture, 12+m), near-IR spectral coverage (extending as red-ward as physical possible, e.g., 2micron), but relatively low to modest resolving power (R~1000). Integration times are likely to extend up to ~50hrs for the faintest highest redshift systems. Hence, the full study will require 50-100 nights of observations (assuming a multiplex factor i.e., ~1000 targets per field-of-view), resulting in a legacy sample for multiple and diverse studies of the chemical evolution of galaxies and AGN.

2. Science Justification

The chemical evolution of galaxies and AGN over cosmic time, and in particular the gas- and stellar-phase metallicities, is a topic of significant current attention (e.g. Zahid et al. 2014, and references therein). Relatively strong evolution has been reported in the stellar-mass metallicity relation (Tremonti et al. 2004) from nearby samples to those close to the peak of cosmic star-formation history. See, for example, samples assembled by Zahid et al. (2013) and Figure 1. However, the sample sizes are relatively modest and arguably biased towards the highest star-forming systems at each epoch. This is because the selection is typically made short-wards of the 400nm break for the very high-redshift intervals, and as such probes only the most UV-bright galaxies. Locally we know that the specific star-formation rate, stellar mass, and metallicity form a fairly complex surface (e.g., Lara-Lopez et al. 2013a). Moreover gas-phase metallicity (usually the only measurement accessible in high-z surveys) is harder to interpret that the stellar-phase metallicity, as the former are very sensitive to recent infall and outflows. Ideally one would wish to study the sSFR-stellar mass-metallicity trifecta using both gas and stellar-phase metallicities, for representative populations at regular time steps. By assuming the earlier population evolves into the later population one can build up a complete picture of the global evolution of both the gas and stellar-phase metallicites over time, and the impact of both sSFR and stellar mass on metallicities (and vice-versa) at a range of epochs. The required infall and outflow models can then be determined through comparisons to simple analytic models, with potentially some additional constraints

coming from the comparison of the emission line-widths (sensitive to dynamics and outflows) to the absorption line-widths (sensitive to just the dynamics) using multi-Guassian line-fitting (e.g., McElroy et al. 2015). However, the measurement of stellar-phase metallicities, essential for such an analysis, require significantly higher-S/N spectra than are typically attained in surveys such as zCOSMOS, VVDS and Deep2 – being reliant on absorption rather than emission line measurements. Modelling of line-broadening through dynamics and outflows also requires significant signal-to-noise levels in the spectral features and for the features to be clean (i.e., away from night sky lines). As one pushes towards higher-redshift this later aspect becomes harder because of the preponderance of telluric features, etc. This can potentially be overcome by using UV metal-lines (e.g. Sommariva et al., 2012., and see Figure 2 which shows the drift of key spectral features with look-back time). By constructing a high-S/N sample of a series of well selected and sufficiently extensive samples we can address a number of compelling questions by:

(1) Providing a fully empirical description of the sSFR-stellar mass metallicity relation for systems with masses greater than $10^9 M_{sol}$ to the peak of the cosmic star-formation history at z~2 (Figure 1). This empirical relation would include measurements of both the gas and stellar-phase metallicities, removing any biases due to recent gas infall/outfall. Such an empirical result would provide an ideal benchmark for the further calibration and development of numerical (hydro-dynamical) and semi-analytic models, which as yet have very few high-z metallicity constraints.

(2) Quantifying the decline in the abundance and frequency of AGN activity within the normal galaxy population at all redshifts to z~2 (the epoch of peak AGN activity) using high S/N emission line diagnostics, such as BPT and WHAN. This would enable the exploration of the co-evolution of galaxies and AGNs by measuring both the star-formation history of the galaxy population, the decline in the luminosity density of AGN and any coupling between these two.

(3) Measuring and comparing the gas-phase and stellar-phase metallicities to constrain the degree of pristine gas infall/outflow as a function of look-back time. Some models suggest galaxies initially evolve according to a closed-box model afterwhich fresh pristine gas arrives significantly reducing the gas-phase metallicity. The clear signature of a closed-box model is a stellar-phase metallicity approximately half that of the gas-phase. Detailed comparisons of the stellar and gas phases will provide constraints on the degree of infall and outflow which can then be monitored over the range of time sampled.

(4) Performing detailed stellar population measurements to determine the progression of stellar-evolution. Earlier epochs of star-formation are typically hidden within later waves of star-formation, however detailed analysis of the complete spectrum on a pixel-by-pixel rather than line basis can reveal the full star-formation histories. These histories of later volume-limited samples need to mesh with what is seen in the earlier volume-limited samples enabling detailed test of our star-formation models. It is also worth nothing that such an analysis as outlined in 3) and 4), combined with ASKAP/SKA HI measurements (at the lower-z end), will provide a comprehensive test of the star-formation history and baryonic composition of individual galaxies, placing strong constraints on likely galaxy

evolution scenarios.

(5) Using multiple star-formation tracers (e.g., Hα v UV v mid or far-IR) to study the onset of star-formation with dynamical separation and/or environment.

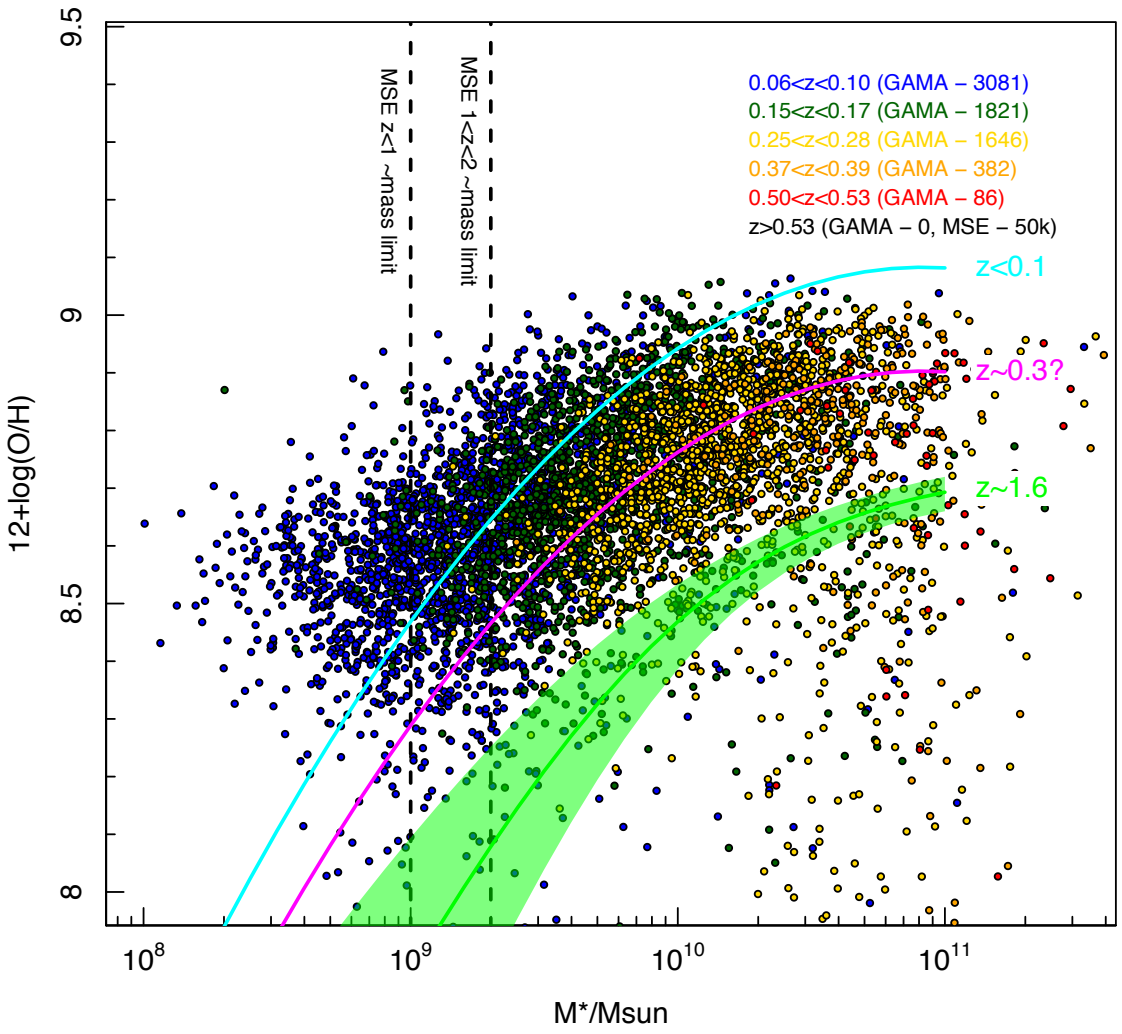

Figure 1: The mass-metallicity relation currently seen by GAMA and with the redshift ranges proposed by the SRO shown ($0.1Z_{sol}$ lies at the lower limit of the plot). The proposed SRO will probe mass limits similar to GAMA at z<0.1 and z<0.2 but out to z<1 and z<2 respectively. The z<0.1 M-Z relation from SDSS+GAMA (Lara-lopez, et al. 2013a) is displayed as the cyan line, the magenta line show the same relation normalized to the 0.25<z<0.39 sample and the green polygon shows the stacked galaxy z~1.6 relation from Zahid et al. (2013). These observations clearly predict a strong evolution in the M-Z relation as a function of redshift. The proposed MSE observations will probe this evolution using individual galaxies, in a comparatively un-biased sample out to z~2.

To identify AGN, star-forming, and inert galaxies, measure their chemical composition, and to achieve the objectives listed above, requires not only a robust redshift measurement, but also sufficient signal-to-noise spanning a broad range of emission and

absorption features. Typically, to robustly distinguish AGN from star-forming galaxies one requires S/N > 5 in the rest-frame 370-680nm (OII → Na), to measure gas-phase metallicity ($0.1Z_{sol}$) and star-formation rates to modest levels ($1M_{sol}$/yr) one requires S/N~10-15 (Choi et al. 2014), and to recover stellar-phase metallicites using, for example Lick indices (400-650nm) or UV metals lines (130-200nm) to $0.1Z_{sol}$, we require S/N ~ 20-30.

Massive samples are not critical here, although in order to fully map out a 3D structure in sSFR, stellar mass and metallicity does require volume-limited samples of ~10k systems. This assumes an average of 20 galaxies per bin and ~ 8 bins each in SF, stellar-mass and metallicity. Here we propose to obtain $S/N_{continuum}$ ~30 spectra from 0.4 to ~2.0micron for 10 samples each containing 10k galaxies, at regular Gyr time steps from the present epoch to a look-back time of 10Gyrs years. This limit of 10Gyrs samples from the peak of the star-formation activity at z~2, to the present epoch. In total, the proposed project would target 100,000 galaxies, which would be either spectroscopically pre-surveyed with MSE itself, or selected from the upcoming photo-z surveys of LSST, EUCLID and WFIRST.

The potential of MSE here is to provide significant statistics to have a transformation impact and fully map the evolution of the mass-metallicity relation to the peak of the star-formation activity at z~2. Existing facilities are capable of constructing modest samples but only with the high throughput, high fibre density and extensive spectral coverage that MSE can provide, do we have the potential to move beyond detections to robust statistics (without unrealistic investments of telescope time). These observations will span, not just the most luminous systems, but those systems which contain the bulk of the stellar mass at the current epoch (and hence the bulk of metals in the Universe).

Driver S., et al., 2013, MNRAS, 430, 2622
Lara-Lopez, M et al., 2013, ApJ, 764, 178
McElroy, M et al., 2015, MNRAS, astro-ph/1410.6552
Sommeriva et al., 2012,A&A, 539, 136
Tremonti, M et al., 2004, ApJ, 613, 898
Zahid, H et al., 2013, ApJ, 771, 19
Zahid, H et al., 2014, ApJ, 791, 130

3. Key astrophysical observables

The required observables are the following spectral features observed for the full range of our target sample from z~0 to z~2: [OII](373nm), Hβ(486nm), [OIII](501nm), Mg b(517nm), NaI(589nm), NII(655nm), Hα(657nm), plus the Lick indices (400-650nm), and redshifted UV metal lines (130-200nm). As such, this requires a combined UV/optical/near-IR spectrograph extending from ~360nm to 1.8micron. Figure 2 shows the progression of the key spectral lines noted above with lookback time/redshift. With the nominal MSE 1.3micron limit, the key metallicity indicators are lost at z~1. However, extending to 2micron would allow all of the the features discussed above to be traced to z~2.0, coincident with the peak of the cosmic star-formation history (although we note that at z>1.7 robust measurments of Hα and NII lines are likely to be problematic due to reduced sky transmission at 1.8-2.0micron – see Figure 2).

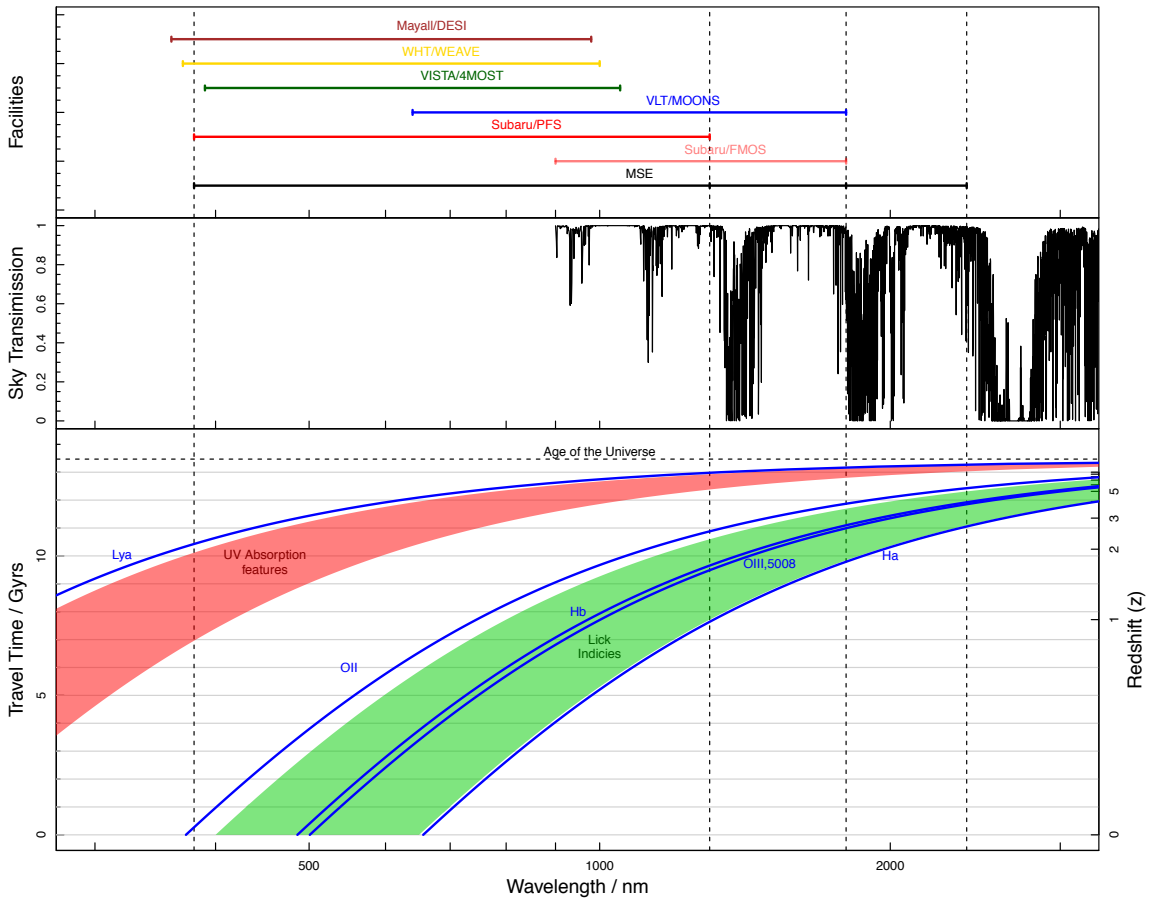

Figure 2 (main/lower panel): The shift of key spectral features versus lookback-time (left-side axis) or redshift (right-side axis) with the prospective wavelength range indicated. The top panel shows the range covered by other notable facilities and the central panel the night sky spectrum.

4. Target selection

Target selection should arise from either a spectroscopic pre-survey of the region to obtain redshifts (preferable – such as in MSE_highz_SRO1) or photo-z selection. LSST and EUCLID will provide deep and vast samples with redshift accuracy of $\Delta z/(1+z) \sim 0.03$ to i~25 or H~24 (AB mags), and one would preferably target fields within their deep imaging regions to obtain the best complementary imaging data. Note: In reality multiple-filters may be used to select stellar mass-limited samples. From these catalogues, samples can be constructed of 10k galaxies in relatively narrow ΔTime intervals (~±0.1Gyr) at redshifts equivalent to 1Gyr time-steps (i.e., 0.08, 0.16, 0.26, 0.38, 0.51, 0.67, 0.88, 1.13, 1.5 and if possible 2.0) over a 10Gyr time-line, to sample the peak of cosmic star-formation history. There is no requirement for the objects to be fully or partially sampled, so source selection can be matched to the final field-of-view and fibre density.

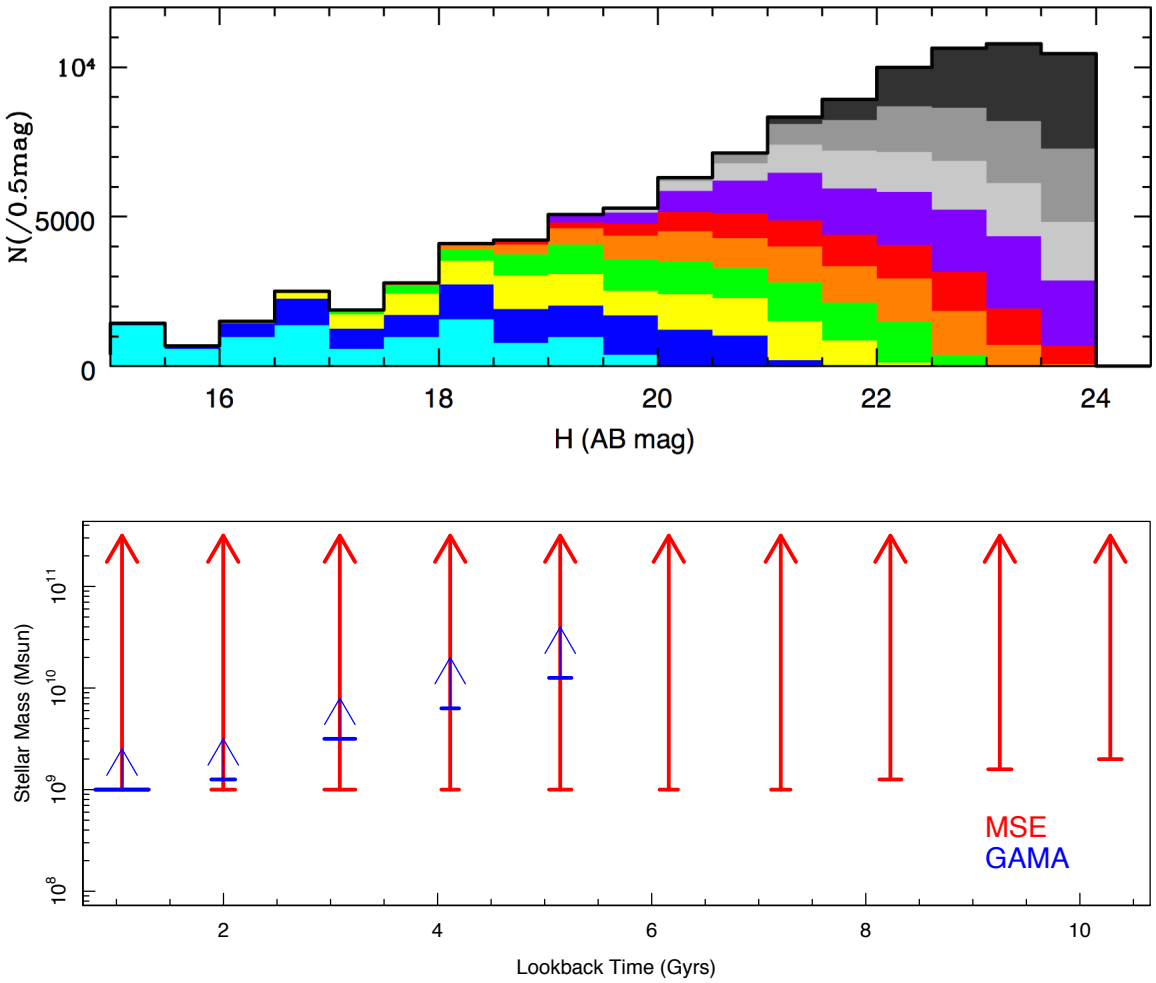

Figure 3: (top) The number-density distribution for each of the volume-limited slices (where cyan is the lowest redshift slice and black the highest). In total there are 100k targets with 10k in each interval. (bottom) the range of stellar-mass probed with lookback time.

In order to estimate the required FOV and integration times required to perform such an experiment we have used the Theoretical Astrophysics Observatory (http://tao.asvo.org.au/tao) and our own number-counts models to simulate a 1sq deg area to H_{AB} < 24.0 mag, and $M_* > 10^9 M_{sol}$ (see Figure 3). The resulting target fibre densities at each redshift are shown in Table1 (note these values will be uncertain to within a factor of 2).

Exposure times to reach S/N ~30 for these sources are extremely uncertain given the current ambiguity in the final MSE characteristics, but are likely to be of order 5/20/100hrs for 22/23/24 K mag (scaling from MSE_highz-SRO1). Hence, the total survey will take of order ~400hrs (50 nights, assuming a fibre density of 5000) – however, we note that this number may easily be in error by a factor of 2.

Table 1: Survey information for MSE-highz-SRO2.

Age	Redshift	Density (/sq deg)	Area (sq deg)
1±0.25	0.06-0.10	51	200
2±0.1	0.15-0.17	284	33
3±0.1	0.25-0.28	479	20
4±0.1	0.37-0.39	1617	5
5±0.1	0.50-0.53	3646	3
6±0.1	0.66-0.69	4500	2
7±0.1	0.86-0.90	5200	2
8±0.1	1.11-1.17	5662	2
9±0.1	1.45-1.54	9439¶	1
10±0.1	1.96-2.10	11385¶	1

¶ values highly uncertain as model dependent

5. Cadence and temporal characteristics

No cadence constrains are required, although numerous repeat visits will be needed. As such, this SRO could be dove-tailed with other SROs which require low-density, but a particular cadence.

6. Calibration Requirements

To measure outflows from emission line diagnostics we require a velocity accuracy of 10km/s. High S/N is the key requirement of our observations, to maximize measurement of both absorption and emission line strengths from UV to NIR wavelengths. As such, we will require high fidelity flux calibrations across the full wavelength range. As we will aim to measure faint absorption line features across a broad range of wavelengths, excellent sky subtraction is also a pre-requisite of our calibration requirements, as minor sky subtraction errors may bias any line diagnostics obtained (especially if binning to lower resolution or stacking to increase S/N).

7. Data processing

Data will need to be de-biased, flat-fielded, flux and wavelength calibrated to a high degree of accuracy, and stacked via signal-to-noise weighting. Line measurements (absorption or emission) will need to be made from multi-Gaussian line-fitting.

8. Any other issues

The main issue for consideration is that of wavelength coverage. Ultimately this sets the upper redshift limit for which meaningful chemical measurements can be made. Otherwise this SRO is massively complimented by high-resolution imaging such as that which might be available from EUCLID and/or WFIRST.

Connecting high redshift galaxies to their local environment: 3D tomography mapping of the structure and composition IGM, and galaxies embedded within it.

Tag: **MSE-highz-SRO3**

Leads*:* **Luke Davies**, Simon Driver, Khee-Gan Lee, Celine Peroux, Patrick Petitjean, Christophe Pichon, Aaron Robotham

1. Abstract

We propose to simultaneously use high-z (z>2.5) Quasi-Stellar Objects (QSOs) and bright galaxy sight-lines to probe the Lyman-α forest and metal content of the IGM at z~2-2.5, and target photometrically selected faint galaxies within ~1Mpc of each sight-line to directly identify sources associated with the IGM structure. Moderate resolution (R~5000), deep spectra would be obtained for all sources to target wavelengths from Lyman-α to OIII, and intervening stellar absorption lines, at z~2-2.5. This will push the capabilities of MSE, requiring good sensitivity and moderate spectral resolution from 3600Å to 1.8μm – with the primary instrumentation requirement of excellent sensitivity at 3600-4250Å. Such a study would allow a reconstruction of the dark matter distribution and associated galaxies at high-z, detailed modeling of galactic scale outflows via emission lines, investigations of the complex interplay between metals in galaxies and the IGM, and the first comprehensive, moderate resolution analysis of large samples of galaxies at this epoch.

2. Science Justification

At high redshift (z > 2), the Intergalactic Medium (IGM) contains the bulk of the baryons in the Universe. As such, it provides the reservoir of gas available for any galaxy to evolve, with IGM accretion fuelling mass growth via star-formation. While mass growth at high-z is likely to be increasingly dominated by mergers (e.g. Conselice, 2014), recent results have indicated that in the majority of cases this does little to affect star-formation (Robotham et al 2013, Davies et al, in prep). Therefore, the primary mechanism through which typical galaxies form new stars is through IGM gas accreting onto their halos. Conversely, star-formation in these galaxies emits highly ionising photons, which heat the IGM and drive superwinds, which expels metals out of the galaxy (e.g. Heckman et al. 1993, Ryan-Weber et al. 2009). Detailed understanding of the complex interplay between the IGM and the galaxies embeded within it is essential to our understanding of the factors driving galaxy evolution and the large-scale baryon distribution in general. By simultaneously probing the IGM structure and composition, and galaxy distributions, nebular gas dynamics and metallicity we can build a complete picture of the interplay between galaxies and their larger scale surroundings. The spatial distribution of the IGM at high-z is also directly related to the dark matter distribution and as such, by fully mapping the IGM will allow a complete reconstruction of the matter density field (the cosmic web) at a given epoch.

i) *3D reconstruction of the Intergalactic medium* – Deep observations of high-z quasar and bright galaxy spectra display numerous absorption lines blue-wards of Lyman-α (e.g. Petitjean & Aracil, 2004). Such features are produced via absorption from line-of-sight intervening gas in a warm photoionised IGM and thus can be used to trace the IGM distribution and composition (Lee et al 2014a,b). The primary diagnostic line for mapping the IGM is Lyman-α absorption (the Lyman-α forest, see Cisewski et al. 2014). By targeting a sufficiently large numbers of bright, background

sources it is possible to use the distribution Lyman-α absorption features to fully reconstruct the IGM distribution at a given epoch using Bayesian inversion techniques – so called, IGM tomography (see Lee et al., 2014a for such a process completed on much smaller volumes than those proposed here). The IGM distribution is directly linked to the dark matter distribution and as such, it is possible to reconstruct the full matter density field on scales of order of the mean separation of lines-of-sight (e.g. Pichon et al 2001; Caucci et al., 2008). In addition to mapping the distribution of the IGM through the Lyman-α, we can also probe its metallicity. Metal absorption lines from the line of sight IGM are also seen in the spectra of high redshift quasars and can be used to map the distribution and evolution of metals in the Universe (Petitjean & Aracil, 2004). By observing systems with sufficient resolution and sensitivity, we can distinguish these metal absorption lines from those of the Lyman-α forest at the same epoch and map the distribution of metals in the IGM.

ii) *The interplay between galaxies and the IGM* – Understanding how the galaxies embedded in this IGM structure interact with the large scale baryonic distribution is key to understanding how these systems evolve with time. By probing the dynamics of nebular material in galaxies in the vicinity of the IGM sight-lines we can build a picture of how they exchange material with the surrounding environment. Detailed analysis of nebular emission line profiles such as Lyman-α and OII (e.g. Verhamme et al. 2008, Weiner et al. 2009) in combination with stellar absorption lines, will allow the identification of galactic scale inflows/outflows and an estimate of the mass exchange between galaxies and thier immediate surroundings (e.g. Pettini et al 2001). Previously, the large samples of high signal-to-noise and moderate resolution spectra required for this analysis have been constrained to a small number of sources. As such, our understanding of both outflows from super-winds and gas accretion is limited. However, the observing strategy required for IGM tomography lends itself to directly to a combined study of the galaxies within the IGM. High signal-to-noise, moderate resolution and good sensitivity over a wide wavelength range are essential for both projects and as such they can be completed simultaneously. With addition of the measurements of galaxy metallicities (see below), it will also be possible to directly compare the chemical content of galaxies and the surrounding IGM, probing the pollution of the circumgalactic medium and the buildup in metals outside of galaxies. With comparable resolution spectra between the IGM mapping and galaxy studies, we will be able to directly associate these galaxies with absorption features in the line-of-sight galaxy/QSO spectrum to investigate the properties of individual neutral hydrogen absorbers and the regions they inhabit.

iii) *The buildup of metals at z >2* – With the high signal to noise and moderate resolution observations discussed above, we will obtain highly robust spectra of a large number of high redshift sources. These spectra will allow the first detailed analysis of both the stellar- and gas-phase metal content of individual galaxies at high-z. Stellar-phase metals of the brighter sources can be obtained through rest-frame UV-continuum stellar absorption lines (using process similar to that discussed in Sommariva et al. 2012), while spectral observations out to 1.8μm will enable the identification of the emission line features required to determine gas-phase metallicities via the R_{23} diagnostic. Current state of the art observations of galaxies at this epoch consist of either tens of sources observed with low resolution spectrographs (R~200, e.g. Popesso et al, 2009 & Henry et al., 2013), which rely on stacking analysis to identify stellar absorption lines and are limited to statistical analyses of the full population, or small numbers of well studied sources at moderate resolution (R~1000-3000, Belli et al., 2013, Maier et al. 2014). With the prosed IGM mapping observations we would target ~140,000 sources at $z > 2$ with the signal-to-noise required to fully investigate stellar absorption/nebular emission lines in individual galaxies. Target spectra could be further binned in resolution elements to increase signal to noise, while retaining sufficient resolution to identify key features required to determine stellar metallicities. In combination with deep photometric data, to derive stellar masses, we will probe the M-Z

relation (e.g. Lara-Lopez et al., 2013) for a large sample of individual galaxies. Though such a study we would, for the first time, produce a detailed large statistical study of the buildup of metals at $z > 2$ and witness the formation of the M-Z relation in a robust sample of galaxies.

MSE is the only current or upcoming facility which can perform such a project. While current 8m+ telescopes and the next generation of ELTs will have the sensitivity to perform these observations, they are limited by their field of view and low simultaneous source targeting. The requirements of the IGM mapping case are a large number of targets simultaneously observed over a large area and as such, would be problematic with non-survey instruments. Other large spectroscopic survey instruments either lack the sensitivity (e.g. 4m class, VISTA-4MOST, WHT-WEAVE and Mayall-DESI) or resolution (e.g. R=2,000 at ~4000Å, Subaru-PFS). Subaru-PFS, at its very upper limits, could attempt an IGM tomography experiment, however, this does not directly form part of the PFS extragalactic science case (Takada et al., 2014). IGM tomography could be undertaken as a bi-product of the proposed PFS galaxy evolution survey. However, such a survey will not have sufficient resolution to determine the metal content of the IGM, will not identify the faint galaxies associated with the IGM structure at $2<z<2.5$ (with a proposed $J<23.4$ limit) and will not have the sensitivity and wavelength coverage to determine the stellar- or gas-phase metallicity of individual galaxies at this epoch. It is therefore unlikely that this science will be successfully undertaken until the construction of MSE and no planned instrument will be able to complete such a project to the high fidelity level of MSE.

By simultaneously probing the IGM and the galaxies embedded within it at $2<z<2.5$ we will build a complete picture of both the IGM and galaxy, distribution and composition at this epoch. We will probe the build-up of metals in both environments, and witness the complex interplay between galaxies and their surroundings. We will preform the first detailed high S/N and moderate resolution analysis of a extensive sample of galaxies at $z>2$ – increasing sample sizes by orders of magnitude, and fully map the IGM distribution on scales inaccessible to any current or proposed instrument other than MSE.

•Conselice, C., 2014, ARAA, 52, 291
•Lee, KG et al., 2014a, ApJ, 795, 12
•Lee, KG et al., 2014b, ApJ, 788, 49
•Caucci, S., et al., 2008, MNRAS, 386,211
•Sommariva, V., et al., 2012, A&A, 539, 136
•Takada, M., et al., 2014, PASJ, 66, 1
•Robotham, A., et al, 2013, MNRAS, 431,167
•Heckman et al., 1993, ASSL, 188,455
•Cisewski, J., et al., 2014, MNRAS, 440, 2599
•Verhamme, A., et al., 2008, A&A, 491,89
•Popesso, P., et al., 2009, A&A, 494, 443
•Maier, C., et al., 2014, ApJ, 792, 3
•Belli, S., et al., 2013, ApJ, 772, 141
•Ryan-Weber, E., et al., 2009, MNRAS, 395, 1476
•Petitjean & Aracil, 2004, A&A, 422, 52
•Picon, C. et al., 2001, MNRAS, 326, 597
•Pettini, M., et al., 2001, ApJ, 554, 981
•Henry, A., et al., 2013, ApJ, 776, 27
•Lara-Lopez, M., et al., 2013, MNRAS, 434, 451
•Weiner, B., et al., 2009, ApJ, 692, 187

3. Key astrophysical observables

To detail the key observables required for this project, we split our observables into those required for the IGM distribution and metallicity mapping, and the study of galaxies associated with the IGM structure:

i) IGM mapping – For a pure mapping of the IGM distribution at $2 < z < 2.5$ a minimum spectral resolution of ~20km/s (R~2,000) is required (comparable to the spatial separation of sightlines). However, in this project we also aim to identify individual Lyman-α absorption features and metal absorption lines associated with the IGM, which requires a velocity resolution of <~10km/s (R~5,000).

To fully map the IGM to the degree required by our science objectives, simulations (Figure 1) predict that 500 randomly distributed targets per deg^2 are required to recover the matter distribution on 1-2' scales at $z \sim 2$. These line of sight sources must fall at $2.5 < z < 3.0$, in order

for their Lyman-continuum region to probe the IGM at $2.0 < z < 2.5$. Using the central 1deg^2 of the COSMOS field as a test region, and the photometric redshifts of Ilbert et al. (2008), which are complete down to r<25.5, we find that $r < 24.0$ sources have the required source density at this epoch. In order to identify IGM column densities of order $\sim 10^{14}$ cm^{-2} we require continuum SN>4 per resolution element. Scaling from current ground based spectrographs, we predict ~20h exposures to obtain this S/N for r~24 sources with MSE, at a resolution of R~5,000. In these observations Lyman-α absorption lines from intervening sources at $2 < z < 2.5$ will fall at ~3600-4250Å. Therefore, **the main technical specification of our IGM tomography observation is high sensitivity at blue wavelengths**. However, we will also target metal absorption lines in the spectra which will extend out to 9800Å (MgII[2800] at $z = 2.5$), and thus we also require good sensitivity across the whole of the optical range. Note, that we will also obtain detailed measurements of the host galaxy properties for all of these sources, as discussed below.

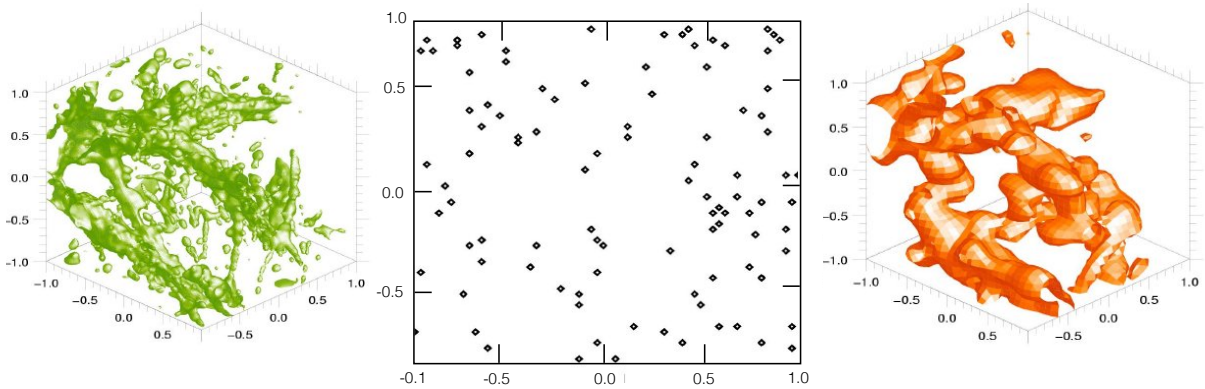

Figure 1: **Left:** The 3D density field in a 50Mpc^3 N-body simulation box. **Middle:** 100 random sight-lines to are draw through this simulation box and a spectrum is simulated for each sight-line. **Right:** The density field is reconstructed using Bayesian inversion. Structure on scales of the mean line-of-sight separations are recovered.

To probe a cosmologically significant volume at $z \sim 2$, and to avoid sample variance, the simulations also predict that observations would have to be undertaken over >20 deg^2 (also see MSE-HIGHZ-SRO1 for a description of the scales required to avoid issues with sample variance at these epochs). However, MSE's great strength over potential competing experiments in this field is survey speed. The prosed PFS extragalactic survey, which could be used to undertake an IGM tomography experiment (modulo the caveats discussed in the science justification), will cover 16deg^2. As such, to remain competitive in purely an IGM tomography sense, we recommend a survey covering 40deg^2. The full set of observations required to map the IGM would be 40×20h, 1deg^2 field observations, targeting at total of 20,000, $z > 2.5$ sources. This yields a total observation time of ~ 1000h (including 20% overheads). We note that this project can be scaled back to a minimum area of 20deg^2 (~500h, 10,000 $z > 2.5$ sources, 60,000 $2<z<2.5$ sources) and still achieve our science goals, albeit at lower fidelity and cosmological significance.

ii) Galaxies associated with IGM – The key physical galaxy properties with we wish to determine for this experiment are: redshift positions to the accuracy of individual Lyman-α absorption features in the IGM tomography observations, nebular outflow velocities from modelling of emission lines, stellar-phase metallicites from UV-continuum stellar absorption line strengths in the brightest sources, and gas-phase metallicites from nebular emission line strengths.

We aim to target sources down to r<25.3 in the region surrounding our IGM tomography sight-

lines but embedded within the IGM structure (see below – this limit is constrained by the robust photo-z range of LSST). Assuming simultaneous observations of both the galaxies and IGM tomography sources we will obtain 20h integrations at R=5,000. For these integration times, we will be able to determine the redshifts of emission line sources to within the accuracy of the IGM mapping experiment (~10km/s) and directly associate individual Lyman-α absorption features with emission line galaxies in the line of sight. Lyman-α emission is the main redshift diagnostic for galaxies at this epoch. However, Lyman-α emission is only seen ~ 20% of sources, and Lyman-α derived redshifts are found to be offset from absorption line redshifts by up to several hundred kms^{-1} – and thus, do not delineate the true systematic redshift of the galaxy. As such, we aim to target both Lyman-α and OII lines simultaneously to obtain a robust measurement of the galaxy redshift. For sources where redshifts are not obtained at R=5,000, we will bin in spectral resolution to increase signal to noise (binning to R~3,000 we will still obtain redshift to a accuracy of ~30km/s and at this resolution we will easily obtain redshifts for all sources in 20h integrations). If OII lines are not available for redshift identification, we will use absorption/emission line features at longer wavelengths (Ca H & K, G-band, Hb and OIII – which will all be covered in our observations out to 1.8μm). Once redshifts have been obtained, all other science goals do not require R=5,000 spectra. As such, will bin to various lower spectral resolutions depending on the specific science goal, as follows:

i) For stellar metallicities we will heavily bin to R~100 for all galaxies and identify UV-continuum absorption line features in the rest-frame 1300-2000Å range (3900-7000Å at $2<z<2.5$). Sommariva et al. (2012) obtain stellar-phase metallicity measurements for $23.0<r<24.5$ sources at R~100 in 38h integrations with VLT/FORS2. Assuming a factor of 2 decrease in MSE integration time for improved sensitivity, throughput and mirror diameter, we will obtain stellar-phase metallicities for the brightest sources in our sample. Thus, **to probe the stellar-phase metallicty of high-z sources we require the maximum possible throughput and sensitivity in the 3900-7000Å region**. Note that we will also obtain steller-phase metallicities for the majority of the 20,000 IGM tomography targets, as all sources will be at $r<24.0$ (brighter than most of the galaxies discussed in Sommariva et al). This will increase the number of $z>2.5$ sources with know stellar-phase metallicities by ~2-3 orders of magnitude.

ii) For gas-phase metallicties we will use the R_{23} diagnostic which requires OII[3727], OIII[4959/5007] and Hβ[4861] emission lines. At $2<z<2.5$, for detection of the OIII[5007] line we need spectral coverage out to ~1.8μm. As such, **to fully map the gas phase metallicity of high-z sources we require a minimum spectral range of 3600Å-1.8μm**. Should the MSE spectrograph be extended to 2.4μm (as in MSE-HIGHZ-SRO1) we will be able to probe H-α and NII lines for our full sample of galaxies, allowing us to determine gas phase metallicites, SFRs and AGN fractions too a much higher degree of fidelity. For spectral line diagnostics we do not require significant resolution, and as such, we do not require an R>1000 spectrograph past ~1.3μm. With 20h integration and no requirement of resolution in our line diagnostics, we shall bin to lower resolution (R~1000) and obtain high S/N, robust measurements of emission line features for our full galaxy sample.

iii) To determine nebular outflow velocities we will bin to R~2,000 to increase signal to noise and model Lyman-α emission lines in a similar manner to Verhemme et al (2008), using systematic galaxy redshifts obtained from the OII emission lines. R~2,000 is sufficient for detailed modelling of the lines and will allow us to determine the nebular dynamics within the system. Such an observation will probe the exchange rate of material between the galaxy and IGM, and allow us to investigate the rate at which metals are being expelling into the galaxy's surrounding environment.

4. Target selection

As discussed above, we will observe 500 randomly distributed r<24.0 sources at 2.5<z<3.0 per deg^2 covering a total of $40deg^2$ to perform the IGM tomography experiment. During these observations all other available fibres would be placed on photometrically pre-selected 2 < z < 2.5 within an angular distance of ~ 1.25' from the IGM mapping line-of-sight (~650kpc at z=2.25). To identify the sources associated with absorption features we must probe to faint magnitudes (r < 25.3 – as discussed above). The number density of r < 25.3 sources using a 2 < z_{photo} < 2.5 preselection is ~ 2 $arcmin^2$, and therefore, ~8 within ~ 1.25' of each line-of-sight (assuming no overlapping sources). For 500 lines of sight per deg^2, and assuming a nominal 3200 MSE fibers all placed in the central deg^2, this gives on average 5.5 fibres per line-of-sight to place on surrounding galaxies. Once again using the COSMOS region as a test-bed, we take 511 sight-lines to r < 24.0 sources at 2.5 < z < 3.0, and identify all r < 25.3 galaxies at 2 < z < 2.5 within 1.25'. In total there are 2827 galaxies which meet this criteria (Figure 2.). This gives a simultaneous observation of ~3400 fibres - close to the nominal MSE fibre density. If the MSE fibre density were increased, we could either simultaneously observe a larger field of view (i.e. for 5000 fibres we could observe ~700 sightlines over $1.4deg^2$ while retaining 6 fibres per sightline for the surrounding r<25.3 sources) or extend the volume around each sightline in which r<25.3 sources are targeted (i.e. to simultaneously probe all r<25.3 sources within a ~1Mpc (2') radius around each sightline with a fixed deg^2 FOV, we would also require ~5,000 fibres).

To estimate the potential fibre collision rate in such an observation, we calculate the minimum separation between all possible r<25.3 sources in each sightline, for the simulated COSMOS observation above. We find that the median separation between the closest galaxies is ~21''. For a typical fibre separation of 10'' we would obtain fibre clashes for 18% of our sample (or in other words, allowing ~5/6, r<25.3 source per sightline to be targeted). This would limit the simultaneous observations to ~3000 sources, for the initial observational setup discussed above (500 sightlines and 5*500 lower-z galaxies). If we were able to pack fibres to within 5'' this fibre collision rate would drop to <7% (simultaneous observations of ~3,300 sources - see Figure 2). Hence, **close fibre density will be highly beneficial to these observations**. However, collisions in our observational setup will not result in unused fibres, as such fibres could be placed on other r<25.3 galaxies slightly outside of the initial sightline radius (i.e. green points which lie close to lines of sight in Figure 2) or target marginally fainter galaxies within the 1.25'' radius.

Photometric source selection for the full project will be obtained from upcoming deep large area surveys such as LSST. We will require accurate photometric redshifts to r < 25.3 over a contiguous 40 deg^2 region, which will be available from LSST by the time MSE is constructed. Choice of field position is non-essential to this project, and is only limited to the deep optical data required for source selection, and would preferably contain the maximum possible bright QSO source density at 2.5<z<3.0. Regions with extensive multi-band coverage are ideal, to provide accurate stellar mass measurements with which to probe the M-Z relation. With these caveats, we are flexible on scheduling and can adapt to the position of deep fields which are available at the time of observations.

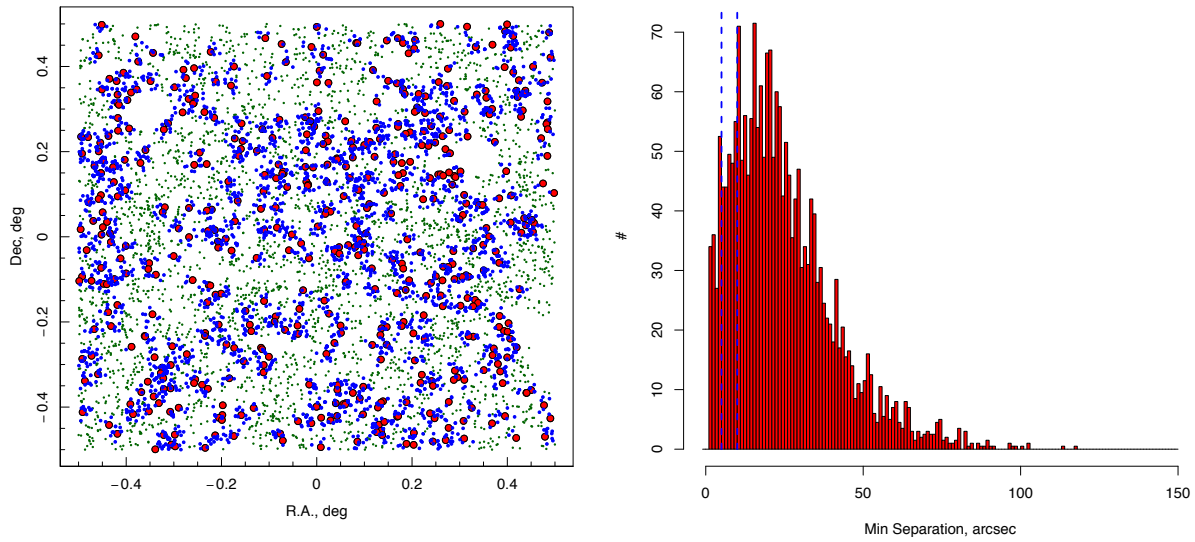

Figure 2: **Left** - Simulated observation of ~500 sight-lines to $2.5<z_{photo}<3.0$ sources in a single 1 deg^2 region of the COSMOS field. Red points display sight-lines, blue points show all r<25.3 sources with $2.0<z_{photo}<2.5$ within 1.25'of a sight line. Green points show all other r<25.5, $2.0<z_{photo}<2.5$ sources. **Right** – The closest separation between r<25.3 galaxies within 1.25' of each sightline. Vertical lines display potential 10'' and 5'' fibre separations, containing 18% and 7% of sources respectively.

5. Cadence and temporal characteristics

No cadence constraints or repeat observations are not required.

6. Calibration Requirements

Our observations will require a high level of spectroscopic fidelity for both the identification of Lyman-α absorbers and galaxy redshifts. We require maximal throughput to obtain good signal to noise, specifically at ~3600-4250Å for the IGM tomography and 3900-7000Å for stellar phase metallicities, and robust flux calibration from ~3600Å -1.8μm to derive accurate faint emission line strengths. As such, we will require accurate wavelength and spectrophotometric calibrations. Excellent sky subtraction is required for stellar absorption features in $2.0 < z < 2.5$ galaxy sample as we will be heavily binning in resolution elements (4500-7000Å). The region probed in the IGM tomography (~3600-4250Å) is largely free from sky emission, however, even minor over subtraction of sky emission can lead to confusion in reconstruction the IGM matter distribution. Hence, we require excellent sky subtraction over the full optical range and robust removal of instrument signatures.

7. Data processing

Data will be debiased, flat-fielded, sky subtracted and, flux and wavelength calibrated to a high degree of accuracy. Bayesian inversion techniques will be used to reconstruct the IGM distribution, Gaussian line fitting will be applied to all emission and absorption line features for metallicity measurements and more complex line fitting will be undertaken to derive nebular outflow velocities. **8. Any other issues** None.

Mapping the Inner Parsec of Quasars with MSE

Tag: **MSE-highz-SRO4**

Leads: **Sarah Gallagher**, Patrick Hall, Yue Shen, Chris Willott

1. Abstract

The centre of every massive galaxy in the local Universe hosts a supermassive black hole that likely grew between a redshift of 1 to 3 through active accretion as a luminous quasar. Despite decades of study, the details of the structure and kinematics of the inner parsec of quasars remain elusive. Because of its small angular size, this region is only accessible through time-domain astrophysics. The powerful technique of reverberation mapping takes advantage of the changing emission-line profiles of gas near the black hole in response to variations from accretion continuum luminosity to measure the sizes and velocities of the line-emitting regions; with this information, we can map the quasar inner parsec and accurately measure black hole masses. This information is essential for understanding accretion physics and mapping black hole growth over cosmic time. We propose a ground-breaking MSE campaign of ~60 observations of ~5000 quasars over a period of several years to map the inner parsec of these quasars from the innermost broad-line region to the dust-sublimation radius. With high quality spectrophotometry and spectral coverage from 400 nm to 2.5 μm, this unprecedented reverberation-mapping survey will map the structure and kinematics of the inner parsec around a large sample of supermassive black holes actively accreting during the peak quasar era. In addition, a well-calibrated reverberation relation for quasars offers promise for constructing a high-z Hubble diagram to constrain the expansion history of the Universe.

2. Science Justification

At the present epoch, supermassive black holes are ubiquitous in the centres of massive galaxies. The black holes grew predominantly around redshifts from 1 to 3 when the universe was approximately a fifth to a half of its current age through active accretion as luminous active galactic nuclei (AGN), also known as quasars. Remarkably, subparsec quasar accretion disks can outshine their host galaxies – thousands of times larger – by two to three orders of magnitude. Despite their small size, black holes are fundamentally linked to their host galaxies as shown through the strong scaling relations between the black hole mass and host galaxy properties. Energy injection during the quasar phase in the form of feedback may regulate these scaling relations; in any case, supermassive black hole growth clearly occurs alongside the build-up of stellar mass in galaxies.
Measuring accurate black hole masses and understanding the inner structure of distant quasars is essential to advancing our knowledge of supermassive black hole growth, AGN physics and phenomenology, the mechanisms for launching quasar outflows, and the co-evolution of supermassive black holes and their host galaxies.

Though quasars have been studied in radio through X-ray wavelengths for decades, there remain fundamental, open questions about accretion physics. For example, the well-known Shakura & Sunyaev (1973) prescription for describing the light distribution of the

UV-optical emitting region of accretion disks underestimates their sizes by factors of several (Blackburne et al. 2011; Jimenez-Vicente et al. 2012). The geometry and kinematics of the region generating the broad emission lines – the most prominent features of quasar optical-UV spectra – are still poorly constrained. These distant, cosmic powerhouses have such small angular sizes that they cannot be resolved with existing or near-term technologies; our only access to constraining their structure empirically is through time-domain astrophysics.

In particular, we can use time resolution to substitute for angular resolution by measuring the rest-frame time lag of the response of a broad emission line to changes in the continuum illuminating the broad line region (Blandford & McKee 1982). The broad emission lines (with widths of 1000s km s^{-1}) reveal the Doppler motions of dense gas close to the central black hole. Strong, broad, resonance lines are seen from ions with a large range of ionization states, from O VI to Mg II; the gas is photoionized with lower-ionization gas at larger radii out to the dust-sublimation radius. The time lags represent light travel times from the continuum to the emitting region and can therefore be converted to physical length – a radius of the emitting region, R_{line}. Once R_{line} is measured, the mass of the black hole is approximately given by $M_{BH} = f(\Delta v)2R_{line}/G$ where G is the gravitational constant, Δv is a measure of the width of the emission line, and f is a factor of order unity which accounts for the geometry and kinematics of the broad-line region (see, e.g., Peterson 2011, and references therein). For each quasar, the time lags and the continuum luminosities generate a radius-luminosity (R_{line}-L_{cont}) relation for each line, enabling the structure of the broad-line region to be mapped. With appropriate velocity resolution and time sampling, high-fidelity velocity-delay maps (line responsivity as a function of line-of-sight velocity and time delay; see Fig. 1) can be obtained with a reverberation-mapping (RM) campaign with a duration $T_{dur} > 3\tau_{line}$, where τ_{line} is the time delay for a given line.

Currently, only ~50 local, low-luminosity AGN have high quality RM measurements of their R_{line}-L_{cont} relations and black hole masses (e.g., Bentz et al. 2009). The largest optical mapping campaign to date is the ongoing, 2 yr SDSS-BOSS program to monitor 849 $i < 21.7$ AGNs with the 2.5 m Apache Point Telescope in a single 7 deg^{-2} field (Shen et al. 2015). Dedicated time-intensive programs that monitor the rest-frame UV through optical of a handful of AGN are currently underway with e.g., HST COS (NGC 5548; PI Peterson) and the VLT X-Shooter (PI Denney). Though these programs will be foundational for taking the next step forward in RM science, MSE promises to go significantly further. Cosmological redshifting means that optical spectroscopic RM campaigns of quasars are fundamentally limited by a mismatch between the high quality data at low-z and what is accessible for high z. The lines sampled in these two regimes – e.g., Hβ and C IV for low and high z, respectively, arise from fundamentally different parts of the broad-line region, and there is significant scatter in the black hole masses derived from these two lines in single epoch spectra as a result of their distinct characteristics (Denney 2012).

The major advantage of MSE over other planned RM programs (e.g., SDSS, OZDES, or 4MOST) is sensitivity (~2-3 mags deeper in 1 hr) because of the planned mirror size and the exquisite Mauna Kea site. The only planned instrument that would be competitive with MSE on these terms is Subaru-PFS; however, there are no current plans to invest the requisite time to a mapping campaign as outlined in this proposal. The

inclusion of near-IR capability (to 1.8 or 2.5 mm) to reverberation-map the rest-frame optical for high-z quasars would make MSE a game-changer in this field (see Fig. 2). There is no other planned facility with optical-NIR multiplexing of this scale.

Ancillary Science: Though the demographics of the quasar population have changed remarkably since z~3, the structure of quasars shows surprisingly little evolution in fundamentals such as metallicity and spectral energy distribution. They are thus promising objects for constructing a high-z Hubble diagram given an appropriate independent estimate of luminosity such as a well-calibrated R_{line}-L_{cont} relation. The size of the line-emitting region can be measured from reverberation; this then yields the average quasar luminosity. From the measured flux and the redshift, a Hubble diagram to z~3 can be made from the proposed MSE high-z quasar reverberation-mapping campaign. Such a high-z Hubble diagram would provide important constraints on general cosmological models (King et al. 2014).

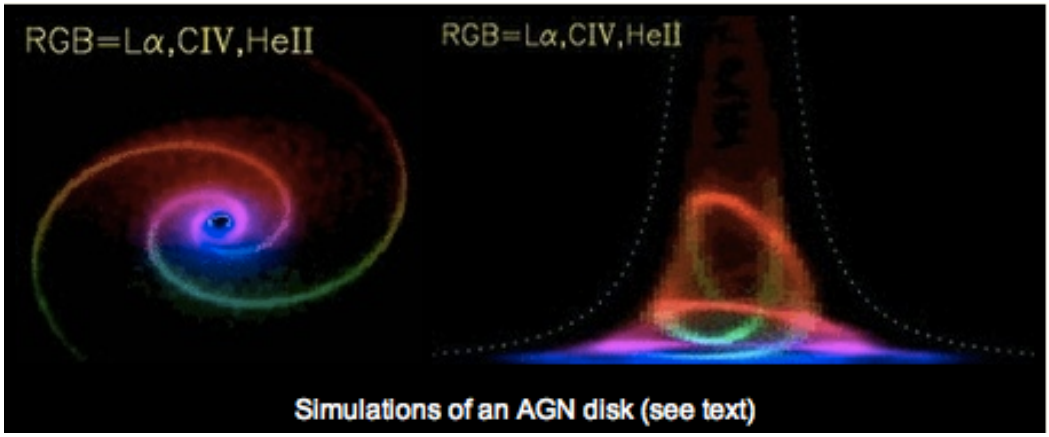

Figure 1: *Left:* An image of a quasar accretion disk with a spiral density wave. *Right:* Time delay vs. velocity map for the Lyα (red), C IV (green), and He II (blue) emission lines. When the continuum emission from the accretion disk varies, the gas giving rise to the broad emission lines responds with a characteristic time delay. The spread of velocity components in each emission line is generated by different locations within the broad-line region, and therefore the line as a whole responds with a range of time delays. With appropriate time sampling, velocity resolution, and absolute flux measurements, the time delay-velocity map can be inverted to reconstruct the accretion disk image. (*Image credit:* K. Horne [star-www.st-andrews.ac.uk/astronomy/research/agn.php])

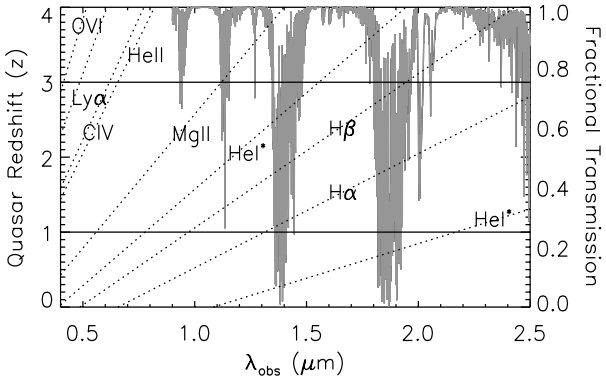

Figure 2: The location of broad emission lines of interest as a function of redshift overlaid on a representative atmospheric transmission spectrum for Mauna Kea. For the peak of the quasar epoch (z = 1–3; bounded by horizontal lines) emission lines from CIV to Hα are accessible with wavelength coverage from 400 nm to 2.5 μm; at least one Balmer line will be at a wavelength of high atmospheric transparency. With wavelength coverage to 1.8 μm, Hβ is accessible for z<2.6. This range of lines probes size scales from the innermost broad-line region (of order light-days) to the dust sublimation radius (of order a few light years; Mor & Netzer 2012). Such broad-band spectral coverage with the proposed time cadence would enable accurate black hole mass measurements for the largest sample of quasars to date and unprecedented mapping of the central parsec.

Bentz, M. C., et al. 2009, ApJ, 697, 160

Blackburne, J. A., Pooley, D., Rappaport,S., & Schechter, P. L. 2011, ApJ, 729, 34

Blandford, R. D. & McKee, C. F. 1982, ApJ, 255, 419

Denney, K. D. 2012, ApJ, 759, 44

Hopkins, P. F., Richards, G. T., & Hernquist, L. 2007, ApJ, 654, 731

Horne, K., et al. 2004, PASP, 116, 465

Jimenez-Vicente, J., et al. 2012, ApJ, 751, 106

King, A. L., et al. 2014, MNRAS, 441, 3454

Mor, R. & Netzer, H. 2012, MNRAS, 420, 526

Peterson, B. M. 2011, ArXiv1109.4181P

Shakura, N. I. & Sunyaev, R. A. 1973, A&Ap, 24, 337

Shen, Y., et al. 2015, ApJS, 216, 4

Zu, Y., Kochanek, C. S., & Peterson, B. M. 2011, ApJ, 735, 80

3. Key astrophysical observables

The essential requirements for a successful reverberation mapping campaign are to accurately measure the time lag between continuum variability and the response of each emission line, and to obtain a root-mean- square (RMS) spectrum of the quasar. The time-lags provide the size scale of the emission-line region, while the RMS spectrum shows the velocity structure of the material responding to the continuum variability. Both of these are required to map the structure of the broad-line region and to obtain accurate black-hole masses.

The quality of these observables depends on the following parameters:

• *Accurate spectrophotometry:* To detect low-amplitude, short-timescale continuum and emission-line variations requires high S/N spectra (S/N~30 per resolution element at line center). Absolute flux calibration of the continuum is critical to detect flux variability at the 10% level. The current state-of-the-art is 6% with the SDSS-RM campaign; we require a minimum of 4% (as achieved with SDSS-I/II with 3” fibres). Systematic errors come from uncertainties in modeling standard star spectra, position-dependent

atmospheric differential refraction, and pointing errors. Obtaining this goal may require allocating a larger fraction of standard star and sky fibres (200–500) than typical per field.

• *Sensitivity:* We aim to achieve S/N~30 at i<24 in 1 hour integration times. Longer integration times compromise accurate spectrophotometry because of changing sky conditions.

• *Spectral resolution:* Quasar broad-emission lines have typical widths of 1000s of km s^{-1}. However, they are highly structured and often blended, and several resolution elements are required to adequately sample their velocity structure. Quasar narrow-emission lines have widths of 100s of km s^{-1} and would ideally be resolved in an individual spectrum. This sets the minimum resolution requirement of 200 km s^{-1} (R~1500) with 100 km s^{-1} (R~3000) being ideal.

• *Wavelength range:* Continuous wavelength coverage in the regions of atmospheric transparency from 400 nm to 2.5 μm maximizes the science return on these time-intensive observations for quasars up to z~4 (Fig. 2). Simultaneous coverage of C IV and Hβ is necessary to map the broad-line region from the innermost regions to the dust-sublimation radius. Furthermore, including rest-frame optical emission lines is essential for tying the typical high-redshift quasar to the extensively calibrated local reverberation-mapped AGN. Cutting the wavelength reach on the red end to 1.8 μm would reduce the redshift range with simultaneous CIV and Hβ coverage to z=1.5-2.6, though this is likely a large fraction of the quasars up to z~3 within a flux-limited survey. Coverage limited to 1.3 μm would effectively eliminate the link to low-z RM campaigns for the redshift range of interest, though a rest-frame UV RM campaign of this magnitude would still be ground-breaking (cf. Fig. 1).

4. Target selection

Given the heroic efforts that have gone into building up large quasar samples with SDSS and follow-on surveys such as UKIDDS/DXS, several fields with known targets appropriate for the quasar variability program will be available prior to 2020. With sensitivity down to i = 24, the sky density of broad-line quasars is ~600 deg^{-2} (from the Hopkins et al. 2007 luminosity function). Therefore, for a 1.8 deg s^{-2} MSE field-of-view, we require 1000–1500 target fibres per pointing. The chosen field(s) should be within the LSST survey area to optimize the opportunity for improving spectrophotometric calibration and the increased time-sampling of continuum monitoring (a factor of 2 to 3; cf., Zu et al. 2011). If MSE is on-sky prior to LSST first-light, other facilities could be used for photometric monitoring. Our ideal sample size is ~5000 quasars (approximately 5 fields) to properly sample the diversity of the quasar population.

5. Cadence and temporal characteristics

Repeat observations to measure continuum and emission-line variability are at the heart of our proposed science program. Quasar variability is a function of timescale (from days to years), luminosity (low luminosity quasars vary more), wavelength (quasars are more

variable at shorter wavelengths and in higher ionization potential broad lines), and redshift (as a result of time dilation). For a given 6-month period of the SDSS-RM campaign, only ~10% of quasars are expected to have successfully measured lags (Shen et al. 2015); multiple seasons are therefore necessary to achieve the science goals.

Horne et al. (2004) discuss the requirements for accurate reverberation mapping (RM). The peak emission-line time delay τ measured in a given RM campaign is the light-crossing time of the broad-line region in that line at that time. The delay resolution is $\Delta\tau \simeq 2\Delta t$ where Δt is the sampling time interval. Therefore, to sample both short lags (days) and long lags (years), we envision a multi-year program with a cadence of several days in the first year, and reduced cadence in each successive year, totaling ≃60 epochs per field over 3–5 years. Given that this program would require less than one-third of the available fibres per pointing, it could naturally be executed concurrently with programs that (1) require repeat observations of very faint targets to build-up S/N in individual spectra, and/or (2) require extremely dense sampling of objects in an extragalactic field. Follow-up spectroscopy to identify interesting LSST transients could also be incorporated into the observing program.

6. Calibration Requirements

• *Wavelength calibration:* As this program encompasses repeat and comparative observations of known targets, standard wavelength calibration should be sufficient.

• *Sky subtraction:* The main sky features will need to be well-subtracted to enable accurate flux calibration. This may require an additional allocation of sky fibres to adequately sample the field-of-view.

• *Flux (spectrophotometric calibration):* As mentioned in §3, the most stringent requirement for the success of the observing program is accurate spectrophotometry. The absolute flux of the continuum must be measured for the experiment.

• *Telluric absorption:* Accurate telluric absorption correction is important for obtaining the high quality broad-band spectra needed for this program. For this reason, it may be desirable to allocate a larger number of sky fibres per pointing than in the typical survey program.

• *Other (e.g., stability):* Absolute flux and wavelength calibration are the primary concerns. As long as they are sufficient, instrument stability is not the focus.

7. Data processing

• *Removal of instrumental signatures:* Instrumental signatures must be removed from the spectra for the proposed analysis.

• *Measurement of astronomical quantities:* For each quasar that varies sufficiently for reverberation mapping: (1) Available photometry, flux and wavelength-calibrated spectra from each epoch will be analyzed together to determine a R_{line}-L_{cont} relation for each

broad line. (2) RMS spectra from each quasar will be constructed and analyzed to determine a black-hole mass. (3) For each quasar in the survey: A high S/N composite spectra will be constructed from the weighted average of individual spectra. These spectra will enable an unprecedented analysis of faint features in typical quasar spectra, such as weak forbidden lines and quasar host galaxy features.

• *Discussion of other data to be combined with MSE:* High quality photometry (e.g., from LSST or other facilities) would be used to improve the spectrophotometry and increase the time cadence for continuum variability monitoring. Quasars in this sample with very high S/N spectra and well-measured black hole masses will be appealing targets for follow-up with other facilities, e.g., ALMA, TMT, and JWST.

• *Desired deliverables:* The minimum deliverables would be flux-calibrated spectra for each epoch and combined, average spectra for all the quasars. Higher level products such as R_{line}-L_{cont} data for each broad line of successfully reverberation-mapped quasars would require additional time and resources to provide.

8. Any other issues

None.

A peculiar velocity survey out to 1 Gpc

Tag: **MSE-highz-SRO5**

Leads: **Helene Coutois,** M. Colless, J. Comparat, H. Courtois, M. Hudson, A. Johnson, N. Kaiser, J. Koda, C. Schimd

1. Abstract

This SRO will propose MSE as a means to realize a velocity survey covering 24,000 square degrees (¾ of the full sky apart from Milky Way) with a minimal requirement of 10,000 square degrees, adopting both the Fundamental Plane and (improved) Tully Fisher techniques to measure the distance of about 1 million of early-type and late-type galaxies up to redshift $z \lesssim 0.25$ with galaxy number density and sampling similar to *Cosmicflows-2*. By exploring the structure and dynamics of cosmic structures up to ~1Gpc from the Milky Way, such a MSE velocity survey will exceed *Cosmicflows-2* by a factor of 150 in volume, and extend the TAIPAN and ASKAP (WALLABY) surveys in the Northern hemisphere by a factor of 14 and 4, respectively. And will be the first and only survey exceeding the scale of homogeneity in both structures and dynamics.

It will allow *(i)* the reconstruction of the velocity-based cosmic web, resolving cosmic structures down to $\lesssim 0.1h^{-1}$Mpc; *(ii)* the high-precision measurement of linear-growth rate of structures, allowing to disentangle modified theories of gravity at 1% level, by the auto- and cross-power spectra of galaxies and velocities, escaping the cosmic variance limit; *(iii)* the direct, genuine probe of the backreaction conjecture arising from the «averaging problem» in General Relativity, dynamically equivalent to both dark matter and dark energy, by measuring the morphology of the velocity potential.

2. Science Justification

In a galaxy peculiar velocity survey the measurements of redshifts are combined with redshift-independent distance estimates to yield a direct probe of galaxy peculiar velocities. In the 1990's peculiar velocity surveys were widely recognized as a powerful tool to constrain the mean mass density on cosmological scales. Though, their analysis was challenging, because of sparsity, noise, and observational selection effects (Malmquist bias). The most recent surveys have increased the samples, reaching size large enough to permit the study not only of the global statistics of large-scale flows but also of the details of the local velocity field.

In 2007, *SFI++* peculiar velocity catalog (Springob et al. 2007) collected about 4,900 field and cluster galaxies over the full sky up to redshift $z \lesssim 0.05$, adopting the Tully-Fisher method (TF) to determine distances along the line-of-sight. More recently, combining six methods to measure the distance including the fundamental plane (FP) method, *Cosmicflow-2* (Tully et al. 2013) probed the peculiar velocities of about 8,000 galaxies in the local Universe ($z \lesssim 0.04$, $cz \lesssim 12{,}000$ km s^{-1}), which ultimately highlighted the dynamics toward the supercluster Laniakea that dominate the local cosmic-web (Tully, Courtois, Hoffman & Pomarède 2014, Nature, 513, 71). In parallel, in the

Southern hemisphere, based on the 6dF Galaxy Survey (6dFGS; Jones et al. 2004, 2009) and applying the FP method (Magoulas et al. 2012), a velocity subsample (6dFGSv) containing about 8900 galaxies at redshift $z \leq 0.055$ has been extracted (Springob et al. 2014) and used to measure the growth-rate by RSD with 13% precision at redshift $z \approx 0.07$ (Beutler et al. 2012).
A successor survey of 6dFGSv is planned to begin in 2015, the *Transforming Astronomical Imaging surveys through Polychromatic Analysis of Nebulae* (TAIPAN), using the UK Schmidt Telescope with upgraded fiber-fed spectrograph to improve the velocity dispersion measurements. It is expected to extend the upper limit of 6dFGSv up to $z \approx 0.1$ and increasing the number density by ~20, collecting 500,000 redshifts over about ¾ of the sky with $r \sim 17$ and $K \sim 14$, of which 50 000 early types galaxies peculiar velocities.
At about a similar depth, the *Australian Square Kilometer Array Pathfinder* (ASKAP), a future HI survey probing the mass and dynamics of over 600,000 emission-line galaxies over 3π up to $z = 0.15$, deserving similar goals of producing 50,000 spiral galaxies peculiar velocities (Wallaby).

MSE could provide the natural extension of *Cosmicflow-2* (CF2), TAIPAN, ASKAP (WALLABY), covering 24,000 deg^2 (optimal requirement), i.e. ¾ of the effective, full sky visible from Mauna Kea, with a viable minimal option at 10,000 deg^2 too. Using the FP method to measure the distance of early-type galaxies and improved TF techniques for late-type galaxies, preserving similar number density, sampling, and sky coverage of CF2 while attaining redshift as high as $z \approx 0.25$ ($cz \leq 75000$ km s^{-1}; note that by adopting a grouping technique, further improved by Wiener filtering as in Tully *et al.* 2014, one can reduce the error on velocity field down to 10%), a MSE velocity survey will improve the CF2 volume by a factor ~150, tracing the velocity of about 1 Million galaxies. **The structure and dynamics of the cosmic web, which accordingly would be explored up to a volume of 3 Gpc^3 largely encompassing the homogeneity scale predicted by WifggleZ (400 Mpc), will represent the pivotal application of such a survey. This will be the only survey that could disentangle the reality of a cosmological bulk flow surviving the 800 Mpc scale as claimed by clusters observations (Kashlinsky et al. 2011).**

The peculiar velocity data collected by MSE will, thanks to its unique observational set-up, further enable breakthroughs in the cosmological field with the following **three additional cosmological probes**:

- With an accurate measurement of the peculiar velocities, one could apply the method by Hoffman et al. (2012) to **reconstruct the velocity-based cosmic web, or V-web,** whose components (sheets, filaments, knots, and voids) are cinematically identified by the local value of the eigenvalues of the velocity shear tensor. Based on *N*-body simulations (see figure 1), this technique has been proven to resolve cosmic structures down to $\lesssim 0.1h^{-1}$Mpc, providing much more details than a similar classification algorithm based on the gravitational tidal tensor obtained from the density field (Hahn et al. 2007, Forero-Romero et al. 2009), which allows one to achieve only $\sim 1h^{-1}$Mpc resolution scale. The higher resolution can be explained by the slower evolution of the velocity field away from the linear-regime than the density field, which therefore

retains less memory of the initial conditions. The V-web further provides a **platform to investigate the segregation of galaxies and halos with respect to their environment and dynamics**, exploiting the high-resolution capabilities of MSE spectra.

- Redshift space distortions are one of the most promising observable to investigate the linear growth of structures, directly probing the **(modified) theory of gravity**. Unlike the standard measurement based on galaxy redshift surveys with single tracers, the **velocity-velocity and velocity-density power spectra that can be directly estimated from velocity surveys avoid the cosmic variance limit**; indeed, by measuring simultaneously the galaxy density and peculiar velocities, which share the same random perturbation, no assumptions about the bias are demanded. Predicting the expected velocities from the smoothed galaxy distribution and comparing with the observed peculiar velocities, the measurement of $f\sigma_8$ or β from angle-averaged auto- and cross-power spectra of galaxy density and line-of-sight peculiar velocities can therefore attain arbitrarily high precision; unlike constraints from RSD by redshift surveys (unless adopting the multi-tracer technique by McDonald & Seljak 2009), the

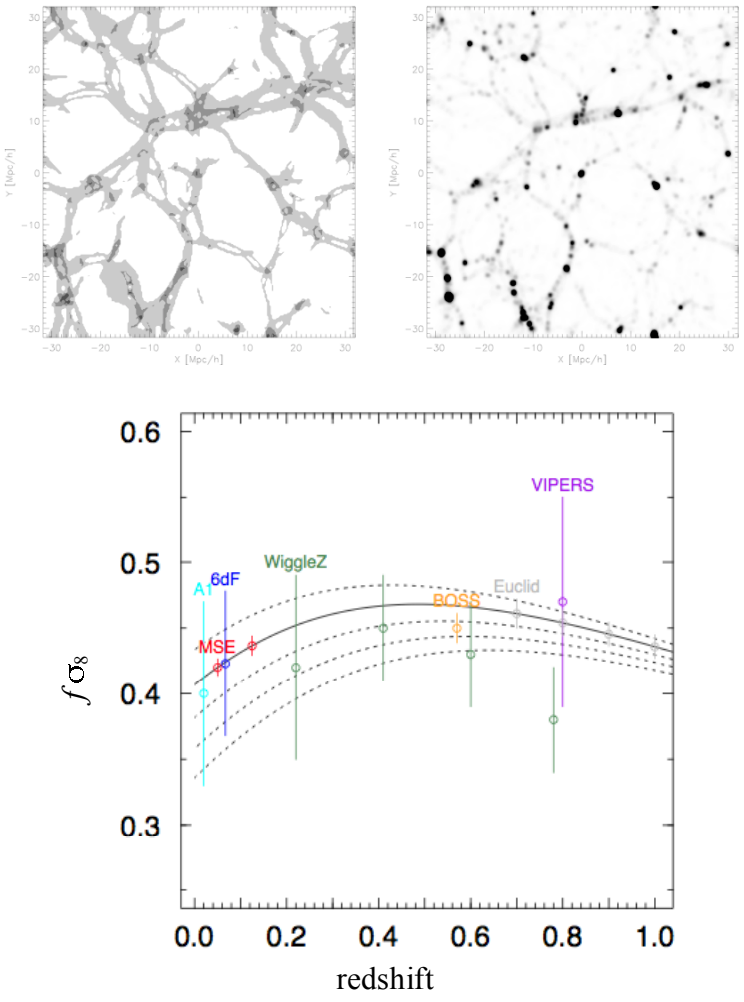

Figure 1: Cosmic-web components (voids, filaments, sheets, and knots in white, light gray, dark gray, and black, respectively) reconstructed from the velocity shear tensor (V-web, *left*) and the density field (*center*), which allows for ~10 times lower resolution scale (adapted from Hoffman et al. 2012, based on N-body simulation study). *Bottom:* Low-z constraints on the linear growth-of-structures from RSD by two-field technique (Fisher-analysis) for a 24,000 deg^2 MSE velocity survey with $n(z = 0.05) = 0.03\ h^3/\mathrm{Mpc}^3$ and $n(z = 0.125) = 0.003\ h^3/\mathrm{Mpc}^3$; for reference, ΛCDM (WMAP9) model with growth rate index $\gamma = 0.55$ (solid) and alternative models with $\gamma = 0.5, 0.6, 0.65$ (dashes, top to bottom).

relative error of these parameters monotonically decreases with the mean number density of sources, n (Koda et al. 2014), yielding an improvement by a factor of ~5 on current constraints by on $f\sigma_8$ and β at low-redshift (see figure 1). The table shows Fisher-analysis constraints that can be achieved by a MSE peculiar velocity survey with two densities; relative error can attain 1% level. Besides, as not affected by cosmic variance, peculiar velocity surveys are also the ideal framework to investigate primordial non-Gaussianities and general-relativistic (gauge) effects specific of large scales (Jeong, Schmidt & Hirata 2012; Villa, Verde & Matarrese 2014).

	$n = 0.003\ h^3/\mathrm{Mpc}^3$		$n = 0.03\ h^3/\mathrm{Mpc}^3$	
	$0<z<0.1$	$0.1<z<0.25$	$0<z<0.1$	$0.1<z<0.25$
$\delta\sigma_8/\sigma_8$	0.0419	0.0183	0.0152	0.0082
$\delta\beta/\beta$	0.0386	0.0166	0.0156	0.0076

Table 1: Optimal option for the survey is reaching a density of peculiar velocities of $n \approx 0.03\ h^3\mathrm{Mpc}^{-3}$ (ie: 2500 gal/deg^2 for 24,000 deg^2) allowing an improvement by a factor ~3 on cosmological parameters as seen in figure 1.

- A unique cosmological application of peculiar velocity surveys is the direct measurement of the so-called **kinematical backreaction** (Buchert 2000) – the pure general-relativistic mechanism due to small-scale inhomogeneities, intrinsic in the non-linearity of the Einstein equations, supplying effective energy sources in the Friedmann equations dynamically equivalent to dark matter (on small/galactic scales) and to dark energy (on large/cosmological scales). In the era of precision cosmology, aiming at validating or disproving the cosmological standard model and the theory of General Relativity, a quantitative measurement of this quantity is mandatory; a not-vanishing value would definitely indicate the necessity to revisit the standard FLRW model. Peculiar velocity surveys provide the genuine key ingredient to probe this concept; as long as the velocity field in redshift space is irrotational, one can directly infer the backreaction term **by the morphology of the velocity potential** (e.g. Nusser & Davis 1994) **probed using the so-called Minkowski functionals** (Buchert 2008, eq. 59).

3. Key astrophysical observables

- Required key measurement of the source spectrum:
  Redshift from VIS-NIR (3900-8600Å, or widest possible), width of emission and absorption lines (MgI, MgII, [OII], Hb, [OIII], NaD, Ha).
- Accuracy of the measurement:
  FP method: similar spectral resolution as TAIPAN, i.e. optimal: 30 km/s still viable option is $\lesssim$ 60 km/s rest-frame.
  TF, BTF, and OTF methods (see below), i.e optimal as in radio-ASKAP: 4 km/s, still viable option is $\lesssim$ 30 km/s rest-frame.
- "Standard" or envisioned technique for extracting the information from the data:
  Standard technique: FP method, based on measurement of stellar radius and velocity dispersion of early-type galaxies; it requires mid-resolution spectra and

exquisite photometry (see section 4).
Envisioned technique: baryonic Tully-Fisher (BTF, Zaritsky, Courtois et al. 2014) and «optical Tully-Fisher» (BTF, to be implemented), allowing the use of late-type galaxies. The successful measurement depends on high signal-to-noise.

4. Target selection

- Pre-imaging data for target selection will be likely provided by Pan-STARRS, CFIS, and Euclid (all sky wide survey), and by LSST and DES for Dec < 30°. Photometric data for extracting distance measurement: accuracy must be < 5%, or 0.1 mag preferably. Photometry in *i* band is best.

- The recommended magnitude limit are $r < 24.5$, $i < 24.5$, $J < 15.2$ (*J*-band similar to TAIPAN). We used to estimate the number of targets the same numbers as in SRO lead by Aaron Robotham:

z<0.25 & Area=24,000 & i<24.1 & M_i < -21.3 (M* and brighter) = 2.3Millions galaxies
z<0.25 & Area=24,000 & i<25.3 & M_i < -21.3 (M* and brighter) = 2.7Millions galaxies

A M* galaxy at z=0.25 with typical size 30 Kpc is 7.7 arcsec across, corresponding to 8 fibers of 0.9 arcsec. We propose to use bundles of 19-Fiber Y Bundle on both spirals and ellipticals in order to reach for the full mapping of the dynamics of the galaxy, measuring an exact velocity dispersion at the effective radius for ellpticals and allowing for an excellent measurement of BTF for spirals.

Best option : 24,000 deg^2, i.e. 3π excluding the Milky Way = 96 galaxie/deg = 144/ MSE FOV
144 targets X 19 fibres = 2736 fibers/FOV
Total data = 43 Million spectra

- Source density: Best option: mean number density of peculiar velocities $n \approx 0.03$ h^3Mpc^{-3} (2500 gal/deg^2 for 24,000 deg^2) allowing an improvement by a factor ~3 on cosmological parameters (see table 1).
Minimal viable option: mean number density of peculiar velocities $n \approx 0.003$ h^3Mpc^{-3}, with even distribution across sky, covering 10,000 deg^2 (1000 gal/deg^2 for 10,000 deg^2).

- Total number of science targets required to be observed to enable science goal:
Best option: about 2.5M L* galaxies over 24,000 deg^2 with i< 24.1.

5. Cadence and temporal characteristics

- Repeat observations are required only for “high value objects”. A spectroscopic success rate as large as large 80% while observing new fields to achieve the largest sky coverage possible is preferred, to reduce the cosmic variance.
- There are no specific issues relating to the timing of the observations.

6. Calibration Requirements

- Wavelength calibration: standard.
- Sky subtraction: standard (using fibres on sky).
- Flux (spectro-photometric) calibration: using standard stars.
- Telluric absorption: standard.

7. Data processing

- The removal of instrumental signatures can be done using standard procedure.
- From standard spectra the following astrophysical quantities will be measured: redshift from emission lines and continuum (Balmer break), velocity dispersion from width of absorption and emission lines.
- Pan-STARRS, CFIS, and Euclid would assure the necessary high-precision photometry of MSE sources; TMT would follow-up of MSE sources).
- The desired deliverables to the science team includes raw data and wavelength calibrated spectra.

8. Any other issues

None.

Mapping the dark matter distribution through velocity shear

Tag: **MSE-highz-SRO6**

Lead: **Carlo Schmid,** Eric Jullo, Jean-Paul Kneib, Johan Richard, Carlo Schimd, Edwar (Ned) Taylor, Ludovic Van Waerbeke

1. Abstract

Gravitational lensing shears the velocity field of disk galaxies in a non-trivial way, yielding to an angle between the maximum- and null-velocity axes that differs from the 90° expected without lensing. Likewise, in presence of lensing, the velocity and morphological position angles do not coincide anymore. Using 7-fibres bundles (IFUs) with total effective diameter 1.8"-2.7" (or 19-fibres bundles for high-value objects) to map at high-resolution the velocity field of spiral galaxies at redshift $z \sim 0.3$-1.0, one can directly point-wise estimate the gravitational shear attaining values as low as $\gamma \sim 0.03$, typical of cosmological weak-lensing, or larger values as due to galaxy clusters typically located at $z \lesssim 0.5$. This technique, so far proposed in the radio domain and based on high-resolution HI velocity maps, can provide an independent measurement of gravitational lensing of galaxies, aiming at improving the mass modeling of the large-scale structure and clusters, with a smaller number of galaxies than required by traditional (statistical) methods.

2. Science Justification

Gravitational lensing, one of the best probes to map the spatial distribution of dark matter and explore cosmology, is traditionally measured looking at the deformation and magnification of background images induced by the intervening matter. In weak and intermediate lensing regimes (κ, $\gamma \lesssim 0.01$-0.1), the required precision is achieved by considering a large number of background sources, eventually averaging over them and looking at the correlation of their shapes. This method is the core of the major weak-lensing projects, e.g. CFHTLenS, RCSLenS, CS82, KiDS, DES, HSC, and will be extraordinarily improved by LSST and ultimately Euclid and WFIRST in the visible and NIR wavelength domain.

Alternatively, one may consider the *effect of gravitational lensing on the velocity field* of the background sources, in particular late-type galaxies; gravitational lensing anisotropically stretches the major and minor axes of the luminosity profile of extended sources, and then their velocity field. As illustrated in the figure, considering as background source an ideal, late-type galaxy of angular diameter ~10 arcmin, i.e. a thin circular disk with a non-trivial

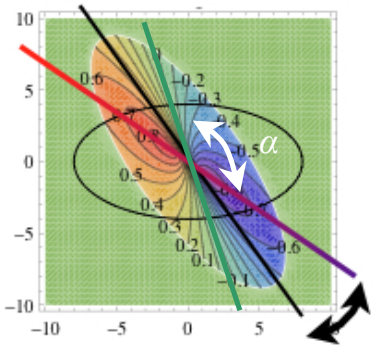

inclination with respect to the line-of-sight (i.e. neither face-on nor edge on, appearing as an ellipse in the source plane; black line) and with a fairly simple rotation curve (here fitting NGC 3145), because of lensing the maximum-velocity axis (aka «velocity position angle», vPA, defined by the locations of maximum and minimum of the velocity map) and the null-velocity axis (colored lines) are not perpendicular anymore. It can be proven (Blain 2002) that the angle between the two axes (in white in figure) depends on convergence κ and absolute value of the shear γ as

$$\alpha = 2\arctan\frac{1-\kappa+\gamma}{1-\kappa-\gamma} \approx \frac{\pi}{2} + 2\gamma - 2\kappa\gamma\,, \qquad (1)$$

the approximation being valid up to intermediate-lensing regime (κ, $\gamma \lesssim 0.1$).

To overcome the difficulty in determining the null-velocity axis, one can instead measure the angle between the velocity and morphological position angles, which in the image plane differs from zero in presence of lensing (black arrow, figure above).

Focusing on the Blain's technique, for a typical accuracy of the velocity position angle, ~5°, and *provided the null-velocity axis is determined with the same accuracy,* one might expect to be able to measure absolute shear larger then $\gamma > 0.03$ to 0.034 for convergence κ ranging from 0 to 0.1, respectively; see figure, illustrating the how an accuracy of 5° on α-90° (dark band; or increased by √2 [light band] if accounting for the error on the null-velocity axis, by linear propagation) does convert into the accuracy on γ.

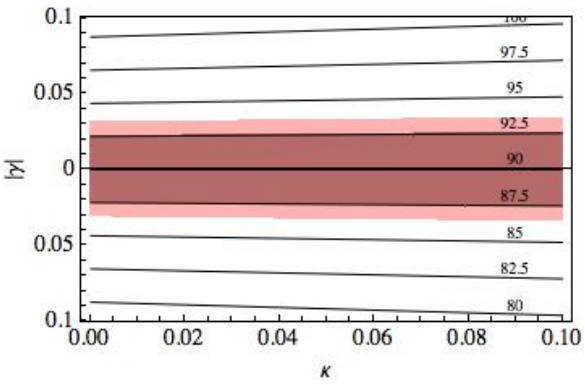

With a perfect velocity measurement based on the full map of the velocity field, such as provided by radio surveys (e.g. SKA), only two lensed galaxies are sufficient to exactly retrieve the intrinsic gravitational shear in weak-lensing limit (Morales 2006). A lower resolution velocity map as probed by high-resolution fibre-bundles (IFUs), eventually improved by a stacking technique of close galaxies, can still bring off the same goal in the *weak- and intermediate-lensing regime* (cosmic-shear and weak-lensing by galaxy clusters). Gravitational lensing estimated by velocity field will be sensitive to totally different systematics with respect to standard measurements based only on luminosity profile of background sources.

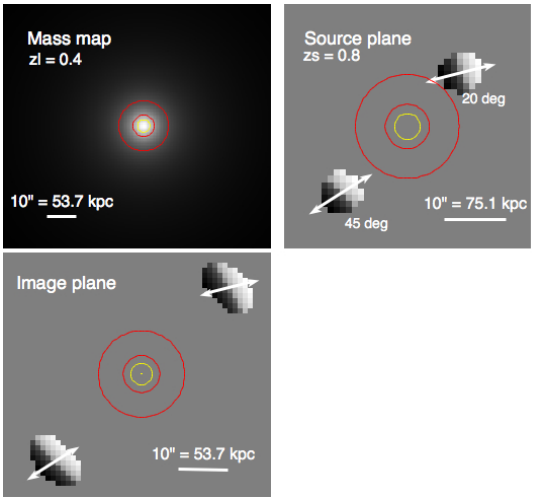

Simulation of the shear-velocity asymmetry, as produced by a foreground galaxy cluster of 10^{15} solar masses with isothermal, spherical profile (colored circles define critical curves and caustics), located at redshift $z = 0.4$ on two background galaxies, which are at $z = 0.8$ and inclined by 45 and 20 deg with respect to the line-of-sight as indicated (Planck cosmology). The velocity field of foreground galaxies is pixelized and shown in gray scale (□=1"). White arrows show the major axes of ellipses fitting the luminosity profile; while in the source-plane (top-right image) it is aligned with the maximum-velocity, in the image-plane it is not. The determination of the angle α (eq.1) strongly depends on the angular size of the fibre-bundle.

3. Key astrophysical observables

- The astrophysical observables (redshift and velocity field) are obtained from emission lines in *g, r, i, Z*, and NIR bands (either [OII] and Hα, or the [OIII] doublet; 3800-13000Å), measured in 7 (or up to 19 for larger IFUs) locations over the image supplied by fibre-bundles arranged in hexagonal (round) configuration.
- This measurement requires:

  1) <u>High spatial sampling</u>, with exceptional seeing conditions to resolve objects, which thus must have size 2-3 times the seeing (≳ 1.2" on Mauna Kea). Adopting fibre-fed IFUs, this requirement can be achieved with 7-fibres bundles with total effective diameter ⌀ = 1.8" (best option) to 2.7" (low-throughput option), corresponding to single fibres with effective diameter of 0.6" to 0.9". An ideal setup would further consider double-ring 19-fibres bundles with total effective diameter ⌀ = 3.0", to be used with galaxies of very large angular size (see e.g. Thorlabs' fibre-bundles).

  2) <u>Spectral resolution</u> $R > 1500$ is in principle sufficient for velocity rotation curves, unless aiming at measuring also the velocity dispersion to further improve the modelling of kinematics and physics of galaxies (in this case, $R > 3000$). Higher resolution, <u>$R \sim 4000$ at $\lambda > 5000$Å</u>, assures more efficient sky-subtraction and better resolution of the [OII] doublet (Comparat *et al.* 2014). The ideal SNR is ~ 10 per resolution element (pixel).
- The <u>standard technique</u> to measure the velocity profile at low redshift is based on the fit of the 2D velocity map by supposing a circular, flat rotator and adopting a model for rotational velocity with at least a 3 parameters (inclination of the galaxy, maximum velocity, and characteristic radius of the rotational velocity, described by tanh or simpler models). The «velocity position angle», vPA, is usually measured with ~5° accuracy for galaxies of diameter $2r_{gal} = 2\times3.2r^* \gtrsim 20$ kpc (r^* is the optical disk, defined for exponential luminosity profile by $I(r) = I_0 \exp(-r/r^*)$). *Without lensing,* the null-velocity axis is supposed orthogonal to the vPA. Dealing with lensing, <u>two techniques</u> are <u>envisioned</u>:

  1) A high-resolution measurement of the velocity map (data-cube) modelled by at least four parameters (i.e. three as in the standard technique along with absolute

shear); the high-resolution is mandatory to allow for a high S/N measurement of determination of the null velocity axis (see eq.1 above).

2) A combined measurement of the velocity map and the morphology of the luminosity profile of galaxies, to extract the difference between the vPA and the «morphology position angle» (mPA, defined by the major axis of the projected elliptical profile). The measurement of morphology will be standard, typically based on numerical tools such as SExtractor or any other shear measurement technique.

For both techniques, further improvements can be achieved by using a Tully-Fisher relation and more sophisticate modelling, e.g. using shapelets. The central fibre of the fibre-bundle, ideally centred on the source and therefore having the maximum SNR, would be used to measure the redshift; it will also help in defining the offset of the velocity map.

4. Target selection

- The pre-imaging can be provided by any imaging survey of the sky with 5σ point source fainter than i_{AB} = 24.5, and with image quality better than 0.6" (the fibre size). Euclid data will perfectly match the required photometric data.
- Luminosity distribution of targets: $r < 25$ or $i < 24.5$.
- Source density:

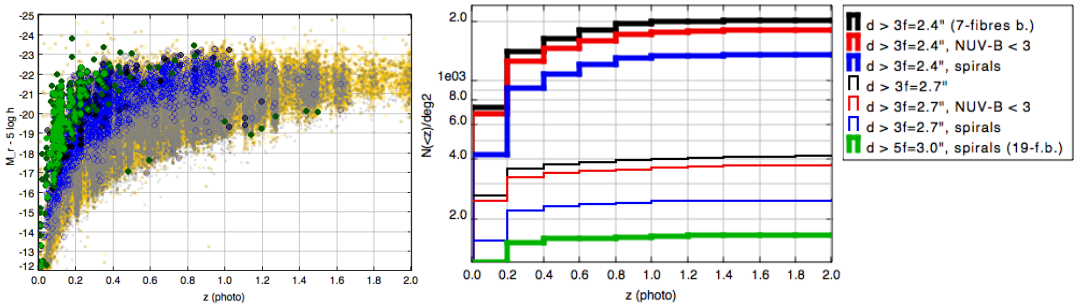

Left: absolute *r* magnitude as function of photometric redshift for galaxies with $i < 24.5$ galaxies and angular size $d > 0.6$" (yellow), 0.9" (gray); spirals (ZEST_TYPE = 2) than can be observed with 7-fibres bundles with fibre diameter $f = 0.6$" (blue) and $f = 0.9$" (black) are shown, along with spirals than can be observed with 19-fibres bundles with $f = 0.6$". *Right:* cumulative number count *N(<z)* per square degree; among the full sample of galaxies with $d > 3f$ (i.e. 7-fibre bundles; black lines), colour and morphological selections (red and blue) are shown for two sizes of fibres (thick: optimal option; thin: minimum requirement). For the morphological selection only, galaxies with size encompassing a 19-fibres bundle are shown (green). Estimation based on ACS-COSMOS.

A survey with magnitude limit $i < 24.5$ is expected to yield:

a) best option, i.e. 7-fibre bundle with fibre diameter $f = 0.6$": ~1300 deg^{-2} spiral galaxies with size larger than $3f = 1.8$" (i.e. ~2000 IFUs over FoV = 1.5 deg^2);

a)* high-value targets, i.e. 19-fibre bundle with $f = 0.6$": ~280 deg^{-2} spiral galaxies with size larger than $5f = 3.0$" (i.e. ~420 IFUs over FoV = 1.5 deg^2);

b) low-throughput option, i.e. 7-fibre bundle with $f = 0.9$": ~250 deg^{-2} spiral galaxies with size larger than $3f = 2.7$" (i.e. ~370 IFUs over FoV = 1.5 deg^2).

These estimations are based on ACS-COSMOS, extrapolating the classification by

spectral type ZEST_TYPE = 2 (if using instead the colour criterion $NUV - B < 3$ to identify late-type galaxies, one would obtain 35-50% more targets per square degree).

- The total number of science targets should be as large as possible, therefore achievable by the largest sky coverage possible, allowing to apply stacking to reduce the statistical errors and in order to maximize the cosmological constraints and the accuracy of the mass modelling of galaxy clusters.

5. Cadence and temporal characteristics

- Considering 3200 (nominal) or 5000 fibres arranged into IFUs units with 7- or 19-fibre bundles, repeat observations are required (see Section 4):

	3200 fibres	5000 fibres
a) *best option* (7-fibres bundles, $d_{\text{fibre}} = 0.6$")	**4-5 passes** (456 IFUs)	**~3 passes** (714 IFUs)
a*) *high-value targets* (19-fibres bundles, $d_{\text{fibre}} = 0.6$")	**2-3 passes** (168 IFUs)	**~2 passes** (263 IFUs)
b) *low-throughput option* (7-fibres bundles, $d_{\text{fibre}} = 0.9$")	**1 pass** (456 IFUs, ~12 not used)	**~1-2 passes** (714 IFUs)

The estimation for option a*) is tentative: high-value targets, i.e. big galaxies with size encompassing a 19-fibre bundle, populate fields containing small galaxies for which a 7-fibre bundle is sufficient. Option a) must be considered as upper bound.

- No requirement for large-scale (cosmological weak-lensing) applications. Only for the modelling of the mass distribution of galaxy clusters one can envisage observing periods specific of the galaxy clusters of interest.

6. Calibration Requirements

Including quantitative discussion of all issues relating to required accuracy, including:

- Wavelength calibration, flux (spectro-photometric) calibration, and telluric absorption: standard calibration is required.
- Sky subtraction: a careful sky subtraction is required in the red part of the spectrum, where emission line of interest will be amongst the OH sky lines. For small galaxies, with size smaller than the fibre-bundle diameter, some fibre might be partially or totally dominated by sky.

7. Data processing

- Removal of instrumental signatures:
  Spatial PSF, spectral PSF as well as angular pixel size and spectral sampling are considered. The total PSF is convolved with a kinematic model of the galaxy.
- Measurement of astrophysical quantities from spectra:
  1) For all the 7-fibres (o 19-fibres) pointing each galaxy: wavelength, width, and

flux of emission lines, to be compared to corresponding values from the centre of the galaxy (central fibre); width of emission lines are used to model the velocity dispersion.
2) SED fitting for morphological confirmation of the pre-selection.

- Ellipticity of spiral galaxies from Euclid photometry.
- Desired deliverables to the science team: raw data, calibrated spectra, photometry.

8. Any other issues

Similar analysis can be done in radio domain; full velocity maps at very-high resolution as measured by SKA will represent an extraordinary test and calibration benchmark for visible-NIR measurements.

MSE Synergy with upcoming facilities

Tag: **MSE-highz-SRO7**

Lead: **Simon Driver**, Matt Jarvis, Jeff Newman, Aaron Robotham, Firoza Sutaria

1. Abstract

This SRO is a placeholder for the many synergistic projects that can potentially take place with MSE as a partner-player. The objective is to ensure that design issues that may be relevant to these projects are considered from the outset. We identify the following serious issues:

Coordination between Euclid, WFIRST, LSST, SKA and MSE is essential, the deep fields of the facilities MUST be coordinated in some way requiring cross-facility collaboration at the earliest possible opportunity.

For GRB research, it is also essential there is coordination between *Swift (*+ any other GRB specific mission*)* and MSE. Further, fast follow-up of rapidly evolving transient phenomenon like GRBs requires short slew times (ideally under a minute).

All MSE extra-galactic survey regions should aim to be near the equator (to aid observability from both hemispheres) but ideally not exactly on it (to improve SKA UV plane rotation). They should avoid the Ecliptic (Euclid, WFIRST) and the plane of the Milk-Way. The latter is a normal constraint, but Euclid in particular is very conservative in its survey design, so it will avoid the Milky-Way by a large margin.

2. Science Justification

From an extra-galactic point-of-view a large number of complementary multi-wavelength information is required to fully describe the physics within galaxies. Table 1 (taken from Meyer et al 2015) presents the most basic characteristics that we would ideally want to measure, and the multi-wavelength tracers that can measure them.

Property	Tracers
atomic gas mass	HI
molecular gas mass	mm emission lines (eg. CO)
stellar mass	optical/NIR multiband photometry (eg. K, g-i), optical spectroscopy
dust mass/temperature	mid/far-IR multiband photometry, (sub)mm continuum
morphology	panchromatic high resolution imaging, fitted structural parameters and decomposition (bulge, disk, bar)
star formation rate	Hα, UV, radio continuum, mid-IR
supermassive black hole	optical emission line diagnostics, radio continuum
chemistry	optical/submm/mm spectroscopy via emission/absorption lines (high R)
dynamics	line fitting (optical, near-IR, CO, HI), spatially resolved (optical IFU, CO, HI)
environment	redshift surveys (low R) + group catalogues (membership, multiplicity, halo mass, central/satellite classification), photo-z (multiband optical/NIR, large scale structure), X-rays (clusters, hot groups, massive halos), radio SZ (clusters, high-z)
distance	redshift (Hubble flow), Tully-Fisher (HI+optical/NIR imaging), Faber Jackson/Fundamental Plane (optical/NIR imaging and spectroscopy)

Table 1: Physical quantities and their multi-wavelength tracers (Meyer et al 2015)

To ensure the full range of extra-galactic physics is measured in future MSE surveys it is extremely important that full care is given to complementary facilities. Facility arrogance, i.e. the assumption that a particular new facility is the most important and will therefore drive the design of other surveys, is a common problem in astronomy. It is particularly prevalent across traditional wavelength divides (e.g. optical and radio), where the issue is one of culture and knowledge than arrogance. The simplest mechanism to overcome this tendency for extra-galactic surveys is to apply a few basic rules that maximize potential synergies without active coordination:

- Design surveys as near the equator as possible (certainly within +/- 30), ensuring they are observable from both hemispheres. Next generation spectroscopic facilities are largely in the North, whilst LSST and most next generation radio surveys (MeerKAT, ASKAP and SKA) are in the South. This target region restricts facilities to 50% of the available sky.
- Avoid the plane of the Milky-Way and Ecliptic by a healthy margin (+/- 15 degrees at least). Euclid, WFIRST and JWST will certainly aim to avoid both. This restriction also restricts facilities to 50% of the available sky.

Combining these two restrictions would suggest a common 25% of the whole sky to

concentrate potential observations on. In fact, since the ecliptic plane largely crosses the equatorial plane the impact is worse, and the available sky for extragalactic synergy observations becomes ~20%, i.e. ~8000 sq deg. For potential synergy science such restrictions are pragmatic and conservative. A strong case could be made that any proposed MSE survey should need a compelling reason to observe outside of this next-generation synergetic zone.

2.1 Transients (*Swift*, Fermi, LSST, ZTF, other transient factories)

Optical spectroscopic studies of GRB afterglows and their host galaxies is essential for

- Establishing or confirming a relationship between the properties of the host-galaxy and the GRB.
- Providing important clues as to the nature of the central engine.
- Determining the role played by the progenitor environment in the various stages of the event's temporal evolution.

So far, deep optical follow-up has not been possible for short duration GRBs, as these have the faintest optical afterglows. While immediate follow-up of optical outbursts will require fast slew times, with its greater sensitivity, MSE should be capable of spectroscopically tracking the afterglows to much fainter magnitudes, and hence in to the late evolutionary stage of the event. For short duration GRBs, this would result in some of the first, deep spectroscopic studies of the optical afterglows. For the long duration events, if the IGC paradigm is true, the all long duration GRBs should show some SNe activity, which may have been missed out by the present generation of optical telescopes because of their intrinsic faintness (SNe spectrophotometric observations have been limited to $z \sim 1$ for that reason), and because of the over-subscription of observing time on large (8m class) telescopes. Dedicated MSE target of opportunity time, combined with surveys like LSST, should be able to pick up these events.

One of the goals of MSE will be to build up a high-resolution spectroscopic database of faint objects, including high-z galaxies. The redshift is unknown for several Swift discovered GRBs, because of magnitude constraints on current photometric catalogues (e.g. this SDSS survey). The limits will be lowered to $i = 25.3$ mag in the post-LSST era, and hopefully, optical sources at the location of such "historical" GRBs may be identified. A high-resolution spectroscopic survey of the host galaxies by the MSE will help resolve questions regarding GRB-host galaxy associations in the high-z, visible universe.

2.2 Photometric redshifts (LSST, Euclid and WFIRST)

Lacking a comprehensive knowledge of galaxy spectral evolution, the only way in which photo-z errors can be reduced and biases characterized is using sets of galaxies with robust spectroscopic redshift measurements. We follow Newman et al. (2014) in dividing the uses of spec-z's into two broad classes, "training" and "calibration." Training constitutes the use of samples with known redshift to develop or refine algorithms, and hence to reduce the random error on individual photometric redshift estimates. In contrast, the problem of calibration is that of determining the true overall redshift distribution of

samples of objects selected in some way; mis-calibration will lead to systematic errors in photo-z's, and hence in dark energy inference. For LSST, for instance, it is estimated that the mean redshift for each sample used for cosmology (typically, objects selected within some bin in photometric redshift) must be known to $\sim 2 \times 10^{-3}(1 + z)$, i.e., 0.2%.

For both training and calibration purposes, we require a set of objects for which the true redshift is securely known; this is only possible with spectroscopy. If spectroscopic redshifts could be obtained for a sufficiently large, fair sample of those objects for which photo-z data is available from LSST, both training and calibration needs can be fulfilled using the same data. However, real spectroscopic samples have fallen well short of this goal (e.g., the DEEP2 Galaxy Redshift Survey obtains secure redshifts for ~ 75% of objects targeted for spectroscopy – a systematically biased subset); hence other methods may well be needed for calibration. MSE surveys can contribute to both aspects of the problem.

2.3 Radio (Square Kilometer Array)

The SKA will be a transformational telescope with the capability of detecting Milky Way-type galaxies via synchrotron radiation into the epoch of reionization, AGN of all types and luminosity, in addition to tracing the neutral hydrogen content of galaxies to z~2. However, optical spectroscopy of such galaxies will still be crucial to maximise the scientific output of the SKA, and to gain the biggest leap in our understanding of galaxy formation and cosmology. The SKA will be predominantly Southern hemisphere, with coverage South of +30 Dec expected. This clearly highlights the importance of any synergetic surveys being close to equator in order to maximize science return. This creates no particular disadvantage for MSE, but it should be noted that it has a clear impact on radio UV plane rotation (there is a preference to be more than 5 deg from the equator, e.g. ASKAP survey design). The precise impact depends on the array design, but it needs some future coordination to ensure no science is overly hindered. A mutually inconvenient field at -5 deg in declination is probably about optimal for combined MSE and SKA surveys.

2.3.1 Tracing the evolution of galaxies

The extreme sensitivity of the SKA means that it will be able to detect star- forming galaxies in radio continuum emission to high ($z >> 1$) redshifts. However, the lack of spectral features in the radio continuum means that additional wavelength observations are required to obtain redshift information, along with obtaining important physical characteristics of the stellar populations via measurement of ages and metallicity etc., or for the presence of AGN activity via emission line diagnostics. Therefore, MSE can play a critical role in providing key information for understanding the evolution of AGN and star-forming galaxies detected with the SKA.

The SKA will also carry out a 3-dimensional survey of the sky, acting like the super-integral-field unit that is sensitivity to neutral hydrogen in emission and absorption. On the HI side, even the SKA will not be sensitive enough to directly detect HI in all but the gas rich galaxies out to z~2. Therefore, much effort is currently being focused on

methods for stacking based on galaxies with known redshifts. The precision required for the redshifts is such that spectroscopic data is far more valuable than the more abundant imaging data from which photometric redshifts can be derived. Thus, MSE could provide the ideal spectroscopic sample to carry out HI stacking analyses of galaxies based on galaxy properties such as age, morphology, redshift etc.

2.3.2 SKA Cosmology

One of the most straightforward and obvious experiments to carry out with MSE and SKA is to perform a redshift survey of all continuum radio sources over a large volume. Such a survey would allow the low-redshift radio sources to be separated out from those faint, and predominantly high-redshifts sources, where obtaining a spectroscopic redshift is all but impossible. This information can then be used to measure the galaxy power spectra in tomographic shell, thus providing novel measurements of the large-sale power on super horizon distances at high redshift (see e.g. Camera et al. 2012).

It is now becoming apparent that cosmology is becoming systematics limited rather than statistics limited. Thus, optimal methods of combining data from experiments with different systematic uncertainties can lead to fully cancelling such issues. One particular area of synergy between MSE and SKA will be the construction of galaxy redshifts catalogues based on different tracers of the underlying density distribution, e.g. precise redshifts for luminous red galaxies from MSE and precise redshifts for lower mass, gas-rich galaxies detected in HI with the SKA. These galaxies trace the underlying dark-matter distribution with vastly different bias, thus allowing the so-called “multi-tracer” technique (Seljak 2009) to be used in order to overcome cosmic variance effects (see e.g. Ferramacho et al. 2014).

A further area of direct synergy will be to obtain spectroscopic redshifts of distant galaxies that are used for weak lensing. In much the same way as for optical surveys, redshift information adds significant power to weak lensing analyses, allowing the growth of structure to be traced. Radio weak lensing is in itself extremely complementary to optical weak lensing surveys, as the systematic uncertainties are different, e.g. the wavelength-dependent PSF is know analytically in radio interferometry but the source density is generally lower (until SKA2), thus the same spectroscopic survey used to supplement optical weak lensing surveys can play the same role in radio weak lensing.

2.4 Space-based imaging (Euclid and WFIRST)

Euclid and WFIRST will provide extremely deep high-spatially resolved imaging (~0.2”) and hence are capable of discerning structure to sub-kpc scales out to redshifts greater than 2.5 at rest-optical wavebands. The emergence of structure on kpc scales is of great interest and a key research area. In Driver et al (2013) it was proposed that galaxies form via two stages, firstly bulge formation via some dynamical hot process (i.e., collapse, rapid merging, disc instabilities and/or clump migration), and secondly disc formation via a more quiescent dynamically cool process (i.e., gas in-fall and minor-merger accretion events) with the pivotal redshift at z~1.5 (see Fig 1).

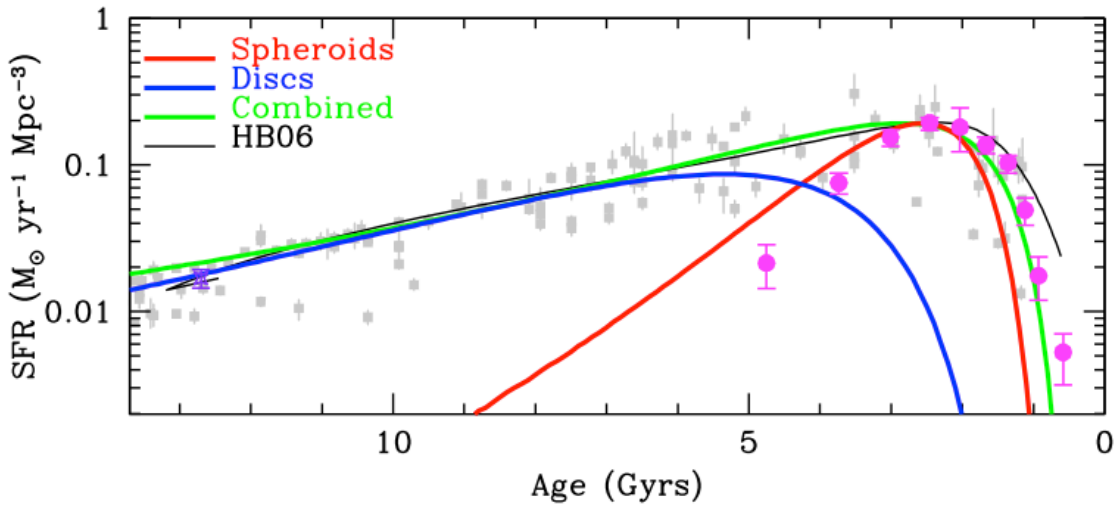

Figure 0: The cosmic star-formation history of spheroids and discs (as indicated) taken from Driver et al. (2013). Also show is the AGN density (pink dots) coincident with spheroid formation. In the above scenario bulges form first followed by disc growth.

At later times during periods of low interaction rates (see Robotham et al 2014) bars emerge along with disc-buckling and pseudo-bulge formation. In the present day Universe systems adhere to the Hubble sequence, at earlier times galaxies appear more lie train-wrecks, as unveiled by the Hubble Space Telescope. While the Hubble Space Telescope and its successor the James Webb Space Telescope have provided this kind of high quality imaging for some time, the fields of view have been very small with only the COSMOS survey extending beyond a square degree. While this provides insight into the morphologies of galaxies at very high redshifts (and higher with JWST) the epochs and process by which each structure (bulge, bar, disc) emerge is empirically unconstrained. Euclid and WFIRST will provide high quality imaging over very extensive areas. This will allow us to directly measure the epochs at which the various structures emerge (e.g., bulge, disc formation) and how they evolve (i.e, growth of spheroids, bulges, and discs).

To fill in the void between the very nearby surveys such as SDSS and GAMA and the very distant surveys with HST and soon JWST requires the *combination* of Euclid/WFIRST imaging with LSST photometric-redshifts and MSE spectra. This will allow us to extract star-formation rates metalicities, and will confirm pair membership to establish merger rates. The combination of data from Euclid/WFIRST/LSST (and even SKA) with MSE spectral analysis should provide a complete blueprint of galaxy evolution from the present epoch to the peak of the cosmic star-formation era (i.e., $z = 0$ to $z \sim 2.5$). Beyond this limit space-based mid-IR spectroscopy would be required. Samples sizes need not be large however. The crucial element will be the ability to obtain reasonable S/N spectra (i.e., ~30) for high-z ($z \sim 2.5$), faint ($i \sim 25$ mag) systems with a high-level of completeness. This requires two key factors: aperture (to reach the S/N levels required) and wavelength coverage (to reach to high redshift). The requirements of this project are essentially identical to those in **MSE-highz-SRO2** and **MSE-highz-SRO2** except with the addition of coordination with Euclid, WFIRST, LSST and SKA.

3. Key astrophysical observables

3.1 Transients

The key science requirement is host galaxy photometric and spectroscopic identification and characterization. Relevant to MSE, we also wish to track the spectral evolution of the GRB afterglow in the optical band.

Having a method to respond rapidly is advantageous if MSE is to be used to observe afterglow. It is worth noting that MSE would offer a relatively inefficient method to observe GRB sources in follow-up mode since they are spatially and temporally rare (Gemini and other 8m facilities would be as competitive for pure follow-up). Where MSE could offer a serious advantage is in pre-characterising galaxies that are subsequently found to host GRB events, and for measuring the large scale environment around known GRB events.

3.2 Photometric redshifts

We wish to obtain secure redshifts for as many objects as possible. This will generally require the identification of multiple features (e.g., multiple emission or absorption lines, or both components of a resolved doublet) to provide an unambigous redshift identification. As a result, broad wavelength coverage (to span multiple features), high throughput and good sky subtraction (to provide a sensitive detection limit), and moderately high resolution (especially in the red part of the spectrum, as the [OII] 3727 doublet is a key redshift diagnostic at $1 < z < 2$) are desirable.

The key result from MSE will be measurements of redshifts with reliable estimates of each object's redshift robustness. For many applications, even a 1% incorrect-redshift rate would cause systematics at a level large enough to compromise dark energy inference. The main approaches to obtaining photo-z are via training and callibration. Below we detail the spectroscopic requirements from MSE for LSST photo-z.

Training: A minimum of 30,000 spectra (ideally $\sim 10^5$) spanning the full range of properties of LSST samples are required to accurately characterize objects in both the core and outlier regions of the photo-z error distribution. To mitigate the effects of sample/cosmic variance, these observations must span a minimum of 15 widely-separated fields that are at least ~ 20 arcminutes (i.e., multiple correlation lengths) in diameter (if the MSE field of view is substantially larger than this, fewer fields may suffice).

Better photometric redshift training will improve almost all LSST extragalactic science, and hence address a wide variety of science goals; the spectroscopy needed for this training would simultaneously provide an extraordinarily rich dataset for studying galaxy evolution down to faint magnitudes, with considerable overlap with other MSE science goals.

Calibration: Given that deep redshift samples have failed to yield secure redshifts for a systematic 20%-60% of their targets, it is a strong possibility that redshift samples

obtained for photo-z training will not be complete enough to solve the calibration problem. The best options in this scenario are provided by cross-correlation methods. These methods cross-correlate positions on the sky of objects with known redshifts with the locations of those galaxies whose redshift distribution we aim to characterize. We can then take advantage of the fact that bright galaxies (whose spectroscopic redshifts may be measured easily) and fainter objects (which can only be studied with photo-z) both trace the same underlying dark matter distribution. As a result, by measuring the cross-correlation signal as a function of the known spectroscopic redshift, one can determine the z distribution of a purely photometric sample with high accuracy.

Cross-correlation calibration for LSST will require spectroscopy of a minimum of $\sim 10^5$ objects (in order to limit shot noise) spanning hundreds of square degrees (to limit the impact of field-to-field variations in measured clustering amplitudes, which dominate errors if field sizes are small). The auto- correlation properties of the spectroscopic sample must also be measured, requiring that, if spectroscopic data is obtained in many small fields, those fields must span several clustering scale lengths ($\sim 5h^{-1}$ Mpc co-moving for typical galaxy samples, corresponding to a minimum field size of 20 arcminutes in diameter at $z \sim 1$). The spectroscopic sample need not be representative in type or magnitude, but it must span the entire redshift range of and overlap spatially with the photometric sample that is to be calibrated. If MSE conducts a dilute survey of both galaxies and QSOs over wide areas of sky, as suggested in Section XYZ the data obtained may well be sufficient to provide an accurate calibration of LSST photometric redshifts, with little or no modification of the survey strategy.

3.3 Radio

The synergy between various future facilities, concentrating in particular on their relationship to the SKA, has been discussed in detail in Meyer et al 2015 (PoS AASKA14 131). Figures 1-3 present various issues that must be addressed, and are presented in Meyer et al 2015. Figure 1 shows the next decade of planned imaging, spectroscopic (including MSE), IFU and radio facilities. Darker colouring indicates a facility that is better for survey science within its particular waveband type (e.g. optical or NIR). Figures 2 and 3 show the complementarity of different depth SKA surveys and fibre spectroscopic surveys. The bottom-left panel of Figure 3 shows that a deep 6 deg^2 2 year integration with SKA-2 is best matched by a $r = 26$ ($i \sim 25.3$) survey. In combination with LSST, this is exactly the type of survey that MSE is prefectly placed to execute.

Regarding future radio observations, SKA MID and Survey are certainly the facilities best matched to

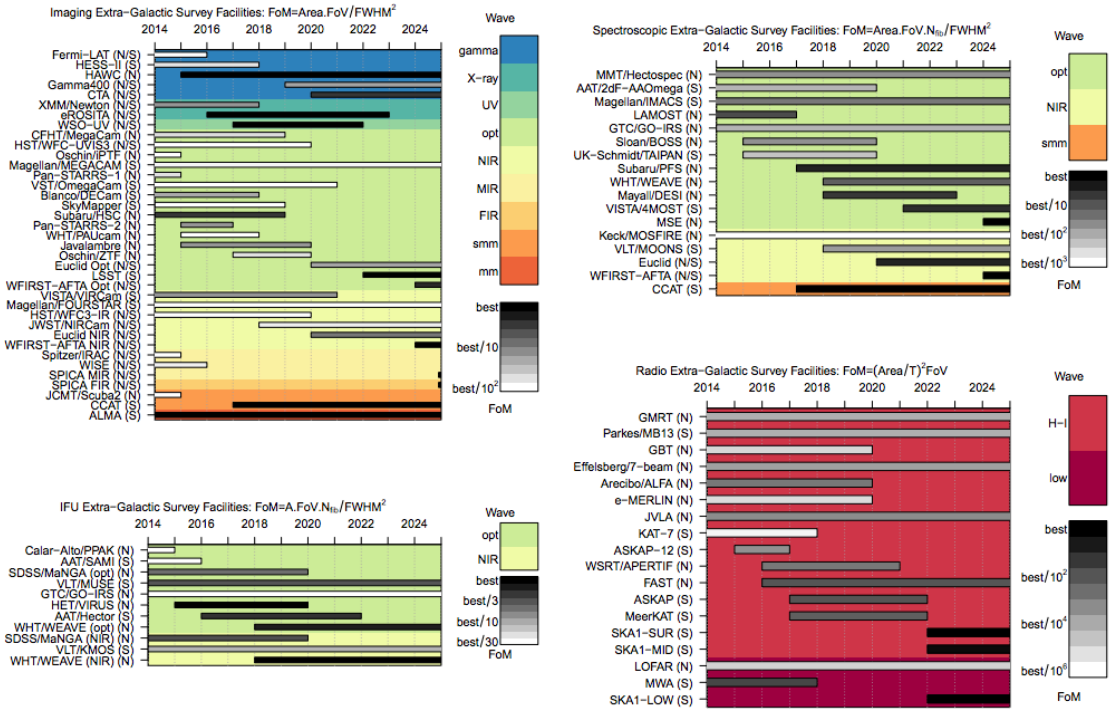

Figure 1: (top left) Comparison of various extra-galactic imaging survey facilities that will operate between now and 2025. Figure of merit (FoM) is calculated using Area.FoV/(FWHM^2). (top-right) Comparison of various extra-galactic spectroscopic survey facilities that will operate between now and 2025. FoM is calculated using Area.FoV.N$_{fib}$/(FWHM^2). (bottom-left) Comparison of various extra-galactic IFU survey facilities that will operate between now and 2025. FoM is calculated using Area.FoV.N$_{fib}$/(FWHM^2). (bottom-right) Comparison of various extra-galactic radio survey facilities that will operate between now and 2025. FoM is calculated using (Area/T)^2.FoV. 'HI' corresponds to facilities able to observe HI in the local Universe, i.e. they can observe at frequencies as high as 1.4 GHz. Note that in all panels FoM shading is scaled within a wavelength subset. The accompanying data for all charts is given in the Appendix. Versions of these charts and table data can be generated online using an interactive tool located at https://asgr.shinyapps.io/ganttshiny.

3.4 Space-based imaging

For Euclid and WFIRST, the main complementarity of MSE will come from the tracing of key emission and metal lines from z=0 to z=2.5 (i.e., [OII] - Ha, Mg b, Na) over extremely large areas on sky. SRO-1 discusses the various considerations that must be made to optimally design such surveys, so this will not be covered in detail here again.

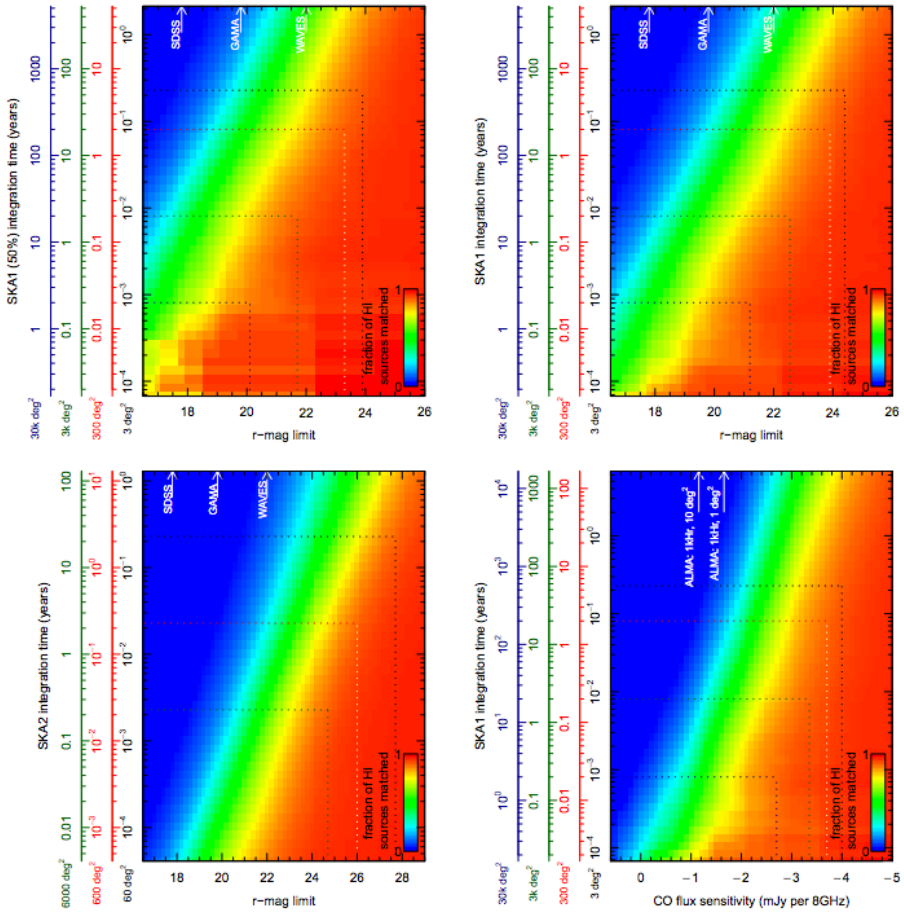

Figure 2: (top-left, top-right, bottom-left) Fraction of HI SKA survey sources (SKA1 50%, SKA1, SKA2 respectively; as a function of integration time) that are detected in an r-band apparent magnitude-limited sample (down to a given magnitude). The colour-scale indicates the value of the metric $F = \frac{A \cap B}{A}$. Different y-axis give the integration time scales for different survey areas. For SKA1 50% and SKA1, four surveys are considered: 3 deg^2 using SKA1-MID (and 50%; black), 300 deg^2 using SKA1-SUR (and 50%; red), 3000 deg^2 using SKA1-SUR (and 50%; green), and 30000 deg^2 using SKA1-SUR (and 50%; blue). For SKA2, three surveys are considered: 60 deg^2 (black), 600 deg^2 (red), and 6000 deg^2 (green). Dotted lines indicate the r-magnitude limit needed to achieve matches for 90% of sources in each SKA survey area (given 2000 hrs of integration for SKA1-MID & SKA2 surveys, and 2 years of telescope time for SKA1-SUR surveys). (bottom-right) Fraction of HI SKA1 survey sources that are detected in a CO(1-0) flux sensitivity limited sample, with colour-scale, colour-axes and indication lines as before.

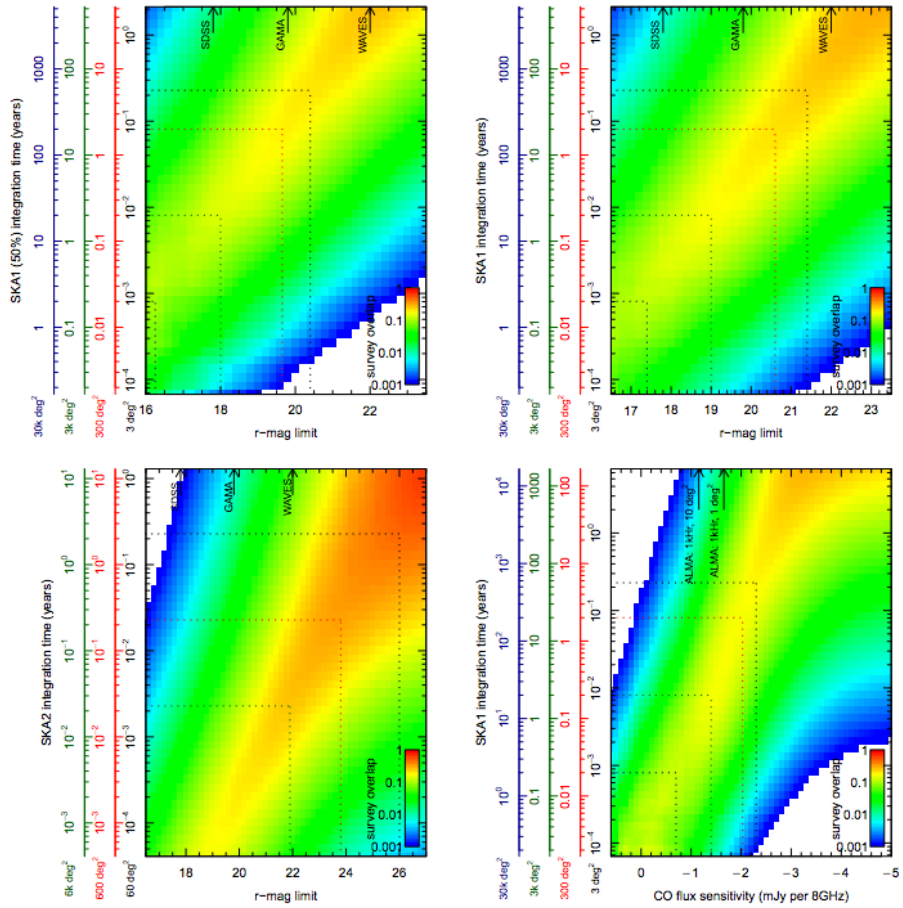

Figure 3: (top-left, top-right, bottom-left) Degree of mutual overlap between the HI sources detected by SKA telescopes (SKA1 50%, SKA1, SKA2 respectively; as a function of integration time) and an optically selected r-band sample (down to a given magnitude). The colour-scale indicates the value of the metric $E = \left(\frac{A \cap B}{A}\right)\left(\frac{A \cap B}{B}\right)$, where $E = 0$ indicates that the two selected populations are disjoint, and $E = 1$ indicates the selected populations are identical. Different y-axis give the integration time scales for different survey areas. For SKA1 50% and SKA1, four surveys are considered: 3 deg^2 using SKA1-MID (and 50%; black), 300 deg^2 using SKA1-SUR (and 50%; red), 3000 deg^2 using SKA1-SUR (and 50%; green), and 30000 deg^2 using SKA1-SUR (and 50%; blue). For SKA2, three surveys are considered: 60 deg^2 (black), 600 deg^2 (red), and 6000 deg^2 (green). Dotted lines show the optimal r-magnitude matching limit for each SKA survey area (given 2000 hrs of integration for SKA1-MID & SKA2 surveys, and 2 years of telescope time for SKA1-SUR surveys). (bottom-right) Degree of mutual overlap between the HI sources detected by SKA1 and a CO(1-0) flux sensitivity limited sample, with colour-scale, colour-axes and indication lines as before.

4. Target selection

4.1 Transients

Targets will be selected from the announcements in the GCN, and by coordination with Swift, Fermi and other gamma ray missions. Optical afterglows being very faint, there may be <4 events a year with V<19. The spectroscopic observations should start off as soon as the GRB is announced.

4.2 Photometric redshifts

For photometric redshift training, the most important requirement is that targets span the full color space of the LSST weak lensing dataset (i_{AB} < 25.3, extended objects). Given the long exposure times required to reach good completeness down to the survey depth, many objects should provide redshifts in considerably less time than the most difficult cases. Therefore, it would be useful to be able to remove objects from the target set and replace them with others as redshifts get measured.

For photometric redshift calibration via cross-correlations, the primary requirement is that the target set span the full redshift range of the photometric sample to be calibrated (for LSST, the limit should be approximately z=3). They do not, however, have to be of similar apparent magnitude; selection of the brightest objects at a given z would be the most efficient strategy. Target selection also must be uniform enough across hundreds of square degrees for the autocorrelation measurements needed not to be compromised.

4.3 Radio

Targets from SKA survey regions will not be selected, rather we expect a large degree of source overlap assuming the SKA and MSE surveys are designed to complementary depths (see Figure 2 and 3 above). For this reason it is important that extra-galactic survey fields are selected with potential SKA overlap in mind. Specifcally this means they must be near the equator.

4.4 Space-based imaging

Target selection should be made from the deepest available imaging capable of selecting redwards of the 4000A-break. Out to z~1.25 this is satisfied by LSST, beyond this the Euclid/WFIRST deep sky regions. The precise sample for obtaining high-S/N spectra can be selected either via an MSE redshift survey or photometric redshifts as provided by Euclid/LSST. To ensure overlap with Euclid extra-galactic survey fields should be designed to avoid the Milky-Way and ecliptic plane.

5. Cadence and temporal characteristics

5.1 Transients

The cadence will be determined by the initial brightness and predicted light curve of the event – most optical afterglows are short lives (few to few x 10 hr), and therefore the cadence would be a few times a night.

5.2 Photometric redshifts

For LSST photometric redshift training, it will be desirable to target based on final-depth LSST imaging; therefore one would prefer to target in the LSST deep drilling fields if the LSST survey is not yet complete, or anywhere within the LSST footprint if the survey is done.

5.3 Radio

For the SKA extra-galactic surveys there is no special temporal constraint to consider.

5.4 Space-based imaging

No special constraints, numerous repeat observations will be required to reach the S/N required (potentially up to 50hrs of intergation time for the very faintest highest redshift systems).

6. Calibration Requirements

6.1 Transients

Standard spectro-photometric calibrators would be used for flux calibration, and standard lamps used for wavelength calibration. No special calibratons other than that would be required. The wavelength calibration needs to only exceed velocities of 10^4 to 10^3 km/s for the supernova / GRB specific lines, though for the host galaxy itself, the line recession velocity would be 100km/s.

6.2 Photometric redshifts

For many objects, well-determined spectral shapes could help in obtaining secure redshifts (e.g., by definitively identifying the 4000 Angstrom break as one feature for determining a redshift). Therefore, spectrophotometry accurate to ~5% would be desirable, though not necessary. High-quality spectrophotometry would also greatly enhance synergistic galaxy evolution science from this sample.

Because targets will be faint compared to night sky lines, extremely accurate sky subtraction will be necessary. This will impose requirements on both flat-fielding and wavelength accuracy (at R~6000 for DEEP2, errors in relative wavelength calibration

needed to be below ~0.01 Angstroms to achieve Poisson-limited sky subtraction).

6.3 Radio

No specific calibration beyond wavelength calibration to better than the line widths. Most systems will have internal dynamics of order 100km/s hence wavelength calibration to better than this value would be required which is not particularly stringent.

6.4 Space-based imaging

No specific calibration beyond wavelength calibration to better than the line widths. Most systems will have internal dynamics of order 100km/s hence wavelength calibration to better than this value would be required which is not particularly stringent.

7. Data processing

7.1 Transients

Standard data processing methods will be sufficient. These will include bias subtraction, flat fielding, flux and wavelength calibration, and stacking if the signal is too faint in a single exposure.

7.2 Photometric redshifts

Standard spectroscopic data reduction pipelines should work. Key attention will need to be made to metrics that can determine redshift reliability. For photo-z training, samples are small enough that all redshifts may be checked by eye. Software/GUIs to enable that checking would be desirable.

It will also be useful to check all objects for multiple redshift solutions, as a few percent of targets at $z>1$ that appear single from the ground are revealed to be blends in space-based imaging, and we want to throw such blends out in training photo-z's.

7.3 Radio

For galaxy evolution and cosmology related science cases the associated MSE spectra will need standard processing. Data will need to be de-biased, flat-fielded, flux and wavelength calibrated and stacked via signal-to-noise weighting. Line measurements (absorption or emission) will need to be made from multi-Gaussian line-fitting.

7.4 Space-based imaging

For galaxy evolution and cosmology related science cases the associated MSE spectra will need standard processing. Data will need to be de-biased, flat-fielded, flux and wavelength calibrated and stacked via signal-to-noise weighting. Line measurements (absorption or emission) will need to be made from multi-Gaussian line-fitting.

8. Any other issues

Deep-field coordination (hemisphere): The deep fields of the key facilities must be coordinated requiring cross-facility communications. Experience has shown this is not easy, as it often requires compromise in selecting regions that are satisfactory for all and hence often sub-optimal for each individual facility. For example Euclid is planning to operate its surveys avoiding the Ecliptic and Milky-Way by large margins (pushing its deep fields south out of MSEs reach). SKA deep fields will need to avoid known bright continuum sources, and will also prefer Southern hemisphere targets avoiding the equator (to maximize UV plane rotation). In a vacuum, LSST would favor deep fields in regions of high visibility (again pushing south out of MSEs reach), but the project is well aware of the desire to have deep drilling fields accessible from the North. We therefore anticipate that most, but not all, LSST deep drilling fields will be accessible from MSE